1. Report No.	2. Government Accession No.	3. Recipient's Catalog No.
DOT-TSC-FAA-71-28		

4. Title and Subtitle	5. Report Date
A Simulation Model for the Boeing 720B Aircraft-Flight Control System in Continuous Flight.	August 1971
	6. Performing Organization Code: PGL
7. Author(s): Dennis Collins, Joseph S. Koziol Jr.	8. Performing Organization Report No.
9. Performing Organization Name and Address: DOT/Transportation Systems Center, 55 Broadway, Cambridge, MA 02142	10. Work Unit No.: PPA FA12 (FY71)
	11. Contract or Grant No.
	13. Type of Report and Period Covered: Preliminary Memorandum
12. Sponsoring Agency Name and Address: FAA/SRDS, 800 Independence Ave. S.W., Washington D.C. 20590	14. Sponsoring Agency Code: FAA/SRDS

15. Supplementary Notes

16. Abstract

A mathematical model of the Boeing 720B aircraft and autopilot has been derived. The model is representative of the 720B aircraft for continuous flight within a flight envelope defined by a Mach number of .4 at 20,000 feet altitude in a cruise configuration down to touchdown in a full landing configuration. Certain data relative to the model were not available but provision has been made for insertion when the data is received from the Boeing Co. In developing the model it was assumed that when used with a cockpit simulator it would be exercised by experienced pilots simulating normal airline operations. This underlying assumption allowed for a reduction in the model complexity for programming purposes.

17. Key Words	18. Distribution Statement
Aircraft-Autopilot Model, Simulation Data, Boeing 720B Aircraft, Flight Control System, Continuous Flight	Unclassified Limited (Distribution Controlled by TSC Landing Systems Programs Branch)

19. Security Classif. (of this report)	20. Security Classif. (of this page)	21. No. of Pages	22. Price
Unclassified	Unclassified	112	

TABLE OF CONTENTS

LIST OF ILLUSTRATIONS

LIST OF ILLUSTRATIONS (Cont)

LIST OF ILLUSTRATIONS (Cont)

LIST OF TABLES

LIST OF ABBREVIATIONS AND SYMBOLS

NOTATION

$\bar{a}$	Speed of sound	feet/second
a	Distance from .25 MAC to cg (positive if cg forward of .25 MAC)	feet
a_n	Measure normal acceleration at accelerometer station	feet/second^2
A/B	Airbrake	-
$\underline{b}$	Wing span	feet
$\bar{c}$	Wing mean aerodynamic chord	feet
C_e, C_a, C_r	Elevator chord (or aileron or rudder)	feet
C_D	Non-dimensional drag coefficient	-
$C_{D()}$	Non-dimensional drag stability derivative	1/degree
$C_{he()}, C_{ha()}, C_{hr()}$	Non-dimensional hinge moment stability derivative	1/degree
C_L	Non-dimensional lift force coefficient	-
$C_{L()}$	Non-dimensional lift force stability derivative	1/degree
C_ℓ	Airplane rolling moment coefficient	-
$C_{\ell()}$	Non-dimensional rolling moment	1/degree
C_m	Airplane pitching moment coefficient	-
$C_{m()}$	Non-dimensional pitching moment stability derivative	1/degree
C_n	Airplane yawing moment coefficient	-
$C_{n()}$	Non-dimensional yawing moment stability derivative	1/degree
C_y	Airplane side force coefficient	-
$C_{y()}$	Non-dimensional side force stability derivative	1/degree

cg	Center of Gravity of airplane	-
FRL	Fuselage reference line	-
F_{sx}, F_{sy}, F_{sz}	Translational forces in stability axes	lbs.
F_{wx}, F_{wy}, F_{wz}	Translational forces in wind axes	lbs.
g	Acceleration of gravity (32.2)	feet/second^2
G	Landing gear	-
GE	Ground Effect	-
h	Altitude	feet
i_{pr}	Incidence of engine thrust axis with respect to fuselage reference axis, positive nose-up	degrees
I_{xx}, I_{yy}, I_{zz}	Moment of inertia about X, Y, or Z axes	slug-feet^2
I_{xz}	Aircraft product of inertia	slug-feet^2
I_e, I_a, I_r	Elevator moment of inertia (or aileron or rudder)	slug-feet^2
K	Ground effect factor	-
L_s	Rolling moment, stability axes (no subscript, body axes)	foot-lbs.
ℓ_E	Distance between cg and engine thrust line in XZ plane	feet
L.E.	Leading edge	-
M	Mach. number	-
MAC	Mean aerodynamic chord	-
m	Aircraft mass	slugs
M_s	Pitching moment, stability axes (no subscript, (body axes))	foot-lbs
N_s	Rolling moment, stability axes (no subscript, body axes)	foot-lbs
p_s	Roll rate about stability axis (no subscript, body axes)	degrees/second
q_s, q_w	Pitch rate about stability axes or wind axes (no subscript, body axes)	degrees/second
$\bar{q}$	Dynamic pressure	lbs/feet^2
r_s, r_w	Yaw rate about stability axes or wind axes (no subscript, body axes)	degrees/second

R_e/R_r	Ratio of elastic to rigid body control effectiveness	-
S	Wing area	$feet^2$
S_e, S_a, S_r	Elevator area (or aileron or rudder)	$feet^2$
S_{FRL}	Horizontal stabilizer angle with respect to FRL	degrees
S_x, S_y	X-axis and Y-axis position coordinates in Earth-fixed coordinate frame	feet
T_1, T_2, T_3, T_4	Engine propulsive thrust	lbs
T_{sx}, T_{sy},	Components of propulsive thrust in X,Y stability axes	lbs
u	Forward velocity	feet/second
V	Total velocity	feet/second
v	Lateral velocity	feet/second
Ve	Equivalent airspeed	knots
w	Normal velocity	feet/second
x_{accel}	Distance from center of gravity to accelerometer station	feet
X_s	Drag force, stability axes	lbs
Y_s	Side force, stability axes	lbs
Z_s	Lift force, stability axes	lbs
α	Angle of attack with respect to fuselage reference line	degrees
β	Side slip angle	degrees
$\delta_e, \delta_a, \delta_r, \delta_s, \delta_F, \delta_{St}$	Elevator deflection (or aileron, rudder, spoiler, flap, or stabilizer)	degrees
$\delta_{te}, \delta_{ta}, \delta_{tr}$	Elevator tab deflection (or aileron or rudder)	degrees
$\delta_{es}, \delta_{as}, \delta_{rs}$	Elevator servo displacement (or aileron or rudder)	degrees
δ_w	Control wheel angle	degrees
θ	Pitch angle	degrees
ϕ	Roll angle	degrees
ψ	Yaw angle	degrees
ρ	Atmospheric density	$slug/feet^3$
$\dot{(\ )}$	Differentiation with respect to time	-

Subscripts

a aileron
B fuselage reference frame
e elevator
F flaps
i inboard
o outboard
r rudder
s spoiler (or airbrake)
S_t horizontal stabilizer

SUMMARY

A mathematical model of the Boeing 720B aircraft and autopilot has been derived. The model is representative of the 720B aircraft for continuous flight within a flight envelope defined by a Mach number of .4 at 20,000 feet altitude in a cruise configuration down to touchdown in a full landing configuration. Certain data relative to the model were not available but provision has been made for insertion when the data is received from the Boeing Co. In developing the model, it was assumed that when used with a cockpit simulator it would be exercised by experienced pilots simulating normal airline operations. This underlying assumption allowed for a reduction in the model complexity for programming purposes. This work was performed under PPA number FA 12-0.

INTRODUCTION

Improvements in instrument landing systems are required to extend the poor visibility operational capabilities of the Civil air transport industry.

Real-time simulation of aircraft and their control systems play an important role in the development of new landing systems and the understanding of significant parameters of existing landing systems. Real-time simulation allows a relatively rapid and inexpensive (when compared to flight testing) closing of the iterative loops in the design process for new systems and provides a useful tool for the design of experiments and for the evaluation and extrapolation of experimental flight test results for existing systems.

Aircraft models can take the form of perturbation models (fixed point) wherein the aircraft parameters are allowed to vary in a restricted fashion about some nominal flight condition or they can be written to allow continuous variations in all of the aircraft parameters over a specified flight envelope. Perturbation models usually make use of linearized equations whereas by their nature continuous models require the full set of non-linear equations. Perturbation models are very useful tools for the design of systems (e.g. control systems) and for the simulation of limited operational situations. However, the general simulation of realistic operational problems requires the increased freedoms allowed by a continuous model in order to better evaluate the complex interrelationships existing between the aircraft/pilot/autopilot system and the related ground based systems.

The aircraft model developed on the following pages allows for the continuous simulation of the Boeing 720B aircraft and autopilot within a flight envelope defined by an altitude of 20,000 feet at mach .4 in a cruise configuration to touchdown in a full landing configuration. Certain simplifying assumptions have been made so that the model could be kept to a manageable size relative to computer capability. In general it was assumed that the aircraft simulation would be operated as in scheduled airline operations as opposed to operating at the design limits of the aircraft. Significant savings in the description of non-linear aerodynamic relationships resulted. The specific assumptions and their consequences are discussed in detail in the text.

Certain data necessary for a complete operational simulation were not available and have been identified. The missing data relates to the powerplant, hinge moments, and

aircraft moments of inertia and products of inertia. The missing data shall be provided upon receipt from the Boeing Company.

The sections entitled Manual Flight Control System Description, Automatic Flight Control System Description, and Approach Landing Mode Description were prepared by H. Zuckerberg and A. F. Robb of the Service Technology Corporation under contract STC-DOT-TSC-43-71-866.

AIRCRAFT MODEL

GENERAL DISCUSSION

The continuous flight regime model for the Boeing 720B consists of rigid body, nonlinear six degree-of-freedom aircraft equations, Euler angle equations, and Earth referenced trajectory equations. These equations are described in the flow diagram in Figure 1. Airplane angles and sign conventions are described in Figure 2. The rotational (moment) equations are referenced to a body axis coordinate frame to preserve constant moments and products of inertia. The translational (force) equations are referenced to the wind axis coordinate frame for ease of obtaining the standard aircraft translational variables, V, β and α.

All force and moment coefficients in the aircraft equations are computed in the stability axis (all the data available is stability axis data) and converted to the wind and body axes appropriately.

In addition to these equations, the aircraft model consists of acceleration equations, hinge moment equations and velocity equations for implementing the wind environment. These are described below.

Finally, the continuous flight regime model requires the calculation of dynamic pressure ($\bar{q} = 1/2\ \rho V^2$), Mach number ($M = V/\bar{a}$) and equivalent airspeed

$$\left(V_e = \sqrt{\frac{\rho}{\rho_{h=0}}}\ V \right) .$$

The atmospheric density, ρ and speed of sound $\bar{a}$, for these calculations must be programmed as a function of altitude and temperature, and are available from any standard atmospheric table such as that given in Reference 6.

DEFINITION OF FLIGHT REGIME, VARIABLE LIMITATIONS, AND CONFIGURATIONS

The flight regime of interest for purposes of this simulation extends from a cruise condition at 20,000 ft. of altitude and Mach .4 down to a landing condition at touchdown. The ranges of parameters and variables are as follows:

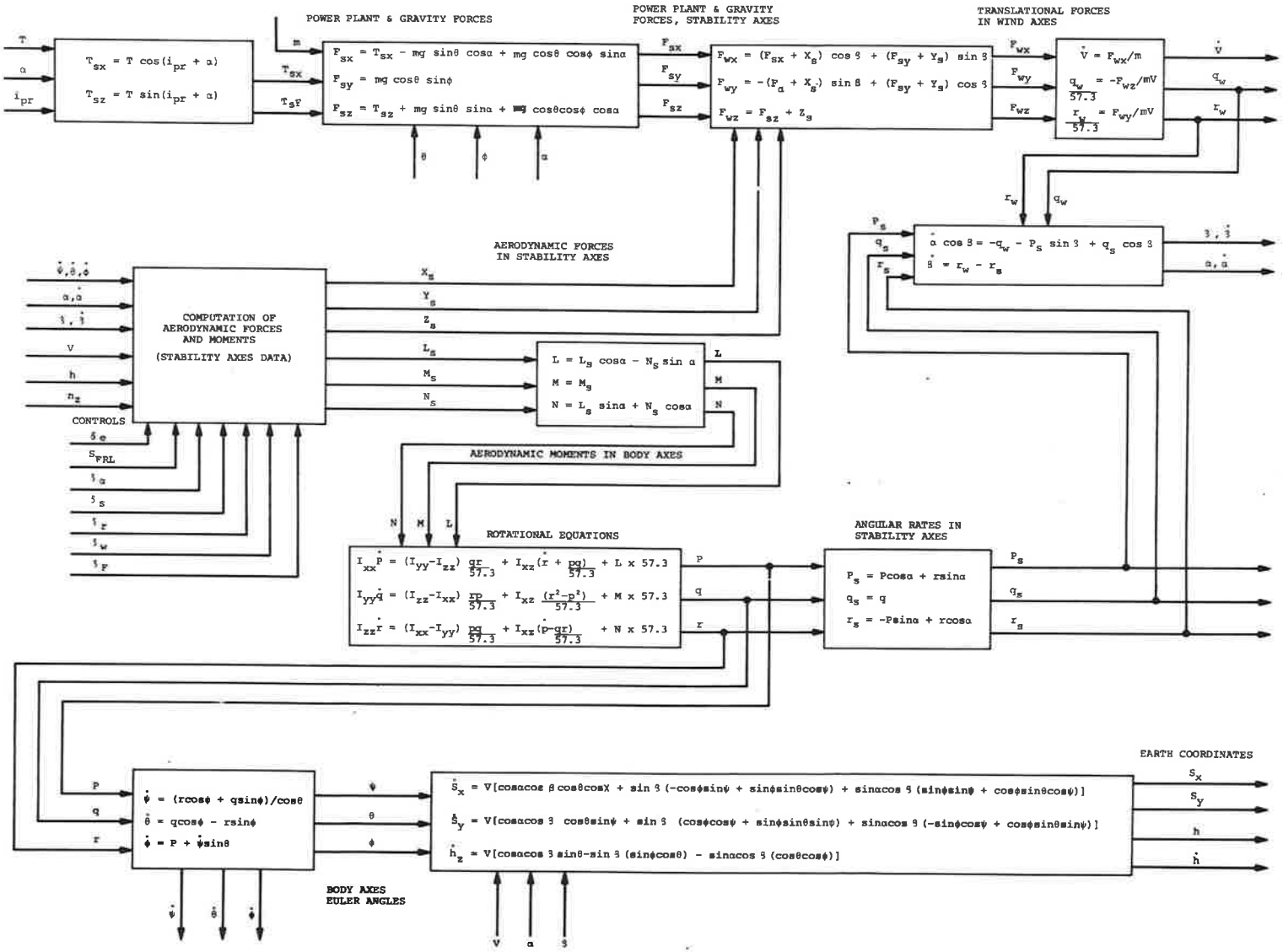

Figure 1. Aircraft Equations

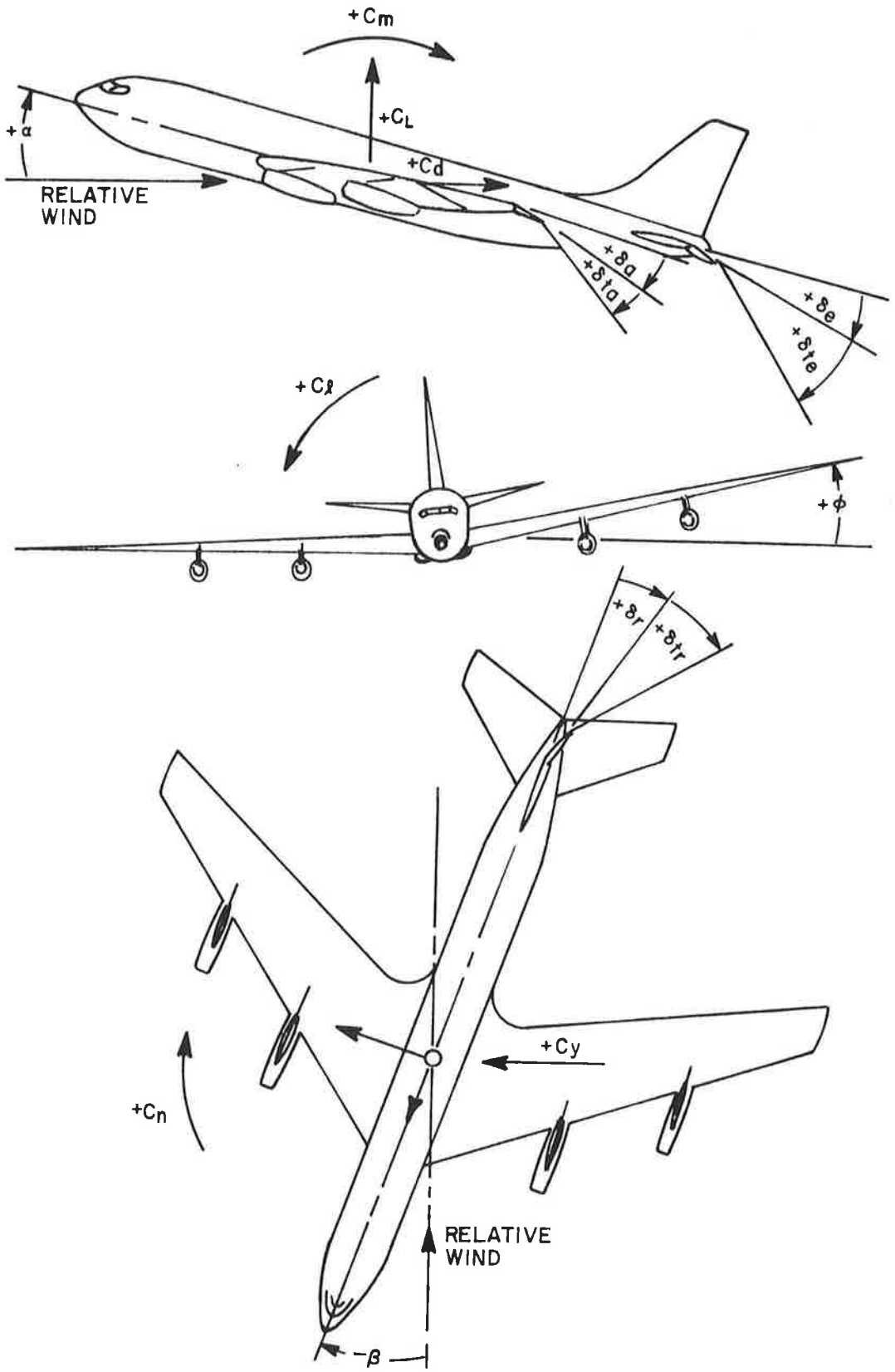

Figure 2 Definition of Airplane Angles and Sign Conventions

a) Altitude (h) : sea level to 20,000 ft.
b) Mach No. (M) : 0.1 to 0.4
c) Thrust (T) : as specified in Figure 31
d) Angle of attack (α) : 0° to + 10°
e) Sideslip angle (β) : $\pm$15°
f) Aileron (δ_a) : $\pm$10°
g) Speed brakes (δ_s) : 0° to 60° } Also used as spoilers; deflection limited as indicated in Figure 3
h) Rudder (δ_r) : $\pm$10°
i) Elevator (δ_e) : $\pm$10°
j) Stabilizer (δ_{st}) 1.5° to -13°
k) Roll angle (ϕ) : $\pm$90°
l) Pitch angle (θ): $\pm$10°
m) Gross wt.: constant } fixed at initial condition
n) C.G. : constant }

In addition, the following configurations are provided for:

a) T.E. Flaps : 0° to 50°
b) L.E. Flaps : Retracted or fully extended
c) Landing Gear: Retracted or fully extended

Information on the rate of change from one configuration to another, and combinations of configurations for proper descent-to-landing procedure is currently not available. These are to be implemented in the simulation either by manual control inputs or programmed commands.

ASSUMPTIONS

The derivation of the continuous flight regime model involved the following assumptions:

a) The aircraft mass is constant.
b) The Earth can be considered an inertial frame.
c) The aircraft is a rigid body.
d) The aircraft is symmetrical about its X-Z plane.
e) The aircraft is initially in trimmed flight with no linear or angular accelerations.

EQUATIONS

ROTATIONAL EQUATIONS

The rotational or moment equations given in Figure 1 are referrenced to a body axis coordinate frame where the X-axis is directed along a fuselage reference line (FRL) as shown in Figure 2. The body axis system is an orthogonal set of axes fixed to the aircraft center of mass. The Y-axis is normal to

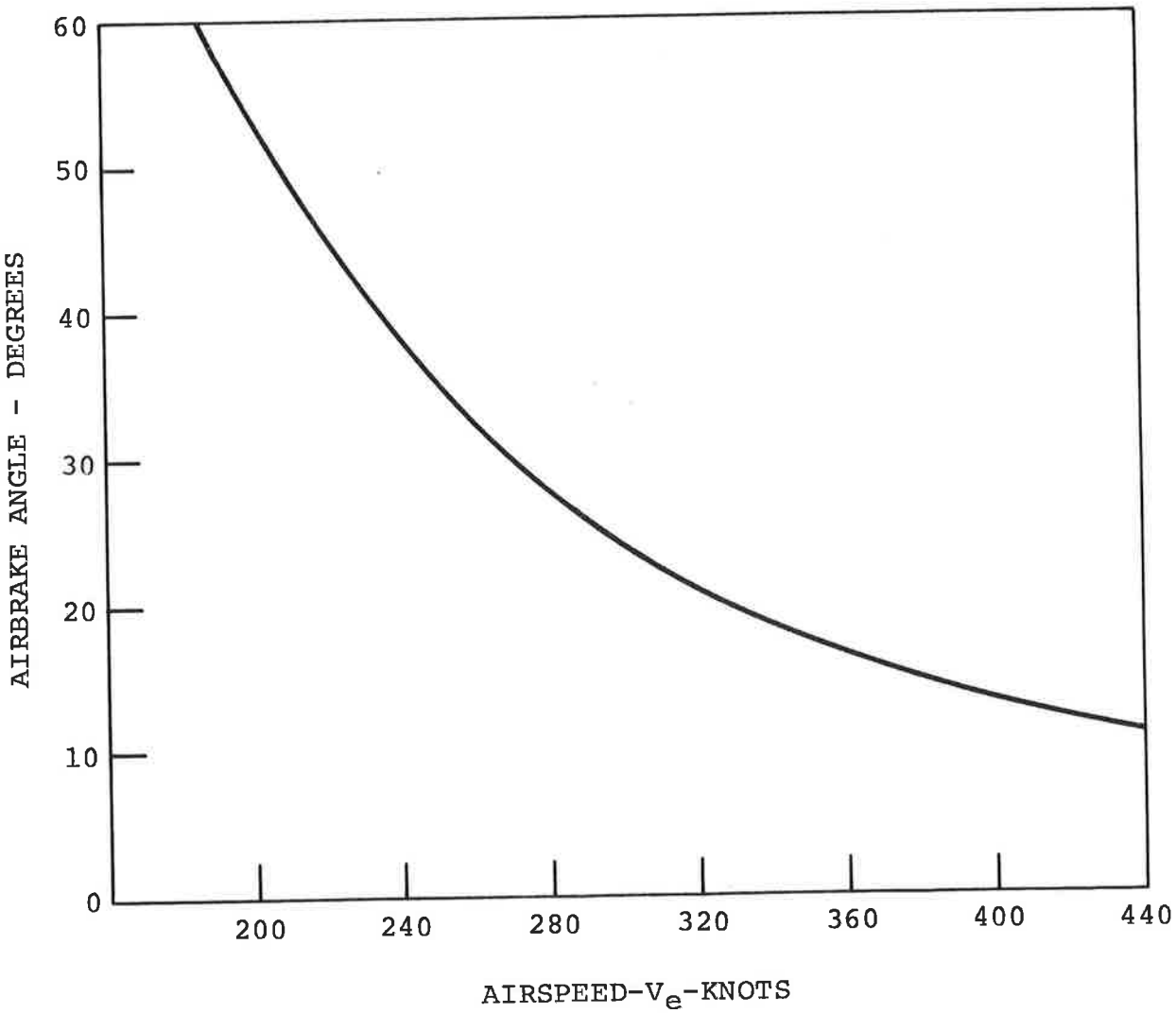

Figure 3. Airbrake Schedule.

the aircraft's plane of symmetry (positive to the right) and the Z-axis is in the plane of symmetry (positive downward) and orthogonal to the X- and Y-axes.

TRANSLATIONAL EQUATIONS

The translational or force equations given in Figure 1 are referenced to the wind axes. The wind axis system is an orthogonal set of axes fixed to the aircraft center of mass. The X-axis points in the direction of motion of the aircraft (positive forward). The Z-axis lies in the aircraft plane of symmetry (positive downward) and is orthogonal to the X-axis. The Y-axis (positive to the right) completes the axes set.

BODY AXIS VELOCITIES

Body axis velocities are required for calculating the accelerations at accelerometer locations. The velocities can be determined from the following equations:

$$V^2 = u_B^2 + v_B^2 + w_B^2$$

$$v_B = V \sin \beta$$

$$w_B = u_B \tan \alpha$$

ACCELERATION EQUATIONS

The aircraft normal accelerations are determined as follows:

Vertical acceleration at center of gravity

$$\dot{w} = V\dot{\alpha}\cos(\alpha)/57.3 + \dot{V}\sin\alpha$$

Vertical acceleration at accelerometer location

$$\dot{w}_{accel} = \dot{w} - x_{accel}\,\dot{q}/57.3$$

Measured Normal Acceleration

$$a_n = \dot{w}_{accel} + p\,v_B/57.3 - q u_B/57.3$$

EULER ANGLES

The Euler angles are used to define the orientation of the vehicle with respect to a local vertical reference axis system. These angles are defined by an ordered sequence of three rotations (ψ,θ,ϕ) which rotates the local vertical

reference frame into the body axis system. The convention normally adopted for the Euler angles and rates is defined in Figure 4.

The Euler angles are calculated by integrating the equations shown in Figure 1 from specified initial conditions.

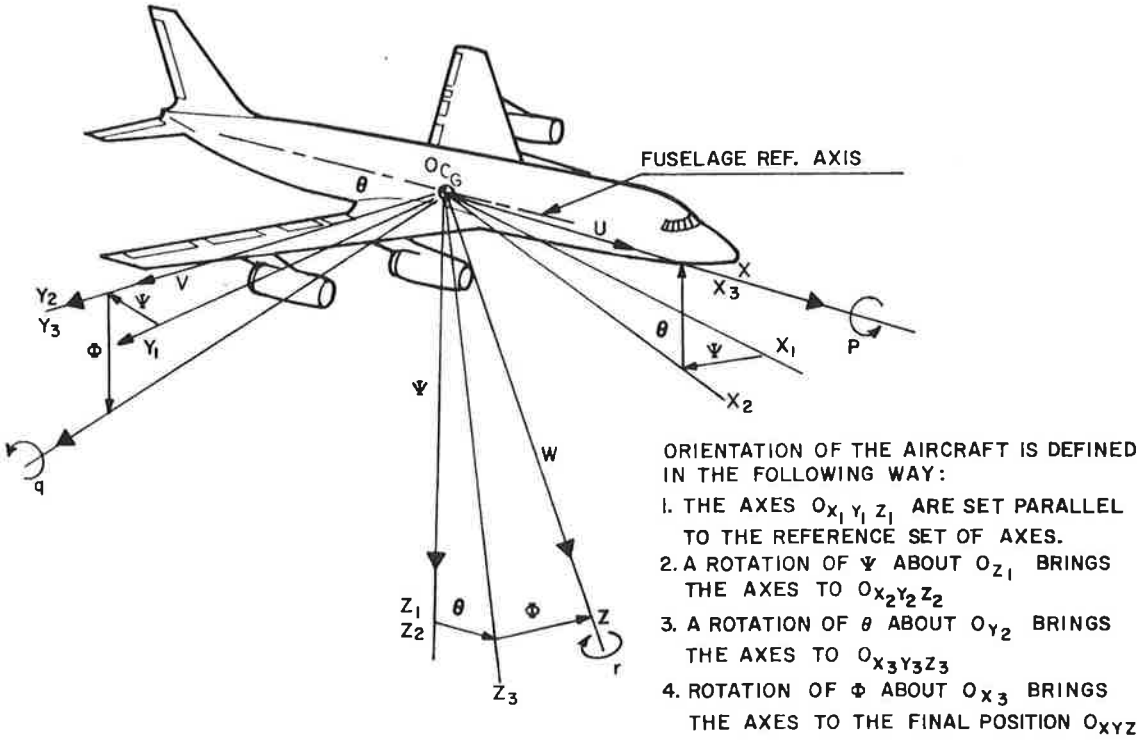

Figure 4. Delineation of Angles and Axes

TRAJECTORY EQUATIONS

The trajectory equations are written with respect to an inertial frame which is earth-fixed. This coordinate frame has

its origin at the center of mass of the aircraft with the X-axis pointing North, the Y-axis pointing East and the Z axis pointing down. The equations are given in Figure 1.

VELOCITY EQUATIONS

The velocity of the aircraft with respect to a stationary axis system is calculated by adding the components of the steady wind to the velocities calculated above. By integrating these velocities from the specified initial conditions the position of the aircraft can be calculated.

HINGE MOMENT EQUATIONS

The primary aerodynamic control surfaces of the Boeing 720B are controlled by means of spring tabs. The control surfaces themselves effectively float freely about their hinge. Therefore, when the tabs are moved by means of the servo, they introduce forces which produce a net moment about the hinge. The control surfaces then move to balance these hinge moments.

The equations which describe this motion of the control surfaces are called the Hinge Moment Equations and are given by

Elevator: $$\ddot{\delta}_e = \left[C_{h_{e_\alpha}} \alpha + C_{h_{e_{\delta_e}}} \delta_e + C_{h_{e_{\delta_{te}}}} \delta_{te} + C_{h_{e_{\dot{\delta}_e}}} \dot{\delta}_e - \left(\frac{2I_e}{\bar{q} s_e c_e} \right) \dot{q} \right] \left[\frac{\bar{q} s_e c_e}{2I_e} \right]$$

Aileron: $$\ddot{\delta}_a = \left[C_{h_{a_\beta}} \beta + C_{h_{a_p}} P + C_{h_{a_{\delta_a}}} \delta_a + C_{h_{a_{\delta_{ta}}}} \delta_{ta} + C_{h_{a_{\dot{\delta}_a}}} \dot{\delta}_a \right] \left[\frac{\bar{q} s_a c_a}{2I_a} \right]$$

Rudder: $$\ddot{\delta}_r = \left[C_{h_{r_\beta}} \beta + C_{h_{r_r}} r + C_{h_{r_{\delta_r}}} \delta_r + C_{h_{r_{\delta_{tr}}}} \delta_{tr} + C_{h_{r_{\dot{\delta}_r}}} \dot{\delta}_r - \left(\frac{2I_r}{\bar{q} s_r c_r} \right) \dot{r} \right] \left[\frac{\bar{q} s_r c_r}{2I_r} \right]$$

The rudder hinge moment equation is not actually included in the simulation model. The rudder surface is the primary controller in the directional axis and is operated directly from the servo. However, to relieve excessive pedal forces, the rudder tab can be operated in the balancing mode (through the hinge moment equations). This information was not available from the reference sources.

AIRCRAFT DESCRIPTION

GENERAL

The Boeing 720-B aircraft is a four engine, low-wing, jet airliner with approximately 35° sweep at 25 percent chord. The maximum take-off gross weight is 221,000 pounds which includes approximately 74,000 pounds of fuel. It is powered by four Pratt and Whitney turbojets mounted on pylons below the wing. A configuration of the 720-B aircraft is shown in Figure 5.

Primary flight controls are operated through spring-tabs. Lateral control at low speeds is provided by outboard and small inboard ailerons supplemented by two hydraulically operated spoilers on each wing which are interconnected with the ailerons. At high speeds, lateral control is by inboard ailerons and spoilers only. Operations of the double-slotted flaps adjusts the linkage between the inboard and outboard ailerons to permit outboard operation only with extended flaps. With this condition only outboard aileron stability derivatives are given. Spoilers may be used symmetrically as speed brakes. Maximum flap deflection is 50°.

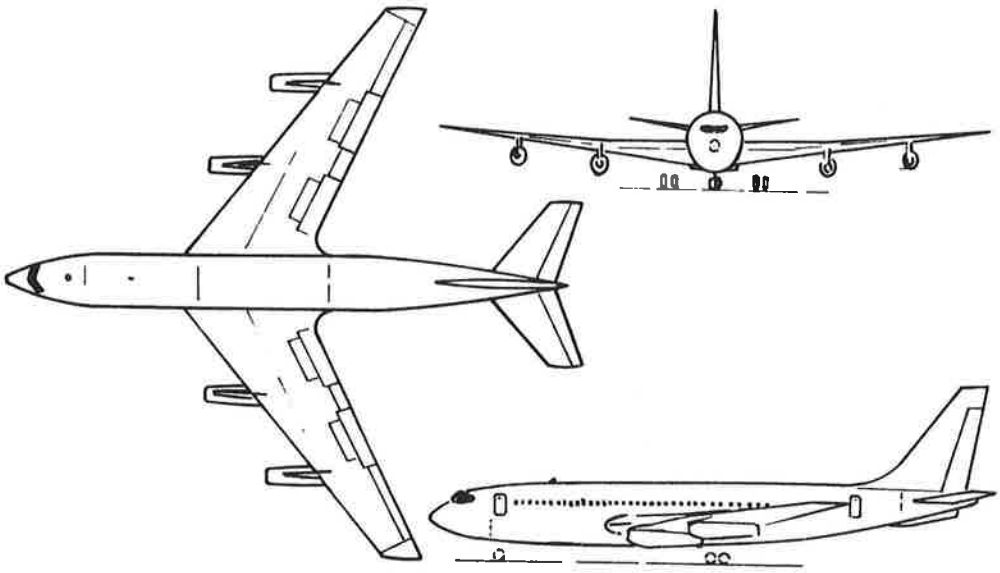

Figure 5 Boeing 720 Four-Engined Jet Transport

PHYSICAL CHARACTERISTICS, MAJOR DIMENSIONS AND INITIAL CONDITIONS

The physical characteristics and major dimensions of the 720B aircraft are given in Tables 1 and 2 respectively. The continuous flight regime model requires that the initial conditions of certain variables be stipulated. These are listed in Table 3.

TABLE 1. PHYSICAL CHARACTERISTICS

Item	Value	Dimension
Weight	185,000	lbs
Mass (m)	5751	Slugs
Center of Gravity Position	.25	% Mac
Moment of Inertia (I_x)	(')	Slug-ft^2
(I_y)	(')	Slug-ft^2
(I_z)	(')	Slug-ft^2
(I_{xz})	(')	Slug-ft^2
(') Data not available		

TABLE 2. MAJOR DIMENSIONS

Item		Value	Dimension
Wing area	(S)	2433	Ft^2
Wing span	(b)	130.83	Ft
Wing mean aerodynamic chord	($\bar{c}$)	20.16	Ft
Elevator area	(S_e)	118	Ft^2
Elevator chord	(c_e)	2.72	Ft
Moment of inertia of elevator	(I_e)	(')	Slug-ft^2
Rudder area	(S_r)	102	Ft^2
Rudder chord	(c_r)	(')	Ft
Moment of inertia or rudder	(I_r)	(')	Slug-ft^2
Aileron area (outboard)	(S_a)	2 X 19.4	Ft^2
Aileron area (inboard)	(S_a)	2 X 39.8	Ft^2
Aileron chord (outboard)	(c_a)	2.09	Ft
Aileron chord (inboard)	(c_a)	2.9	Ft
Moment of inertia of aileron	(I_a)	(')	Slug-ft^2
Mean distance of engine thrust axis below CG	(ℓ_e)	2.28	Ft
Incidence of engine thrust axis	(i_{pr})	0	Degrees
(') Data not available			

TABLE 3. INITIAL CONDITIONS REQUIRED

Landing Gear Position	
Flap Position	(δ_F)
Speed Brake Position	(δ_s)
Altitude	(h_{cg})
Velocity	(V)
Roll Rate	(p)
Pitch Rate	(q)
Yaw Rate	(r)
Angle of Attack	(α)
Angle of Sideslip	(β)
Roll Angle	(ϕ)
Pitch Angle	(θ)
Yaw Angle	(ψ)
Thrust	(T)
mass	(m)

COMPUTATION OF AERODYNAMIC FORCES AND MOMENTS

This section describes the representation of the continuous aerodynamic forces and moments as required in Figure 1. The mechanization scheme is left as a further exercise. The data have been extracted from Reference 3 and are the results of both flight test information, and wind tunnel tests. All important contributions are included. The results are expressed in terms of force and moment coefficients. These are described below and summarized in Tables 4 through 9.

LIFT CHARACTERISTICS, Z_s

$$Z_s = \frac{1}{2} \rho V^2 S C_L$$

where $C_L = C_{Lo} + \Delta C_{Lo} + \Delta C_{L\alpha}\alpha + C_{L_{S_{FRL}}}(S_{FRL} + 4) + C_{L_{\delta e}}\delta e + \Delta C_{L_{GE}} + \Delta C_{L_{A/B}}$

C_{Lo} = Basic lift coefficient given in Table 10 as a function of α and δ_F.

ΔC_{Lo} = Deviation from basic lift coefficient due to Mach number and altitude and given in Table 11.

$\Delta C_{L\alpha}\alpha$ = Deviation from basic lift coefficient due to variation in lift curve slope. $\Delta C_{L\alpha}$ is given in Table 12 as a function of Mach number and altitude.

TABLE 4. SUMMARY OF LIFT CHARACTERISTICS

Coefficient	Value, Reference or Representation	Variables Required for Programming
C_{L_o}	Table 10	α, δ_F
ΔC_{L_o}	Table 11	M, h
ΔC_{L_α}	Table 12	M, h
$C_{L_{S_{FRL}}}$	.01/degree	-
$C_{L\ \delta_e}$	.0042/degree	-
$\Delta C_{L_{GE}}$	$K(.0125+.009\ \delta_F+.004\alpha)$	K, δ_F, α
$\Delta C_{L_{A/B}}$	Figures 7, 8, 9	M, h, $\Lambda_{A/B}$, δ_F
K	Figure 6	h

TABLE 5. SUMMARY OF DRAG CHARACTERISTICS

Coefficient	Value, Reference or Representation	Variables Required for Programming
C_{D_o}	Figure 10	C_L, δ_F, L.E. flap
ΔC_{D_M}	negligible	-
$\underline{\Delta C_{D_{GE}}}$	$K\ \overline{\Delta C_{D_{GE}}}$	K, $\overline{\Delta C_{D_{GE}}}$
$\overline{\Delta C_{D_{GE}}}$	Figure 11	C_L, δ_F
$\Delta C_{D_{A/B}}$	Table 13, Figure 12	C_L, $\Lambda_{A/B}$, δ_F
ΔC_{D_G}	.0221	-
$\Delta C_{D\ \beta}$	Table 14	β, δ_r

TABLE 6. SUMMARY OF PITCHING MOMENT CHARACTERISTICS

Coefficient	Value, Reference or Representation	Variables Required for Programming
C_{mo}	Figure 13	α, δ_F, L.E.flap
ΔC_{mo}	$.015\left[\frac{20,000-h}{20,000}\right]$ M	M,h
$\Delta C_{m\alpha}$	$(.022M-.0018)-\frac{h}{20,000}(.01M-.005)$	M,h
$C_{m_{S_{FRL}}}$	.01M-.3065	M
$\Delta C_{m\,\delta_e}$	$[-.01352\,\delta_e+.000003167\,\delta_e^3]\,[.98-.000667(V_e-100)]$	δ_e, V_e
$\Delta C_{m(a/\bar{c})}$	$[(.068M-.13)-\frac{h}{20,000}(.048M-.007)]$ $[1+.156\,\delta_F-.00104\,\delta_F^2]$	M,h, δ_F
$\Delta C_{m_{\alpha(a/\bar{c})}}$	Table 15	M,h
$\Delta C_{m_{GE}}$	$K(.0208-.14604C_L+.04476C_L^2)$	K,C_L
$\Delta C_{m_{A/B}}$	Figures 14, 15, 16	M,h,A/B, δ_F
ΔC_{m_G}	$.014-.0003\,\delta_F$	δ_F
$C_{m_{\dot{\alpha}}}$	$-.096+.04\left[\frac{20,000-h}{20,000}\right]$ M, per degree	M,h
$C_{m_{\dot{\theta}}}$	$-.25+\left[.04+\left(\frac{20,000-h}{20,000}\right)(.064)\right]$ M per degree	M,h
C_{m_T}	$.0321\left(\frac{T_1+T_4}{V_e^2}\right)+.0462\left(\frac{T_2+T_3}{V_e^2}\right)$	T_1,T_2,T_3,T_4, V_e

TABLE 7. SUMMARY OF ROLLING MOMENT CHARACTERISTICS

Coefficient	Value, Reference or Representation	Variables Required for Programming
C_{ℓ_β}	Figure 17	C_L, δ_F
$C_{\ell_{\dot{\phi}}}$	$(.000372V_e-.436)/57.3$, per degree	V_e
$C_{\ell_{\dot{\psi}}}$	$(.054+.230C_L+.0005\ \delta_F)/57.3$, per degree	C_L, δ_F
ΔC_{ℓ_s}	$(R_e/R_r)\overline{\Delta C}_{\ell_s}$	(R_e/R_r), $\overline{\Delta C}_{\ell_s}$
(R_e/R_r)	Figure 21	h, V_e
$\overline{\Delta C}_{\ell_s}$	Figures 18, 19, 20	C_L, δ_s, M, δ_F α
$\Delta C_{\ell_{\delta a}}$	$(R_e/R_r)_i C_{\ell_{\delta a_i}} \delta_{a_i}+(R_e/R_r)_o C_{\ell_{\delta a_o}} \delta_{a_o}$	$(R_e/R_r)_i$, $(R_e/R_r)_o$, $C_{\ell_{\delta a_i}}$, $C_{\ell_{\delta a_o}}$, δ_{a_i}, δ_{a_o}
δ_{a_o}	$[.05\ \delta_F]\delta_{a_i}$, $\delta_F \leq 20°$ $[1+.011(\delta_F-20)]\ \delta_{a_i}$, $20° \leq \delta_F \leq 50°$	δ_{a_i}, δ_F
$C_{\ell_{\delta a_i}}$	$[.00058+.0000108\ \delta_F]\ [1-.1087C_L]$, $0 \leq C_L \leq .92$ $[.00058+.0000108\ \delta_F]\ [.9-2.5(C_L-.92)]$, $.92 \leq C_L \leq 1.2$	C_L, δ_F
$(R_e/R_r)_i$	$.91-.00185V_e$	V_e
$C_{\ell_{\delta a_o}}$	$[.00145]$, $0 \leq C_L \leq 1.05$ $[.00145]\ [1-.878(C_L-1.05)]$, $1.05 \leq C_L \leq 1.75$	C_L
$(R_e/R_r)_o$	$.865-.00315V_e$	V_e
$C_{\ell_{\delta r}}$	$.00065+.000006\ \delta_F-.0004C_L$, per degree	C_L, δ_F

TABLE 8. SUMMARY OF SIDE FORCE CHARACTERISTICS

Coefficient	Value, Reference or Representation	Variables Required for Programming
C_{Y_β}	Figure 22	C_L, δ_F
$C_{Y_{\dot{\beta}}}$	Figure 23	C_L, δ_F,h,M
C_{Y_ϕ}	Figure 24	C_L
C_{Y_ψ}	Figure 25	C_L, δ_F
$C_{Y_{\delta_w}}$	negligible	-
$\Delta C_{Y_{\delta_a}}$	.00394	-
$C_{Y_{\delta_r}}$		

TABLE 9. SUMMARY OF YAWING MOMENT CHARACTERISTICS

Coefficient	Value, Reference or Representation	Variables Required for Programming
C_{n_β}	Figure 26	C_L, δ_F, gear position
$C_{n_{\dot{\beta}}}$	.0003/degree	-
C_{n_ϕ}	Figure 27	C_L, δ_F
C_{n_ψ}	Figure 28	C_L, δ_F
$C_{n_{\delta_r}}$	-.001625/degree	-
$C_{n_{\delta_w}}$	Figure 29	C_L, δ_F

TABLE 10. BASIC LIFT COEFFICIENT*

α (DEG)	$C_{L_O}(\delta_F = 0°)$	$C_{L_O}(\delta_F = 30°)$	$C_{L_O}(\delta_F = 50°)$
0	.12	.575	.755
4	.475	.93	1.115
8	.825	1.29	1.465
10	1.0	1.45	1.60
12	1.155	1.57	1.70
14	1.245	1.635	1.75
16	1.27	1.645	1.75

* Interpolate for intermediate values of flap deflection.

TABLE 11. DEVIATION FROM BASIC LIFT COEFFICIENT, ΔC_{L_O} *

Mach NO.	ΔC_{L_O}		
	h = sea level	h = 10,000 ft	h = 20,000 ft
0	0	0	0
.2	-.005	0	0
.4	-.02	-.015	-.005

* Use linear interpolation for intermediate values of Mach number and altitude

TABLE 12. DEVIATION FROM BASIC LIFT COEFFICIENT, ΔC_{L_α} *

Mach NO.	ΔC_{L_α}		
	h = sea level	h = 10,000 feet	h = 20,000 feet
0	0	0	0
.2	-.004	-.00225	-.001
.4	-.0135	-.009	-.005

* Use linear interpolation for intermediate values of Mach number and altitude

TABLE 13. EFFECT OF AIRBRAKES* ON DRAG CHARACTERISTICS - FLAPS UP

Airbrake Angle (DEG)	$\Delta C_{D_{A/B}}$				
	C_L=0	C_L=.2	C_L=.4	C_L=.6	C_L=.8
20	.0050	.0055	.0060	.0070	.0082
40	.0116	.0131	.0144	.0165	.0300
60	.0200	.0220	.0245	.0310	.0415

*$\Delta C_{D_{A/B}}$ is given for either inboard or outboard airbrake. To obtain the effect of inboard and outboard airbrake at the same angle, double the value given.

$C_{L_{S_{FRL}}}(S_{FRL} + 4)$ = variation in lift coefficient due to change of stabilizer angle from $S_{FRL} = -4$. $C_{L_{SFRL}}$ is constant over the flight range of interest and is equal to .01/degree.

$C_{L_{\delta_e}} \delta_e$ = increment of lift coefficient due to elevator angle. $C_{L_{\delta_e}} = .0042$/degree over the flight range of interest.

$\Delta C_{L_{GE}}$ = increment of lift coefficient resulting from ground effect $\Delta C_{L_{GE}} = K(.0125 + .009\,\delta_F + .004\alpha)$ over the flight regime of interest where K is the ground effect factor described in Figure 6.

$\Delta C_{L_{A/B}}$ = increment of lift coefficient due to airbrakes (spoilers). The effect of inboard and outboard airbrake operation for the flaps up condition is given in Figures 7 and 8 respectively as a function of Mach number, altitude and airbrake angle. Note that this data is presented only for the $\alpha = 2.5°$ condition. It is unknown from the information available whether or not different α's will have significant effects on the increment of lift coefficient due to the airbrake operation. The effect of the airbrakes for the flaps down condition is given in Figure 9 as a function of airbrake angle and flap angle.

DRAG CHARACTERISTICS, X_s

$$X_s = \tfrac{1}{2}\,\rho V^2 S C_D$$

$$C_D = C_{Do} + \Delta C_{D_M} + \Delta C_{D_{GE}} + \Delta C_{D_{A/B}} + \Delta C_{D_G} + \Delta C_{D_\beta}$$

C_{Do} = Basic drag coefficient given in Figure 10 as a function of C_L, δ_F and L.E. flap position.

ΔC_{D_M} = Increment of drag coefficient due to Mach number. This effect is negligible over the flight regime of interest.

$\Delta C_{D_{GE}}$ = Increment of drag coefficient due to ground effect. $\Delta C_{D_{GE}} = K\,\overline{\Delta C_{DGE}}$ where $\overline{\Delta C_{DGE}}$ is plotted in Figure 11 as a function of C_L and δ_F. K is described in Figure 6.

$\Delta C_{D_{A/B}}$ = Increment of drag coefficient due to airbrakes. The effect of either inboard or outboard airbrake operation for the flaps up condition is given in Table 13 as a function of C_L and airbrake angle. The effect of the airbrakes for the flaps down condition is given in Figure 12 as a function of airbrake angle and flap angle.

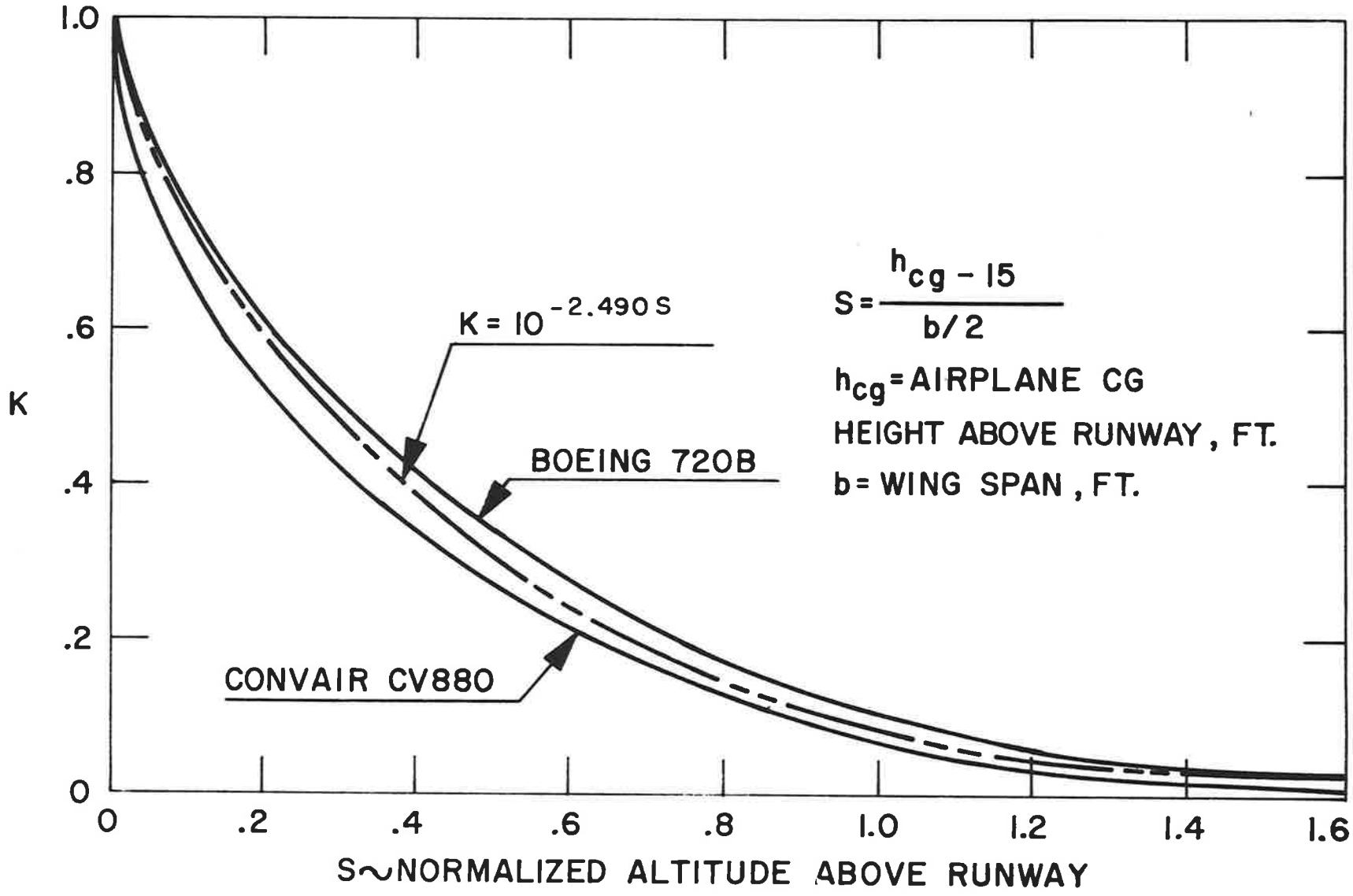

Figure 6. Ground Proximity Effects on Coefficients

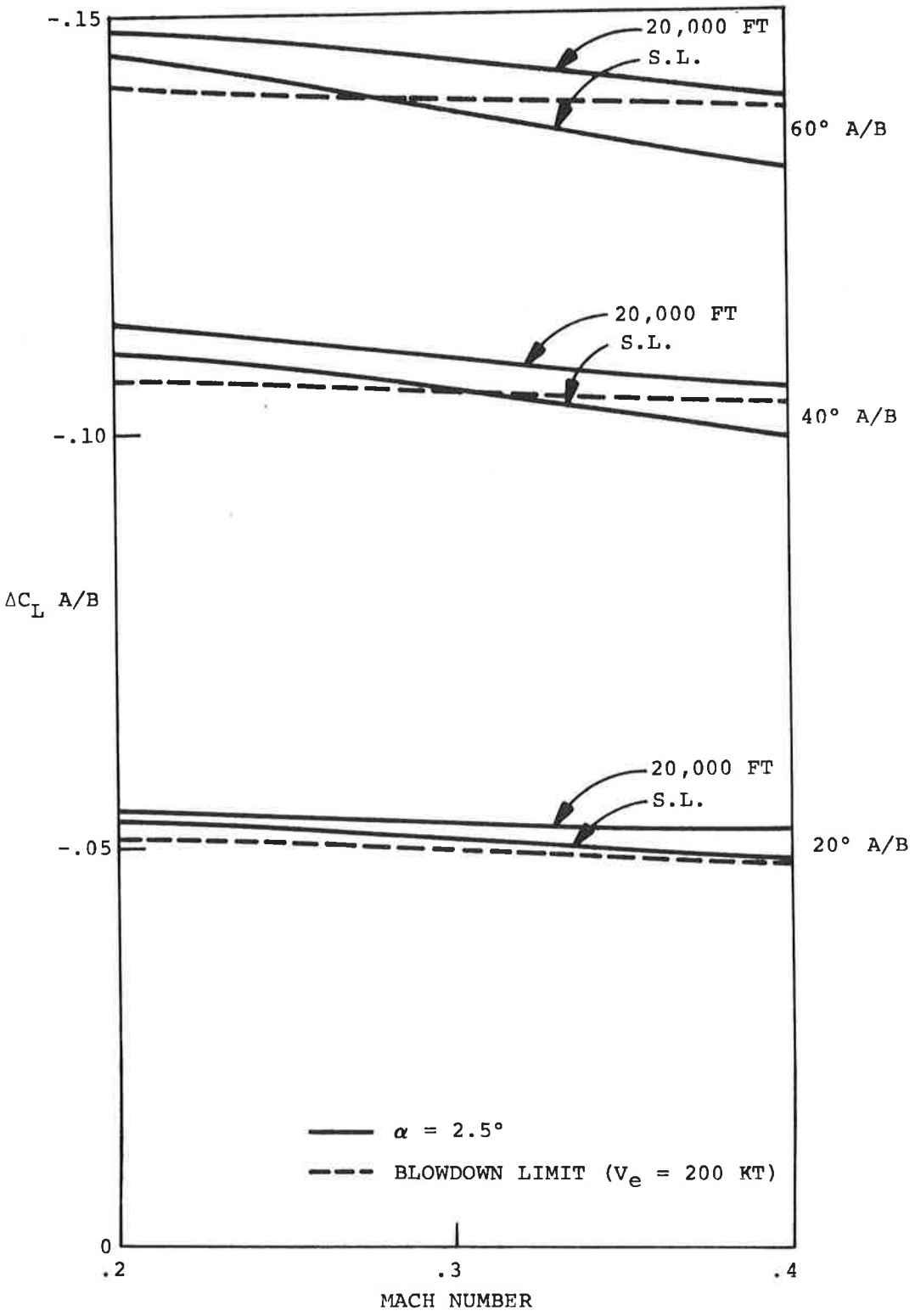

Figure 7. Effect of Inboard Airbrake Operation-Flaps-Up.

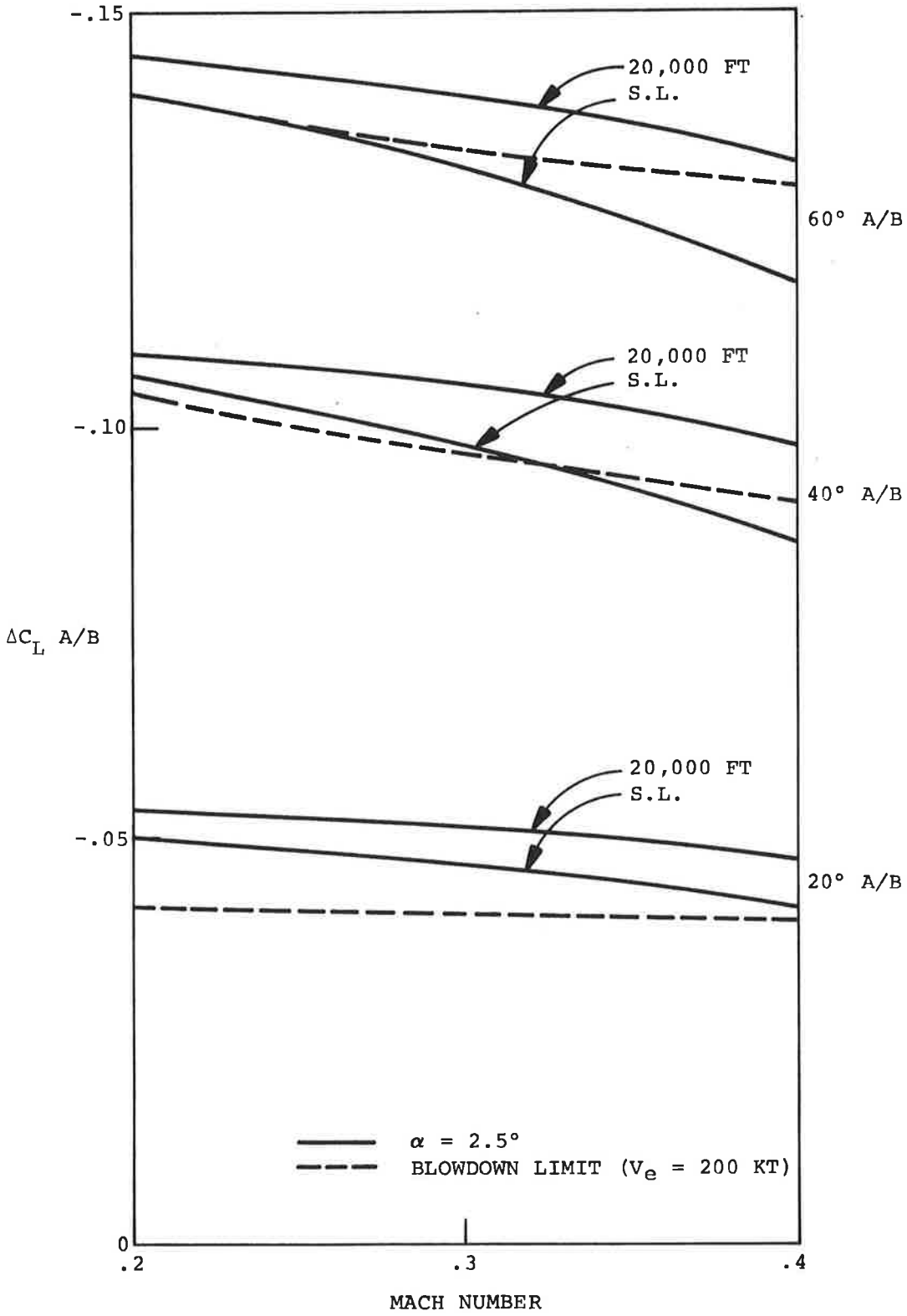

Figure 8. Effect of Outboard Airbrake Operation-Flaps-Up.

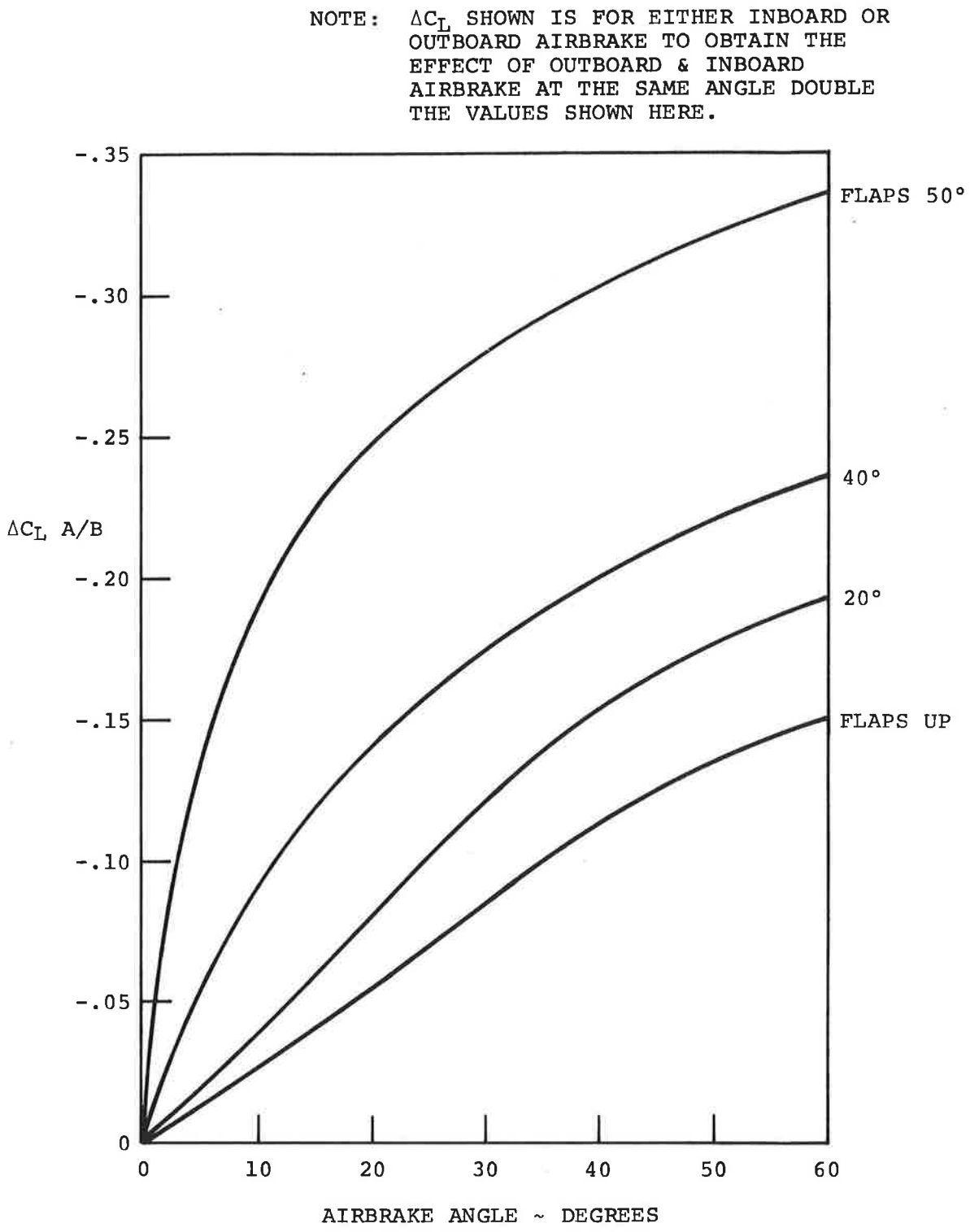

Figure 9. Effect of Airbrakes-Flaps-Down.

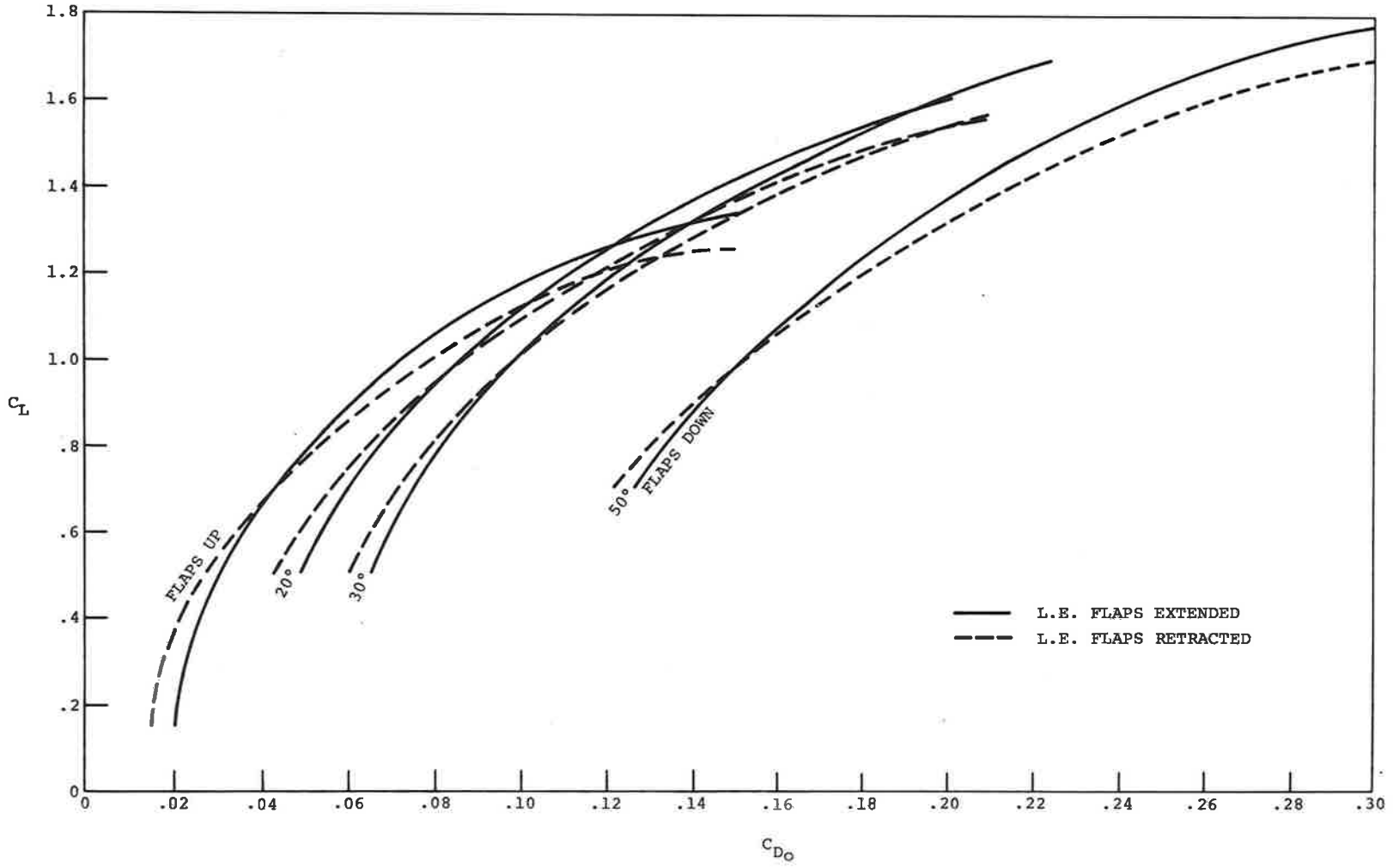

Figure 10. Basic Drag Coefficient.

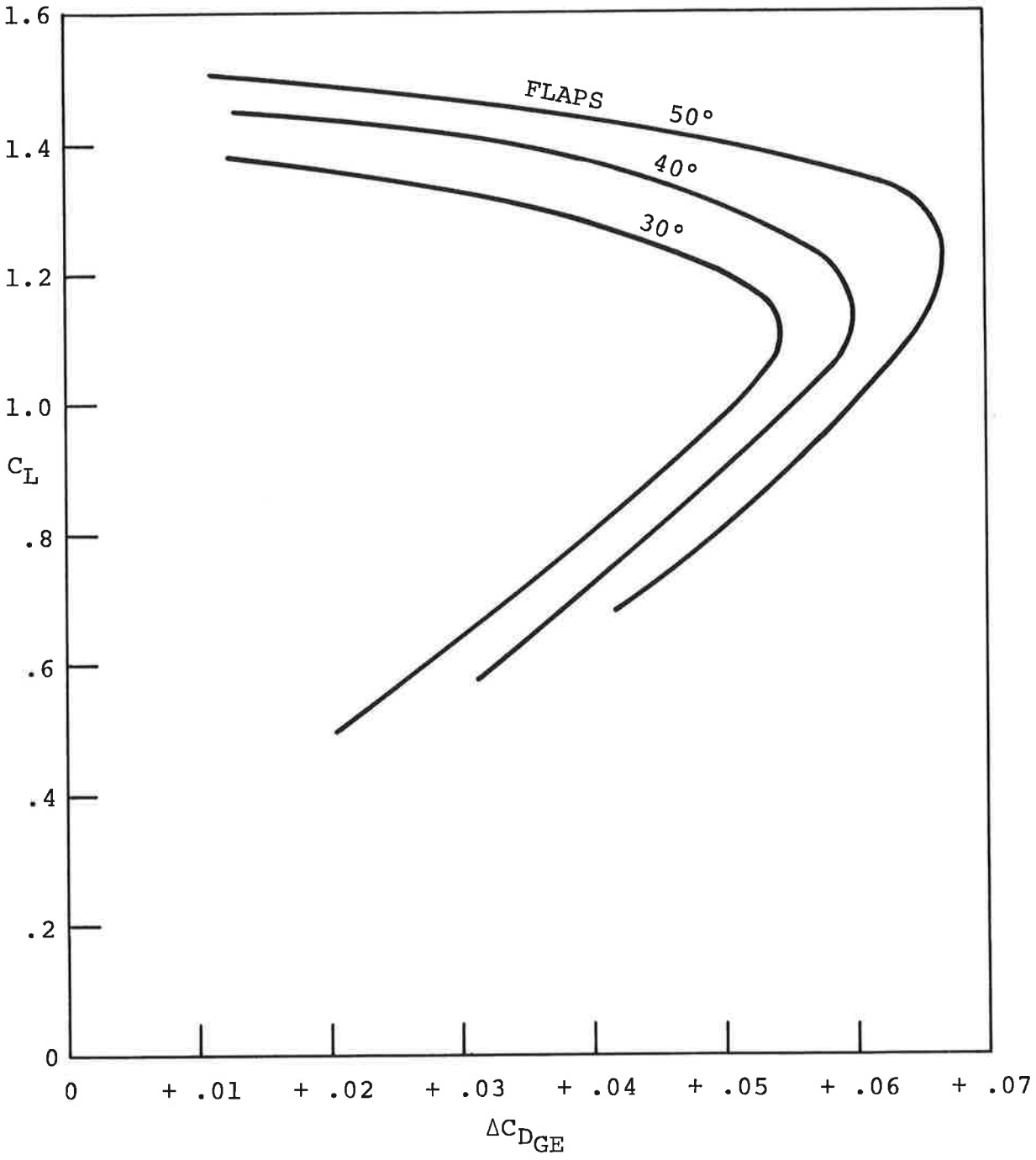

Figure 11. Ground Effect on Drag Characteristics.

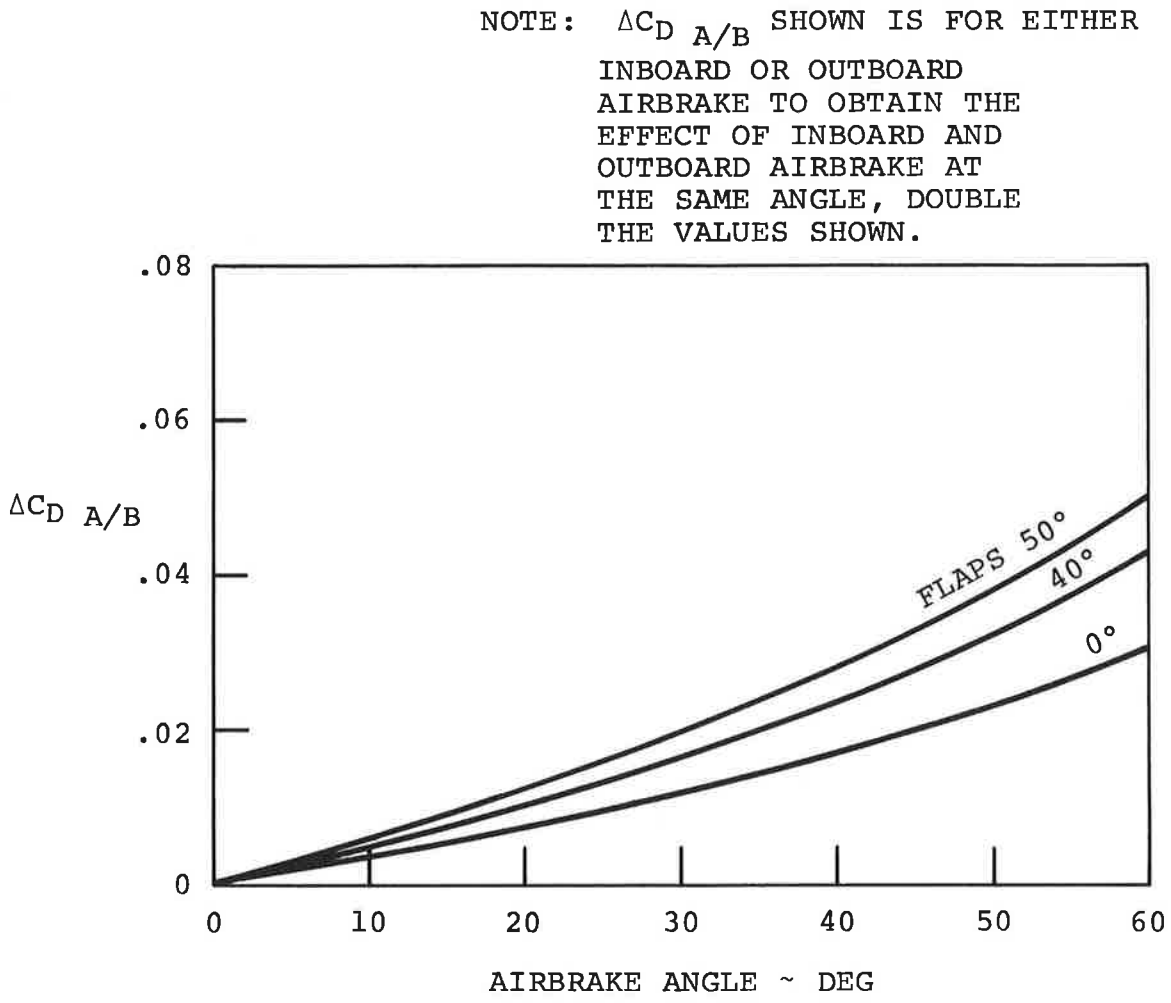

Figure 12. Effect of Airbrakes on Drag Characteristics-Flaps-Down.

ΔC_{D_G} = Increment of drag coefficient due to landing gear. ΔC_{D_G} = .0221 for the flight regime of interest.

ΔC_{D_β} = Increment of drag coefficient due to sideslip. ΔC_{D_β} is shown in Table 14 as a function of sideslip angle and rudder deflection

PITCHING MOMENT CHARACTERISTICS, M_s

$$M_s = \tfrac{1}{2} \rho V^2 S \bar{c} \, C_m$$

where

$$C_m = C_{m_O} + \Delta C_{m_O} + \Delta C_{m_\alpha}\alpha + C_{m_{S_{FRL}}}(S_{FRL} + 4) + \Delta C_{m_{\delta_e}} + \Delta C_{m_{(a/\bar{c})}} x\left(\frac{a}{\bar{c}}\right) + \Delta C_{m_{\alpha_{(a/\bar{c})}}} x \left(\frac{a}{\bar{c}}\right)\alpha + \Delta C_{m_{GE}} + \Delta C_{m_{A/B}} + \Delta C_{m_G} + \frac{\bar{c}}{2V} C_{m_{\dot{\alpha}}} + \frac{\bar{c}}{2V} C_{m_{\dot{\theta}}} + \Delta C_{m_T}$$

C_{m_O} = Basic coefficient of moment about quarter chord position for rigid wing airplane. C_{m_O} is plotted in Figure 13 as a function of α, δ_F and L.E. flap position.

ΔC_{m_O} = Deviation from basic moment coefficient due to Mach number and altitude. ΔC_{m_O} can be approximated by

$$.015 \left(\frac{20{,}000-h}{20{,}000}\right) M$$

over the flight regime of interest where h is the altitude in feet and M is the Mach number.

$\Delta C_{m_\alpha}\alpha$ = Deviation from basic moment coefficient data due to variation in slope of moment versus α curve. ΔC_{m_α} can be approximated by

$$(.022M-.0018)- \frac{h}{20{,}000} (.01M-.0005)$$

over the flight regime of interest where h is the altitude in feet and M is the Mach number.

$C_{m_{S_{FRL}}}(S_{FRL} + 4)$ = Variation in moment coefficient due to change of stabilizer angle from $S_{FRL} = -4°$. $C_{m_{S_{FRL}}}$ can be approximated by .01M-.3065 over the flight regime of interest where M is the Mach number.

TABLE 14. EFFECT OF SIDESLIP ANGLE ON DRAG CHARACTERISTICS

β (DEG)	ΔC_{D_β} (δ_r=0)	ΔC_{D_β} (δ_r=15°)	ΔC_{D_β} (δ_r=25°)
-20	.076	.09	.099
-15	.041	.054	.0625
-10	.017	.027	.036
-5	.004	.011	.02
0	0	.004	.0125
5	.004	.008	.014
10	.018	.02	.023
15	.042	.04	.039
20	.076	.068	.062

TABLE 15. EFFECT OF $C_{m_{CG}}$ CHANGE WITH α WHEN CENTER OF GRAVITY SHIFTS, ON MOMENT COEFFICIENT

Mach Number	$\Delta C_{m_\alpha}(a/\bar{c})$		
	h=0 ft	h = 10,000 ft	h = 20,000 ft
.15	-.0862	-.0877	-.0885
.2	-.085	-.0866	-.088
.3	-.0805	-.0835	-.086
.4	-.0756	-.08	-.084

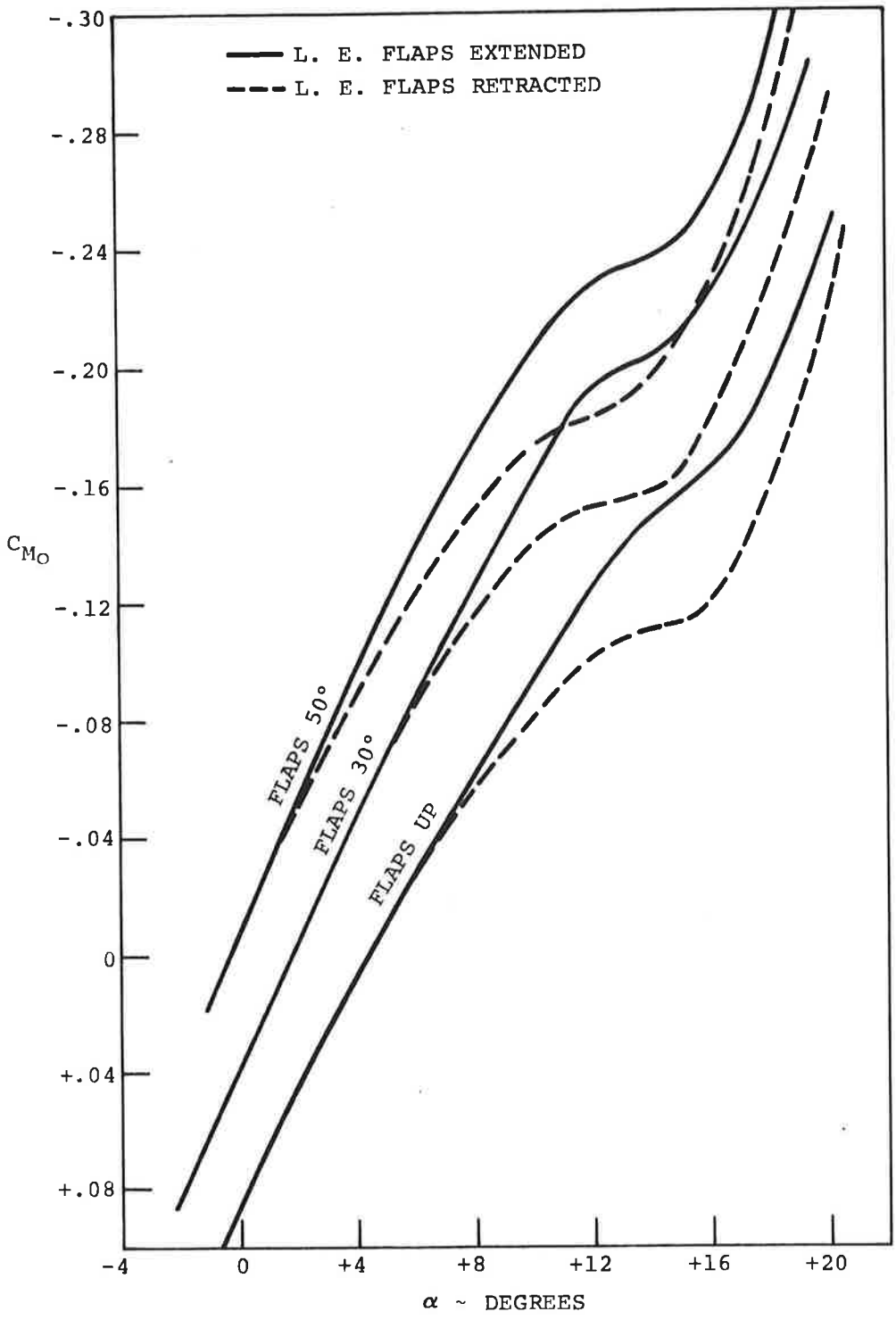

Figure 13. Basic Pitching Moment Coefficient.

$\Delta C_{m_{\delta_e}}$ = Increment of moment coefficient due to elevator. $\Delta C_{m_{\delta_e}}$ includes static aeroelastic effects and over the flight regime of interest is given by $[-.01352\,\delta_e + .000003167\,\delta_e^3]\,[.98-.000667(V_e-100)]$ where δ_e is the elevator angle in degrees and V_e is the equivalent airspeed in knots. The elevator deflection for this representation is restricted to $-23.5° < \delta_e < 15°$

$\Delta C_{m_{(a/\bar{c})}} x\left(\frac{a}{\bar{c}}\right)$ = Variation in moment coefficient due to center of gravity shift. Over the flight regime of interest $\Delta C_{m_{(a/\bar{c})}}$ is given by

$$\left\{(.068M-.13)-\frac{h}{20{,}000}\,(.048M-.007)\right\}\left\{1+.156\,\delta_F-.00104\,\delta_F^2\right\}$$

where h is the altitude in feet, M is the Mach number and δ_F is the flap angle in degrees.

$\Delta C_{m_{\alpha_{(a/\bar{c}}}} x\left(\frac{a}{\bar{c}}\right)\alpha$ = Change in moment coefficient due to variation of $C_{m_{cg}}$ change with α when center of gravity shifts. $\Delta C_{m_{\alpha(a/\bar{c})}}$ is given in Table 15 as a function of Mach number and altitude

$\Delta C_{m_{GE}}$ = Increment of moment coefficient due to ground effect $\Delta C_{m_{GE}}$ for the flaps down condition is given by

$$\Delta C_{m_{GE}} = K(.0208-.14606C_L+.04476C_L^2)$$

where K is the ground effect factor described in Figure 6.

$\Delta C_{m_{A/B}}$ = Increment of moment coefficient due to airbrakes. The effect of inboard and outboard airbrake operation for the flaps up condition is given in Figures 14 and 15 respectively as a function of Mach number, altitude and airbrake angle. The effect of the airbrakes for the flaps down condition is given in Figure 16 as a function of airbrake angle. Linear interpolation may be assumed between the flaps up and the flaps down conditions.

ΔC_{m_G} = Increment of pitching coefficient due to gear. Over the flight regime of interest ΔC_{m_G} is given by

$$\Delta C_{m_G} = .014-.0003\,\delta_F$$

where δ_F is the flap angle in degrees.

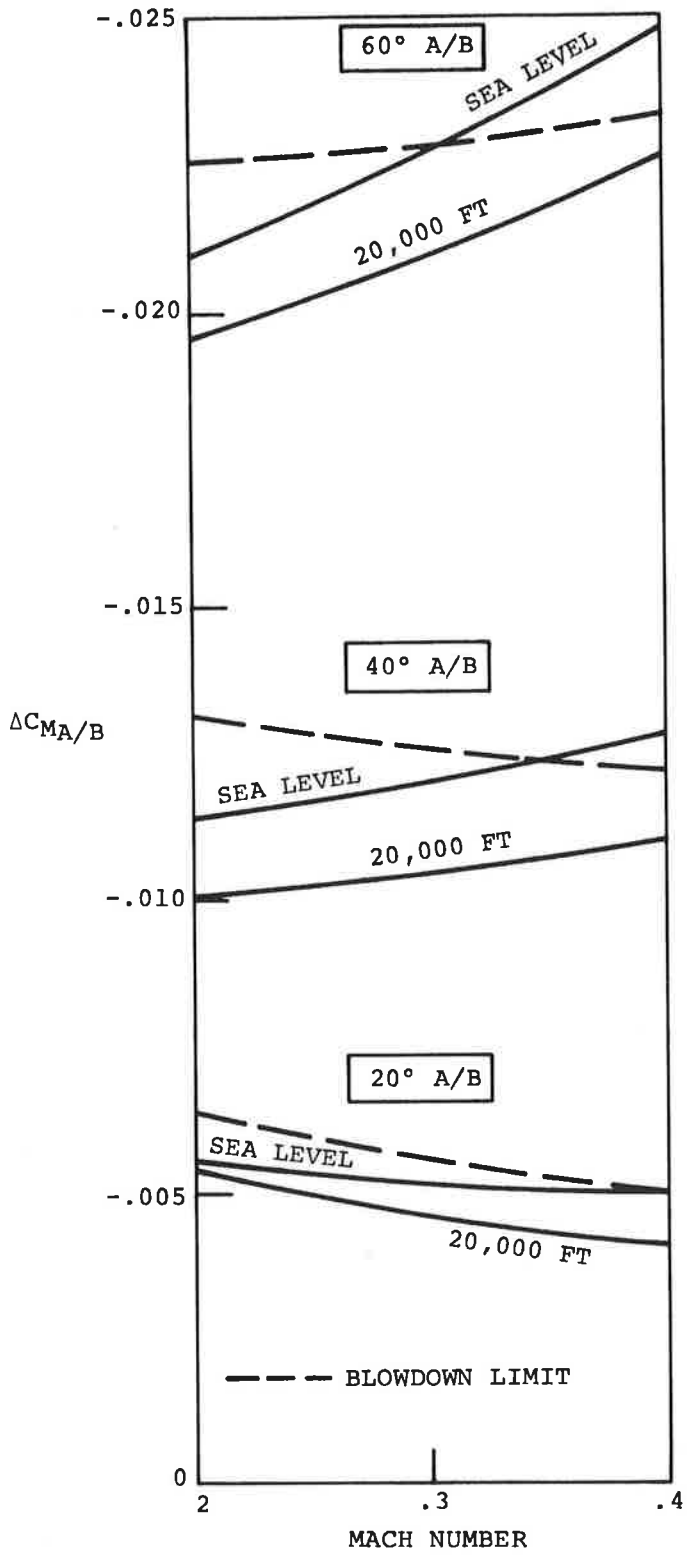

Figure 14. Effect of Inboard Airbrake Operation-Flaps-Up.

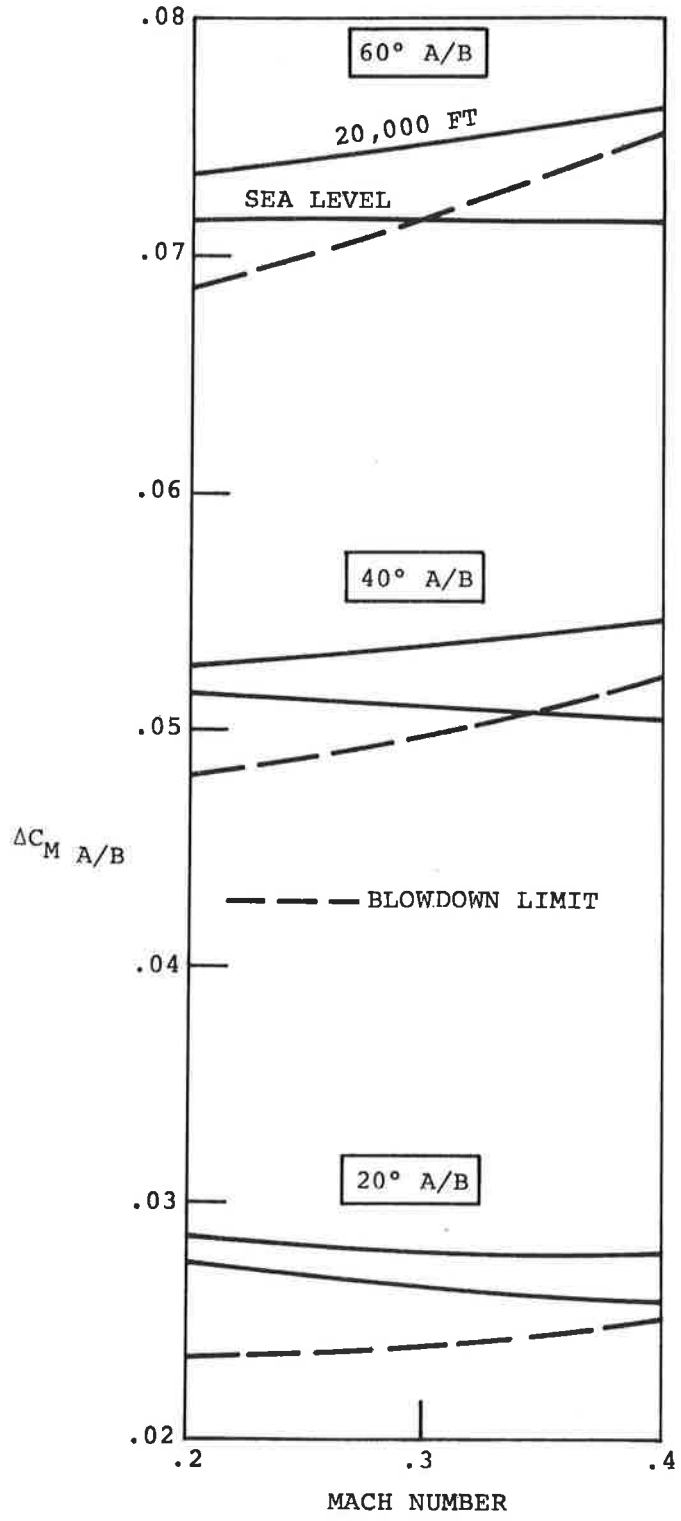

Figure 15. Effect of Outboard Airbrake Operation-Flaps-Up.

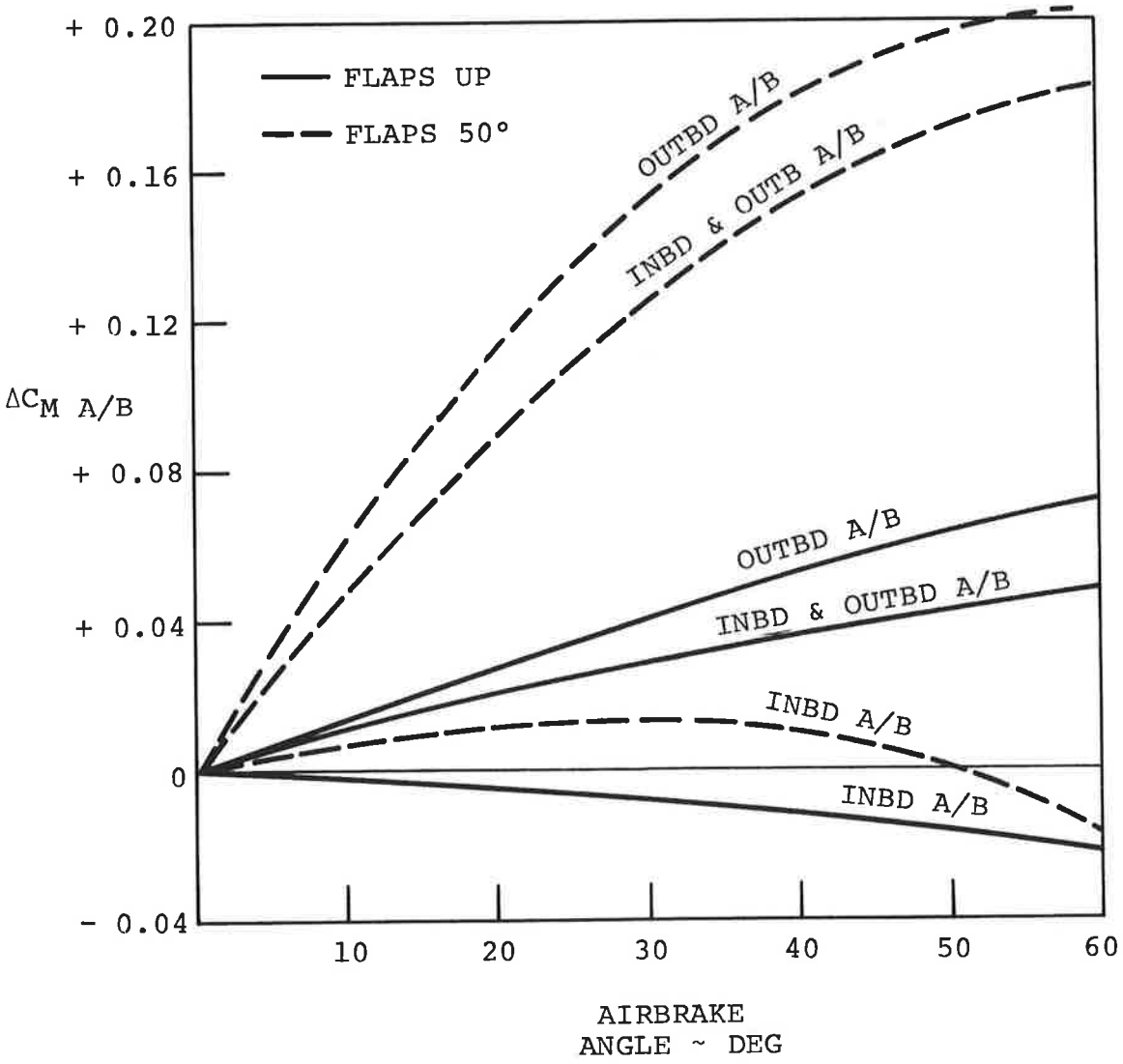

Figure 16. Effect of Airbrakes-Flaps-Down.

$\frac{\bar{c}}{2V}C_{m_{\dot{\alpha}}}\dot{\alpha}$ = Increment of moment coefficient due to $\dot{\alpha}$. Over the flight regime of interest

$$C_{m_{\dot{\alpha}}} = -.096 + .04\left[\frac{20{,}000-h}{20{,}000}\right] M$$

where M is the Mach number and h is the altitude in feet.

$\frac{\bar{c}}{2V}C_{m_{\dot{\theta}}}\dot{\theta}$ = Increment of moment coefficient due to $\dot{\theta}$. Over the flight regime of interest

$$C_{m_{\dot{\theta}}} = -.25 + \left[.04 + \left(\frac{20{,}000-h}{20{,}000}\right)(.064)\right] M$$

where M is the Mach number and h is the altitude in feet.

ΔC_{m_T} = Increment in pitching moment due to engine thrust. ΔC_{m_T} is given by

$$\Delta C_{m_T} = .0321\left(\frac{T_1 + T_4}{V_e^2}\right) + .0462\left(\frac{T_2 + T_3}{V_e^2}\right)$$

where $T_1 + T_4$ = thrust of outboard engines

$T_2 + T_3$ = thrust of inboard engines

V_e = equivalent airspeed in knots

ROLLING MOMENT CHARACTERISTICS, L_s

$$L_s = \tfrac{1}{2}\rho V^2 S b C_\ell$$

where $$C_\ell = C_{\ell_\beta}\beta + \frac{b}{2V}C_{\ell_{\dot{\phi}}}\dot{\phi} + \frac{b}{2V}C_{\ell_{\dot{\psi}}}\dot{\psi} + \Delta C_{\ell_s} + \Delta C_{\ell_{\delta_a}} + C_{\ell_{\delta_r}}\delta_r$$

$C_{\ell_\beta}\beta$ = Contribution to rolling coefficient due to sideslip. C_{ℓ_β} is plotted in Figure 17 as a function of C_L and δ_F.

$\frac{b}{2V}C_{\ell_{\dot{\phi}}}\dot{\phi}$ = Contribution to rolling coefficient due to $\dot{\phi}$. This represents the roll damping characteristics. Over the flight regime of interest $C_{\ell_{\dot{\phi}}}$ is given by

$$C_{\ell_{\dot{\phi}}} = (.000372\ V_e - .436)/57.3 \text{ per degree}$$

where V_e is the equivalent airspeed in knots.

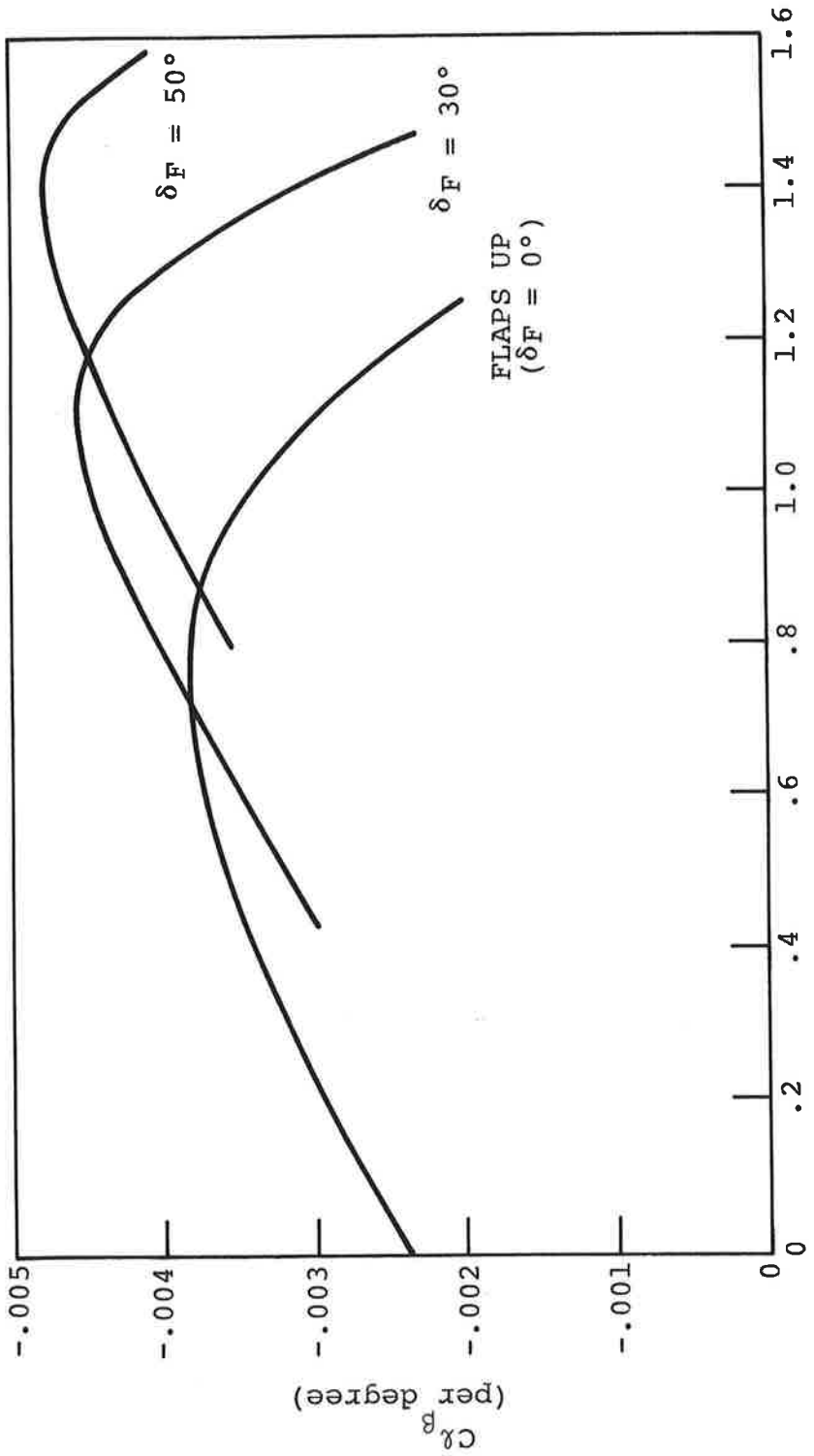

Figure 17. Roll Due to Sideslip.

$\frac{b}{2V} C_{\ell_{\dot{\psi}}} \dot{\psi}$ = Contribution to rolling coefficient due to $\dot{\psi}$. Over the flight regime of interest $C_{\ell_{\dot{\psi}}}$ is given by

$$C_{\ell_{\dot{\psi}}} = (.054 + .230 C_L + .0005 \delta_F)/57.3 \text{ per degree}$$

where C_L is the lift coefficient and δ_F is the flap angle in degrees.

ΔC_{ℓ_S} = Increment of rolling moment coefficient due to spoiler deflection. $\Delta C_{\ell_S} = (R_e/R_r)\overline{\Delta C}_{\ell_S}$. $\overline{\Delta C}_{\ell_S}$ is described in Figures 18, 19 and 20 for the flaps up, flaps = 30° and flaps = 50° conditions respectively. Note that the data for the flaps up condition is presented for $\alpha = 1.6°$. It is unknown from the information available whether or not different α's will have significant effects on the increment of rolling coefficient due to spoiler deflection. The aeroelastic effect R_e/R_r is plotted in Figure 21 as a function of altitude in feet and equivalent airspeed in knots.

$\Delta C_{\ell_{\delta_a}}$ = Increment of rolling moment coefficient due to aileron deflection $\Delta C_{\ell_{\delta_a}}$ is given by

$$\Delta C_{\ell_{\delta_a}} = \left(\frac{R_e}{R_r}\right)_i C_{\ell_{\delta_{a_i}}} \delta_{a_i} + \left(\frac{R_e}{R_r}\right)_o C_{\ell_{\delta_{a_o}}} \delta_{a_o}$$

where the subscript "i" refers to the inboard aileron and the subscript "o" refers to the outboard airleron. The outboard airleron is slaved to the inboard aileron and flap condition according to the following relationships.

$$\delta_{a_o}/\delta_{a_i} = .05 \delta_F, \quad \delta_F \leq 20°$$

$$\delta_{a_o}/\delta_{a_i} = 1 + .011(\delta_F - 20), \quad 20° < \delta_F \leq 50°$$

The aeroelastic effect R_e/R_r, and the non-dimensional roll stability derivative due to aileron deflection $C_{\ell_{\delta_a}}$, are described below over the flight regime of interest.

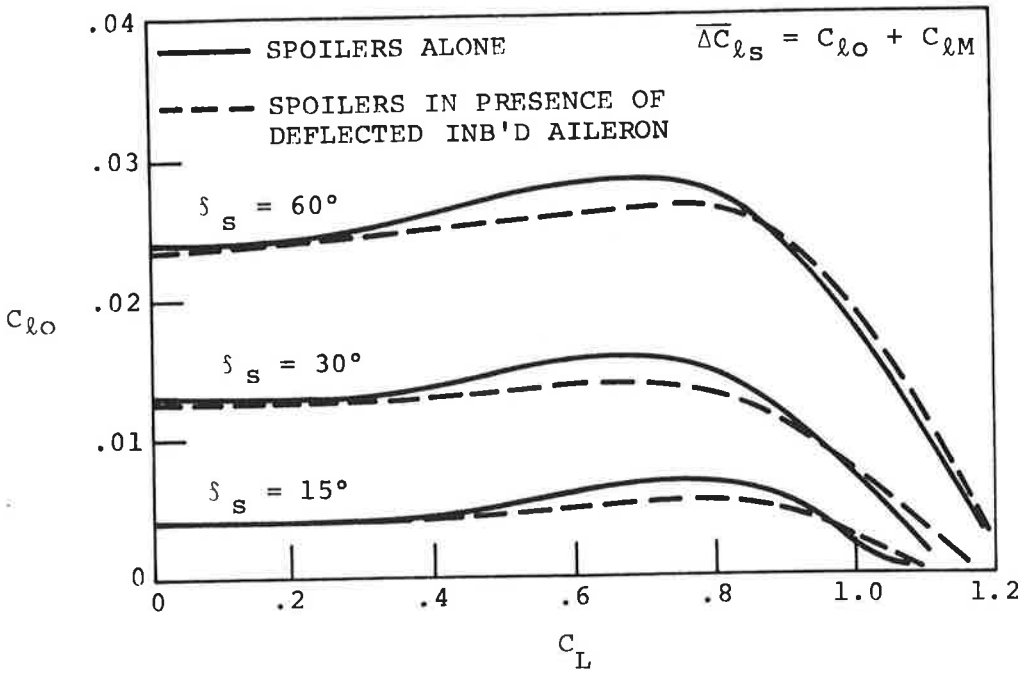

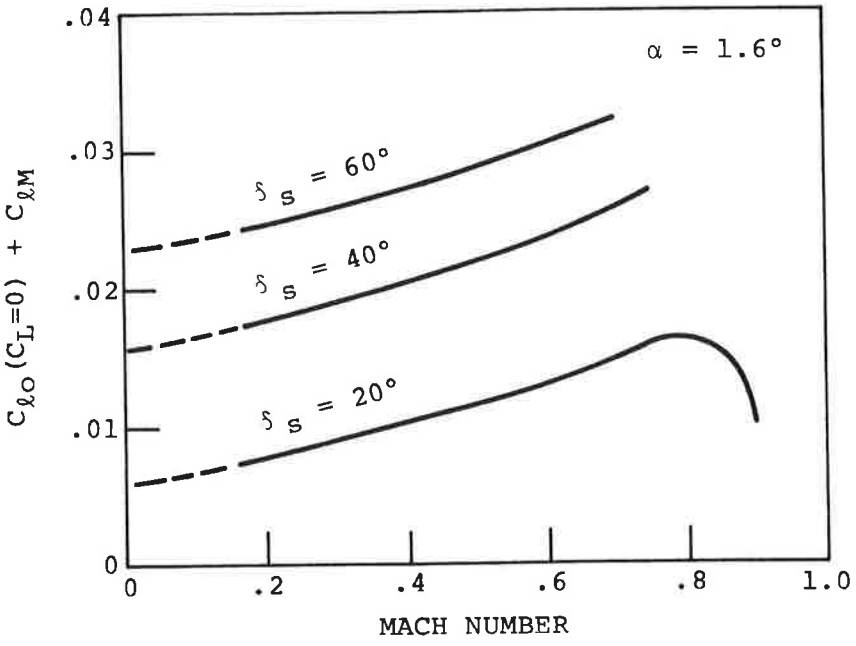

Figure 18. Spoiler Roll Effectiveness-Flaps Up.

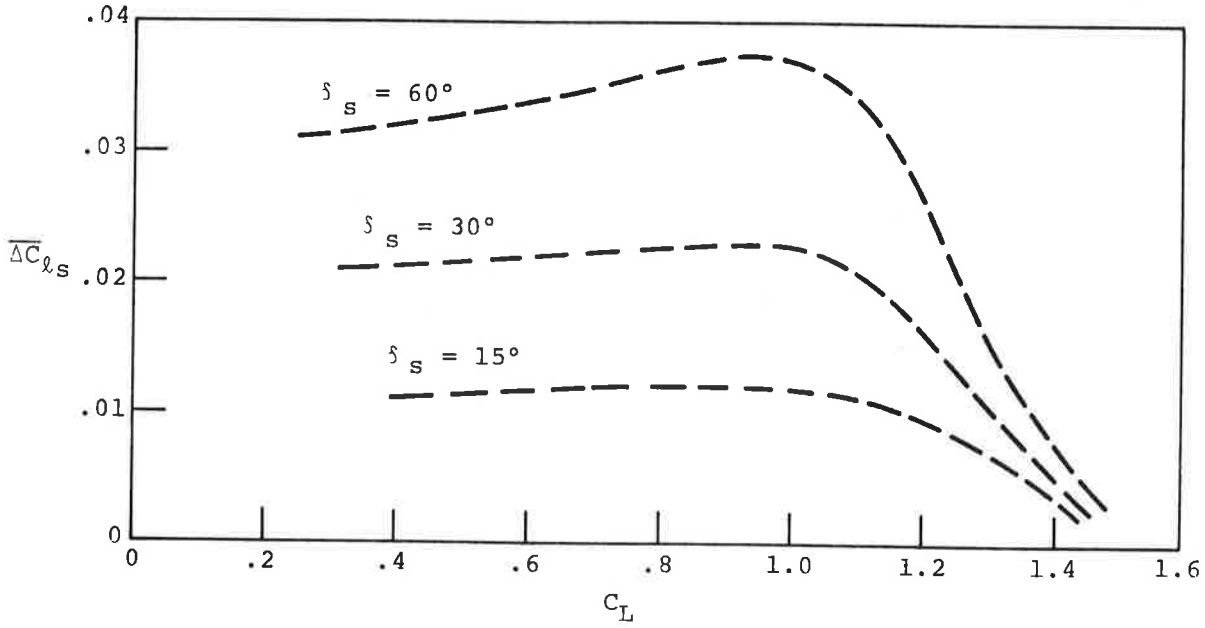

Figure 19. Spoiler Roll Effectiveness-Flaps 30°.

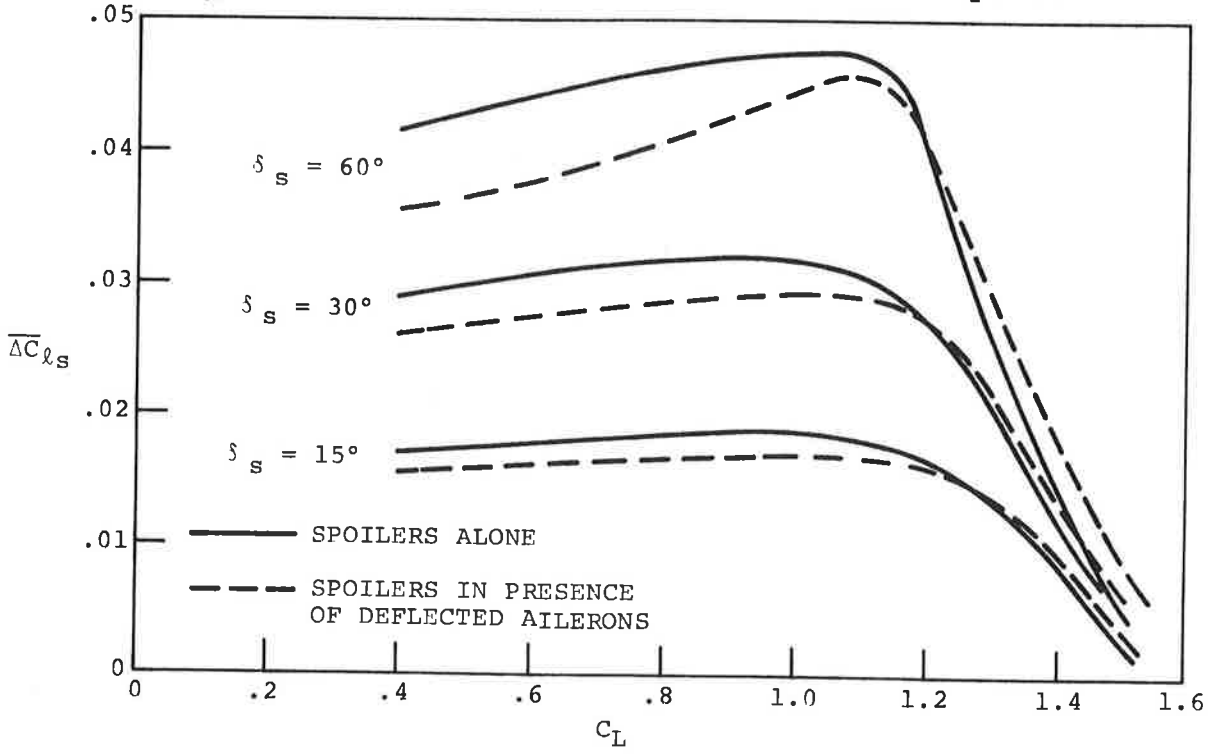

Figure 20. Spoiler Roll Effectiveness-Flaps 50°.

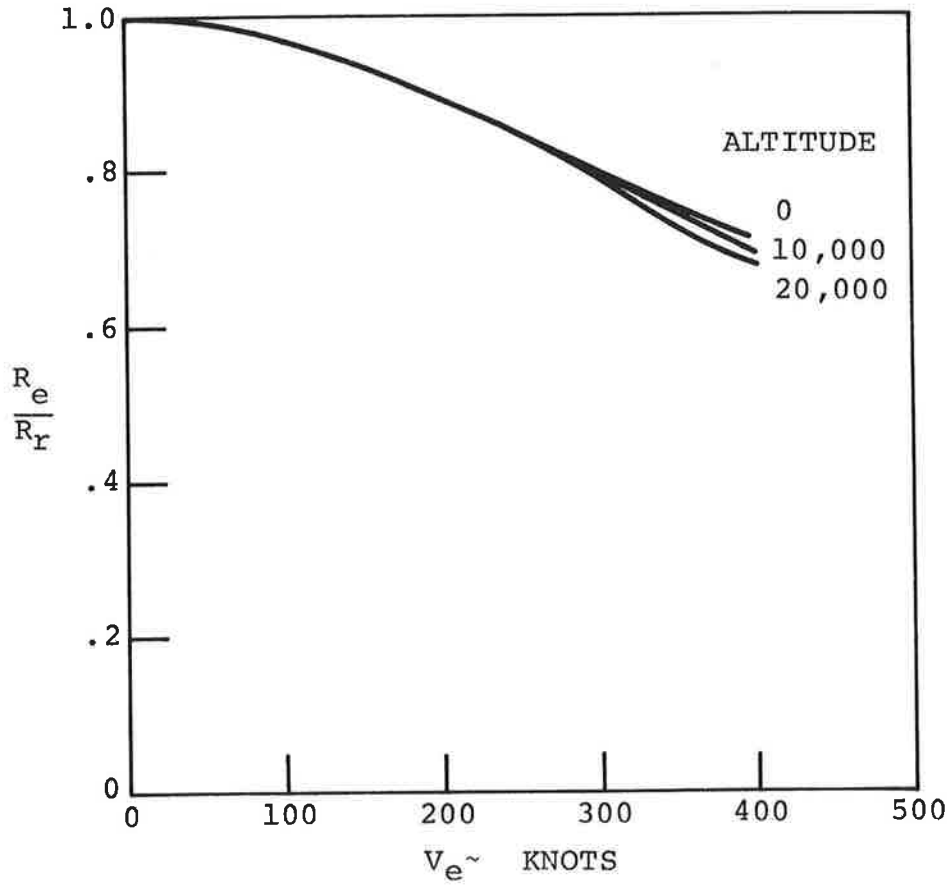

Figure 21. Spoiler Aeroelastic Effect.

$$C_{\ell_{\delta_{a_i}}} = \begin{cases} [.00058 + .0000108\,\delta_F]\,[1-.1087C_L], \\ \quad 0 \le C_L \le .92 \\ [.00058 + .0000108\,\delta_F]\,[.9-2.5 \\ \quad (C_L-.92)], \quad .92 < C_L \le 1.2 \end{cases}$$

$$(R_e/R_r)_i = .91-.00185V_e$$

$$C_{\ell_{\delta_{a_o}}} = \begin{cases} [.00145], \quad 0 \le C_L \le 1.05 \\ [.00145]\,[1-.878(C_L-1.05)], \\ \quad 1.05 < C_L \le 1.75 \end{cases}$$

$$(R_e/R_r)_o = .865-.00315V_e$$

δ_F is the flap angle in degrees, V_e is the equivalent airspeed in knots, and δ_a is the aileron angle in degrees.

$C_{\ell_{\delta_r}}\delta_r$ = contribution to rolling coefficient due to rudder deflection. Over the flight regime of interest, $C_{\ell_{\delta_r}}$ is given by

$$C_{\ell_{\delta_r}} = .00065 + .000006\,\delta_F - .0004C_L, \text{ per degree } (\delta_r \le 11°)$$

where δ_F is the flap angle in degrees.

SIDE FORCE CHARACTERISTICS, Y_s

$$Y_s = \tfrac{1}{2}\rho V^2 S C_y$$

where

$$C_y = C_{y_\beta}\beta + \frac{b}{2V}C_{y_{\dot\phi}}\dot\phi + \frac{b}{2V}C_{y_{\dot\psi}}\dot\psi + C_{y_{\delta_w}}\delta_w + \Delta C_{y_{\delta_a}} + C_{y_{\delta_r}}\delta_r$$

$C_{y_\beta}\beta$ = contribution to side force coefficient due to sideslip. C_{y_β} is plotted in Figure 22 as a function of C_L and δ_F.

$\frac{b}{2V}C_{y_{\dot\phi}}\dot\phi$ = contribution to side force coefficient due to $\dot\phi$. $C_{y_{\dot\phi}}$ is described in Figure 23 as a function of C_L, δ_F, altitude, and Mach number.

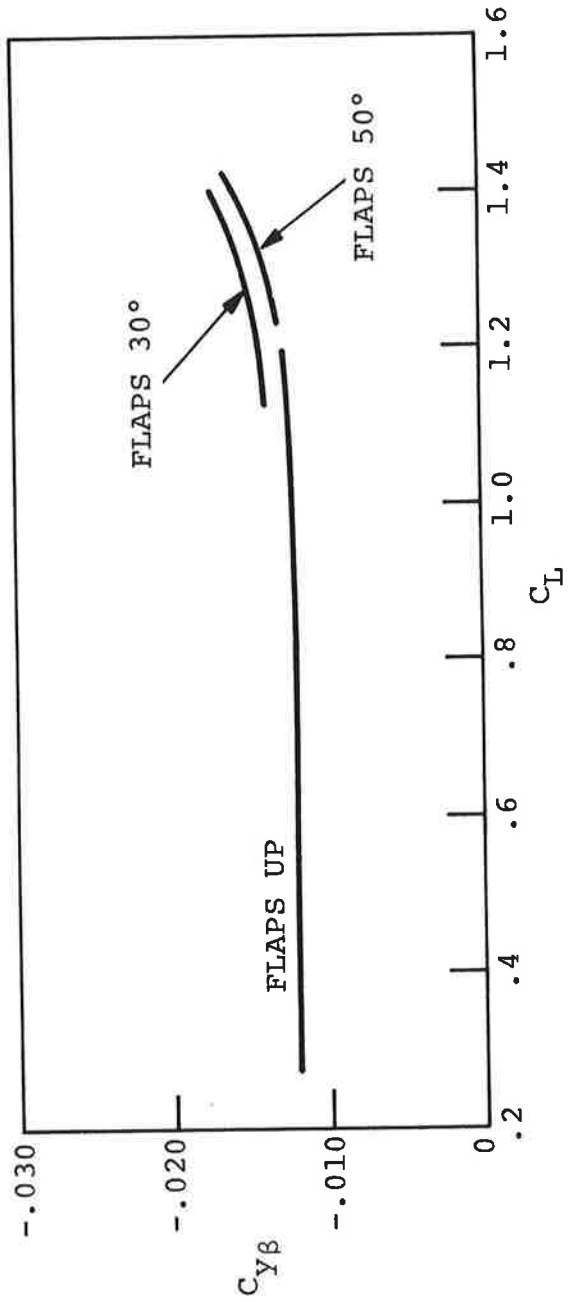

Figure 22. Side Force Effect Due to Sideslip.

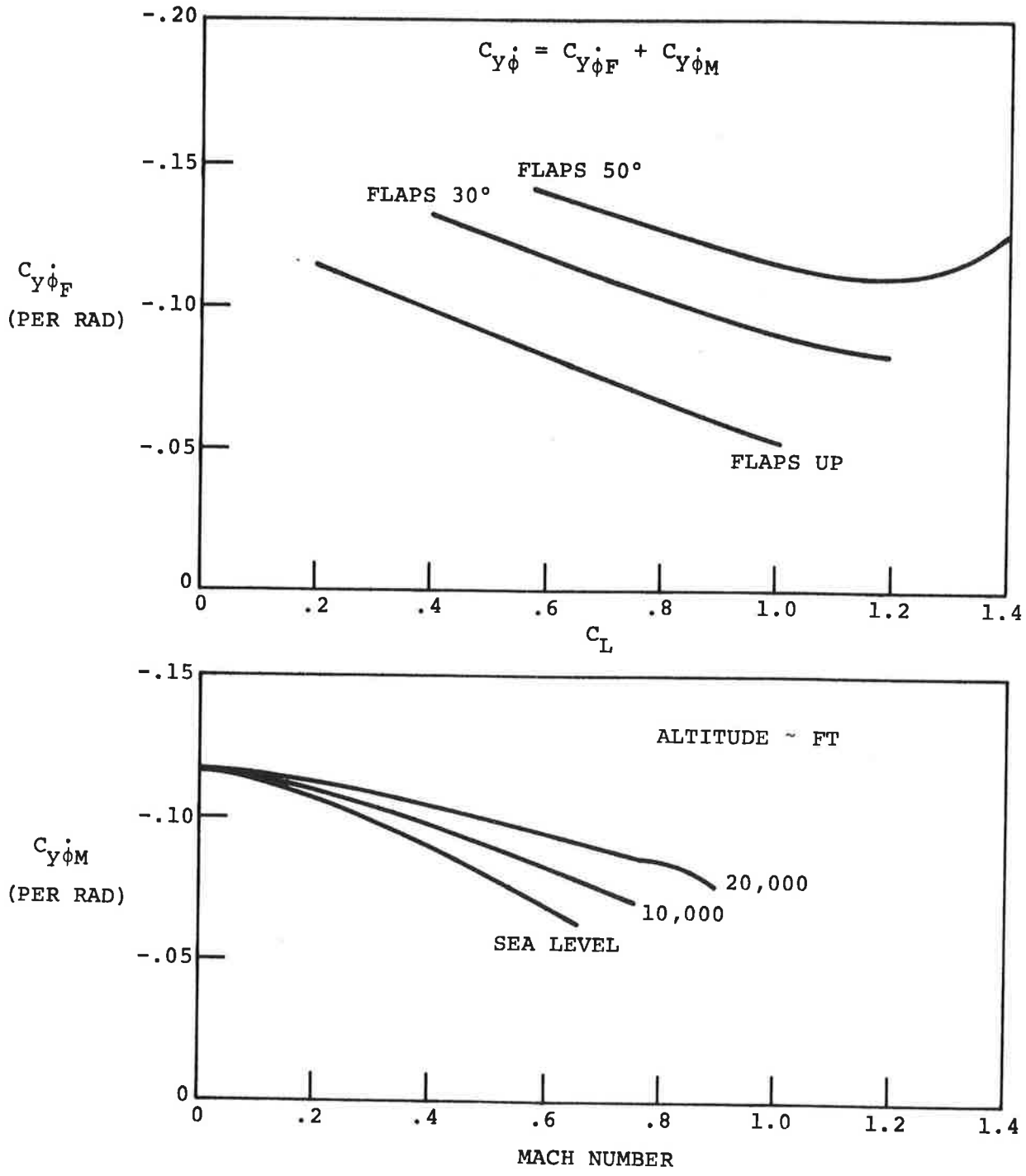

Figure 23. Side Force Effect Due to $\dot{\phi}$.

$\frac{b}{2V}C_{y_{\dot{\psi}}}\dot{\psi}$ = contribution to side force coefficient due to $\dot{\psi}$. $C_{y_{\dot{\psi}}}$ is plotted in Figure 24 as a function of C_L.

$C_{y_{\delta_w}}\delta_w$ = increment of side force coefficient due to lateral control. $C_{y_{\delta_w}}$ is given in Figure 25 as a function of C_L and flap angle.

$\Delta C_{y_{\delta_a}}$ = increment of side force coefficient due to aileron deflection. $\Delta C_{y_{\delta_a}}$ is negligible over the flight regime of interest.

$C_{y_{\delta_r}}\delta_r$ = increment of side force coefficient due to rudder deflection. $C_{y_{\delta_r}} = .00394$ over the flight regime of interest.

YAWING MOMENT CHARACTERISTICS, N_s

where

$$C_n = C_{n_\beta}\beta + \frac{b}{2V}C_{n_{\dot{\beta}}}\dot{\beta} + \frac{b}{2V}C_{n_{\dot{\phi}}}\dot{\phi} + \frac{b}{2V}C_{n_{\dot{\psi}}}\dot{\psi} + C_{n_{\delta_r}}\delta_r + C_{n_{\delta_w}}\delta_w$$

$C_{n_{\dot{\beta}}}\dot{\beta}$ = contribution to yawing moment coefficient due to sideslip. $C_{n_{\dot{\beta}}}$ is plotted in Figure 26 as a function of C_L, δ_F and gear position.

$\frac{b}{2V}C_{n_{\dot{\beta}}}\dot{\beta}$ = contribution to yawing moment coefficient due to $\dot{\beta}$. $C_{n_\beta} = .0003$/degree over the flight regime of interest.

$\frac{b}{2V}C_{n_{\dot{\phi}}}\dot{\phi}$ = contribution to yawing moment coefficient due to $\dot{\phi}$. $C_{n_{\dot{\phi}}}$ is plotted in Figure 27 as a function of C_L and flap angle.

$\frac{b}{2V}C_{n_{\dot{\psi}}}\dot{\psi}$ = contribution to yawing moment coefficient due to $\dot{\psi}$. $C_{n_{\dot{\psi}}}$ is plotted in Figure 28 as a function of C_L and flap angle.

$C_{n_{\delta_r}}\delta_r$ = contribution to yawing moment coefficient due to rudder deflection. $C_{n_{\delta_r}} = -.001625$/degree over the flight regime of interest.

$C_{n_{\delta_w}}\delta_w$ = increment of yawing moment coefficient due to lateral control. $C_{n_{\delta_w}}$ is given in Figure 29 as a function of C_L and flap angle.

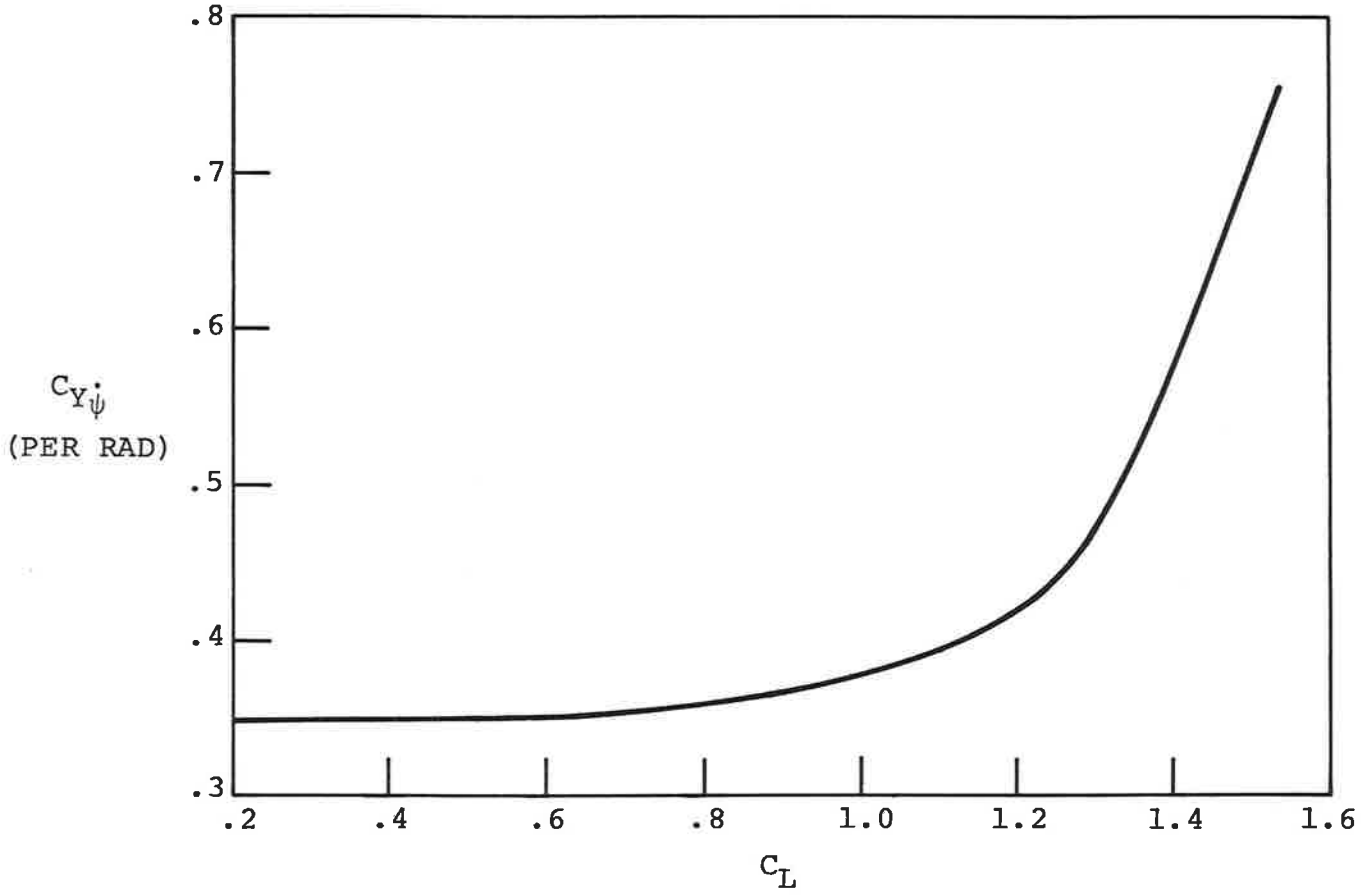

Figure 24. Side Force Effect Due to $\dot{\psi}$.

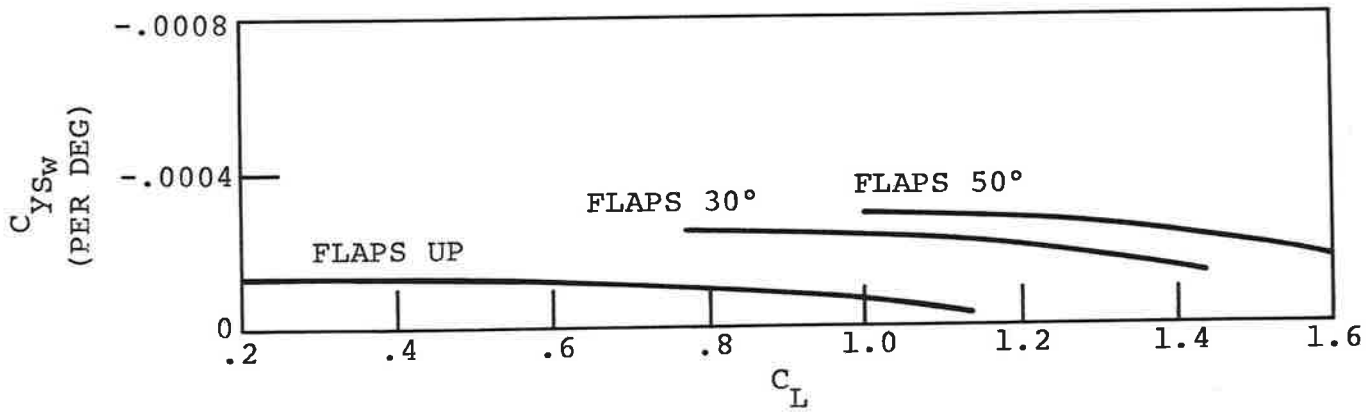

Figure 25. Side Force Effect Due to Lateral Control.

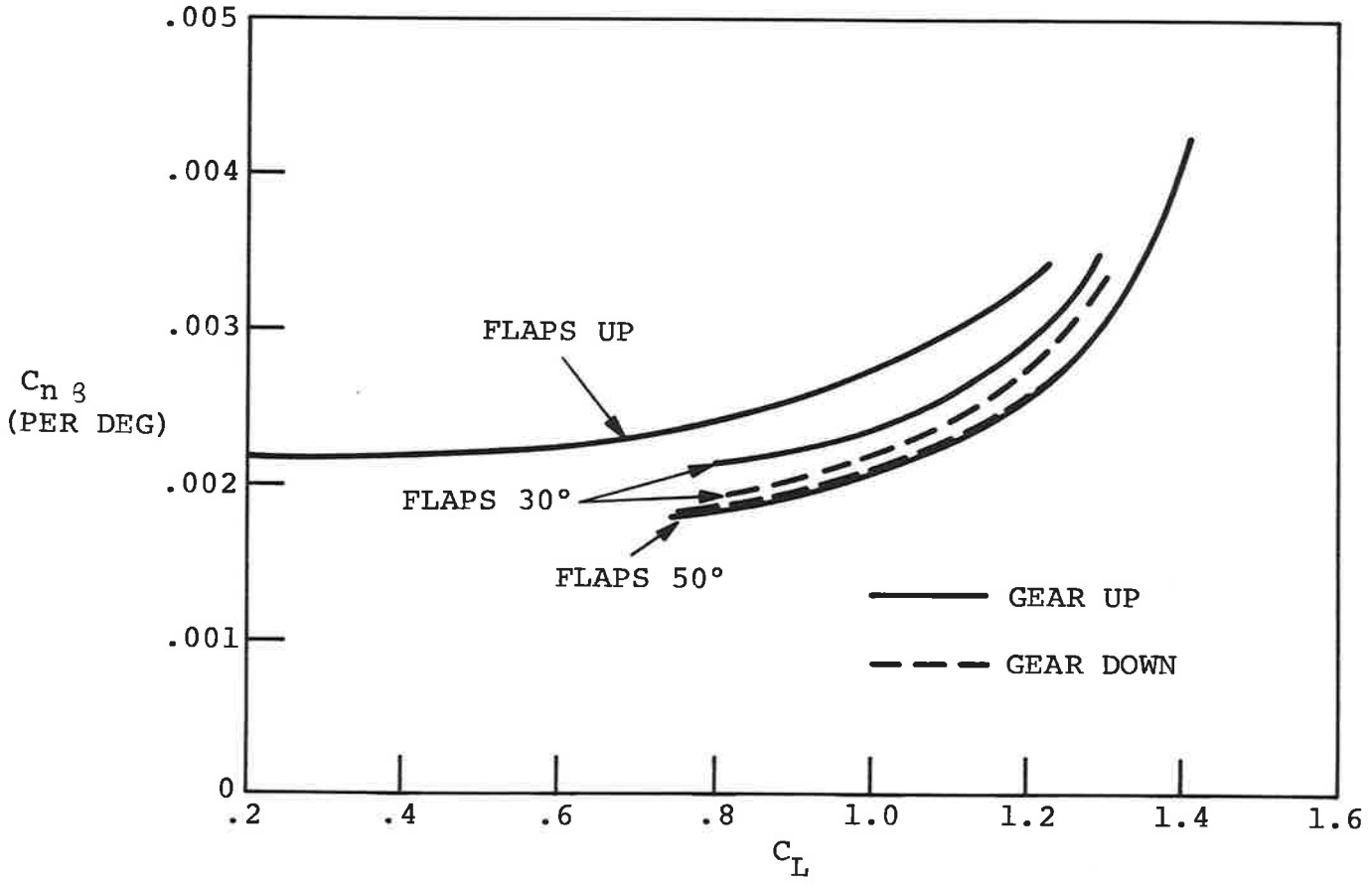

Figure 26. Yawing Moment Effect Due to Sideslip.

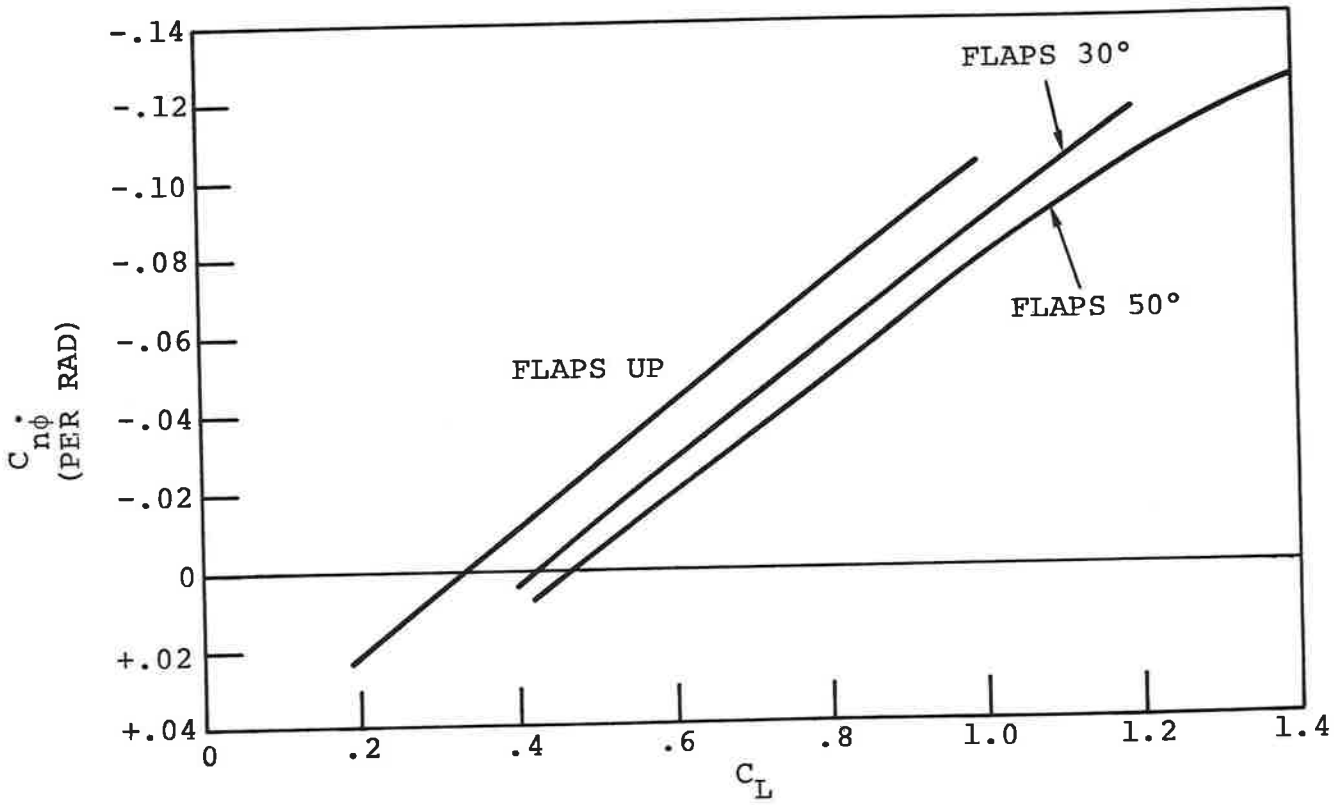

Figure 27. Yawing Moment Effect Due to $\dot{\phi}$.

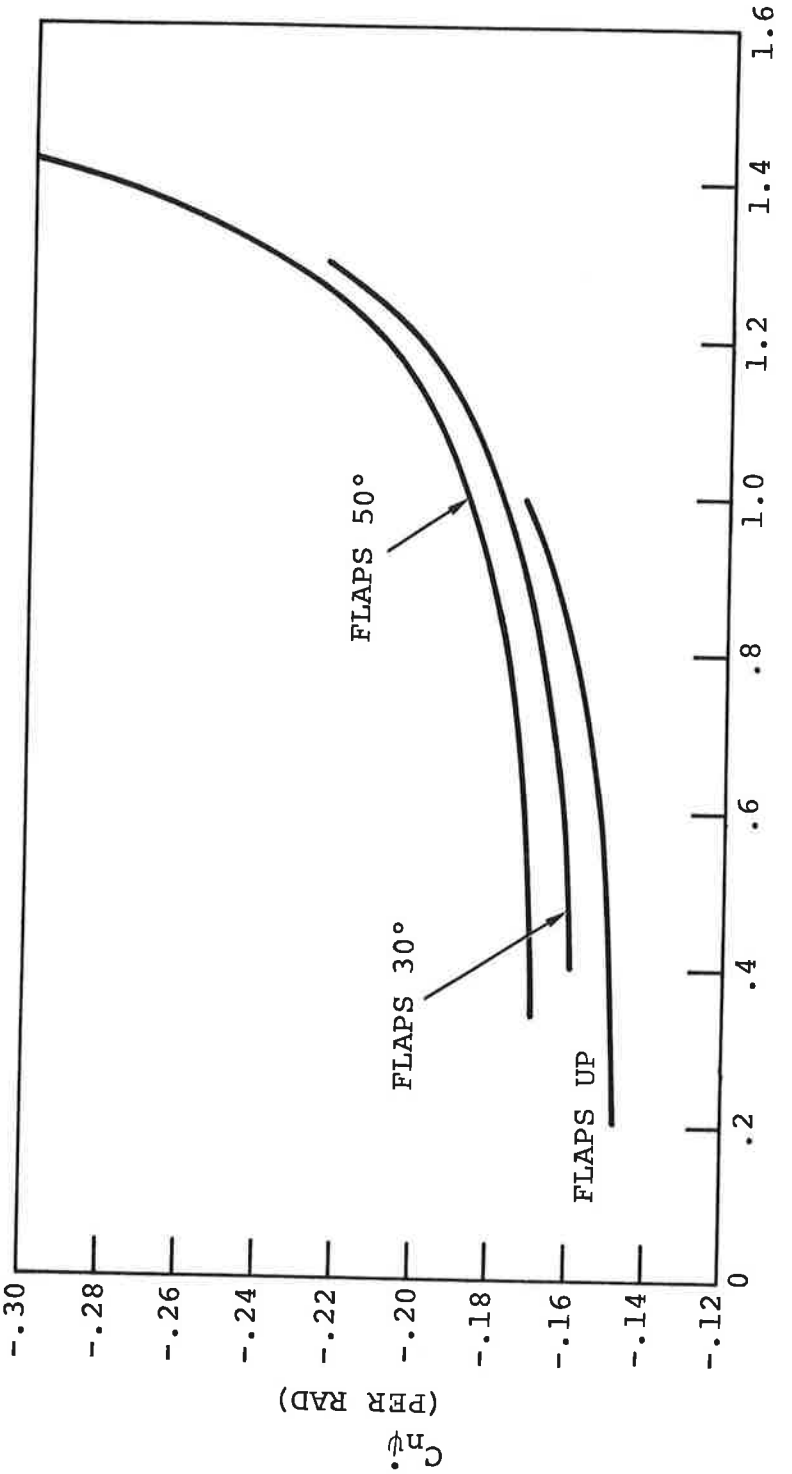

Figure 28. Yawing Moment Effect Due to $\dot{\psi}$.

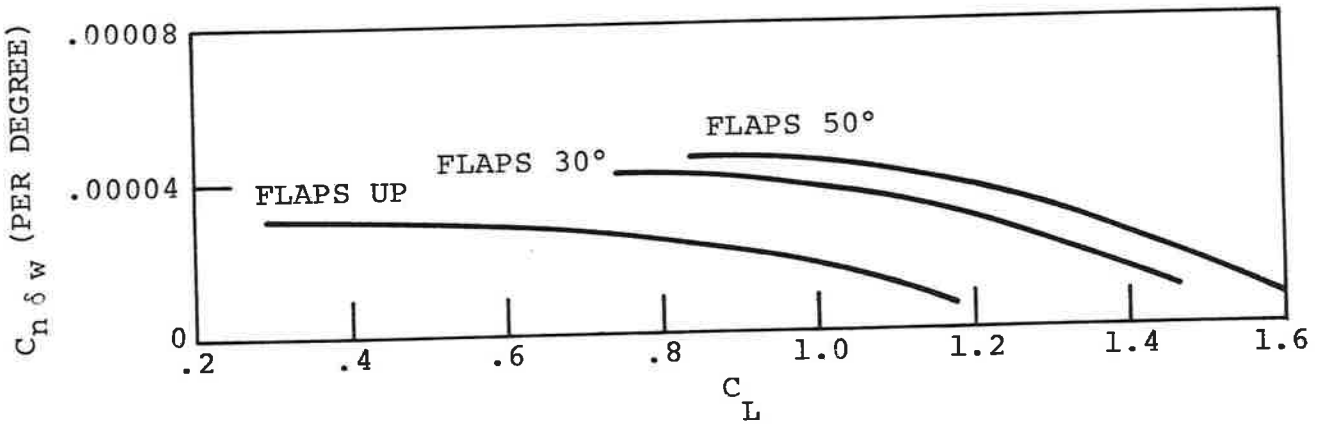

Figure 29. Yawing Moment Effect Due to Lateral Control.

ENGINE THRUST DATA

The only available engine thrust data from Reference 2 is summarized in Figures 30 through 36.

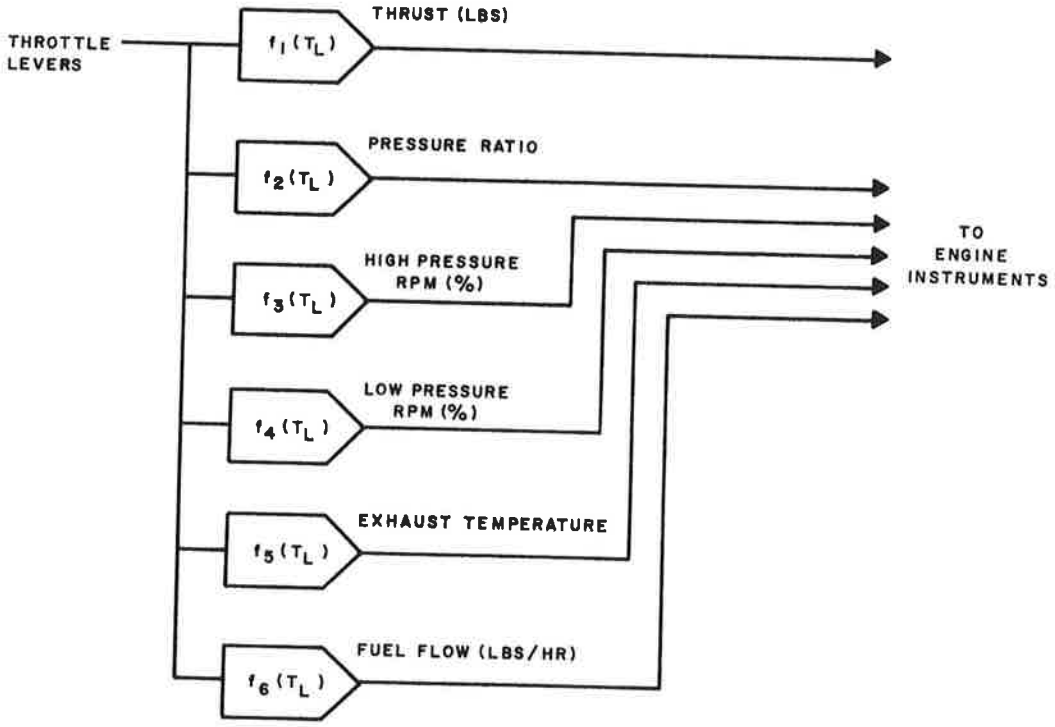

Figure 30. Engine Mechanization

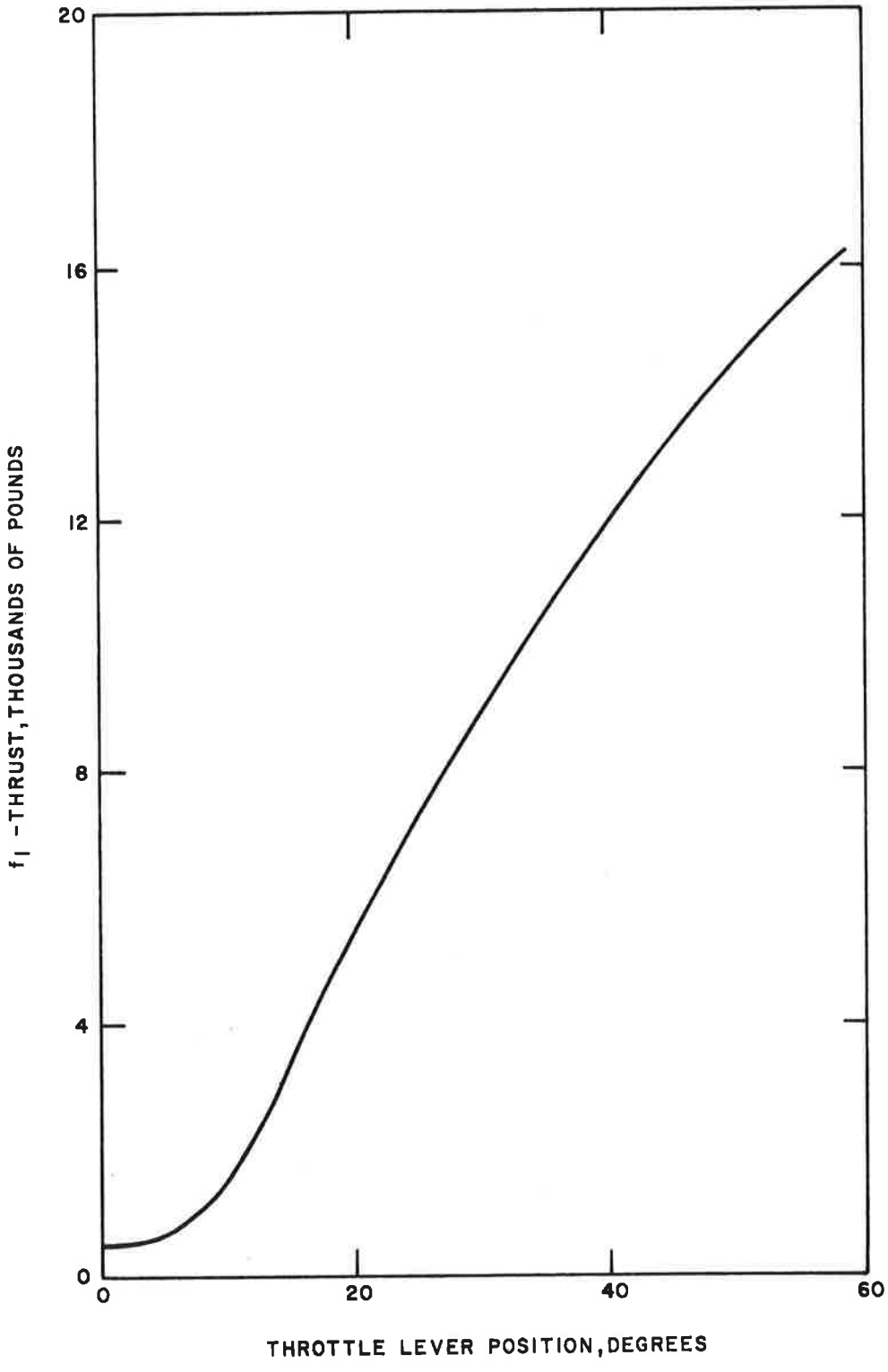

Figure 31. Thrust, Pounds

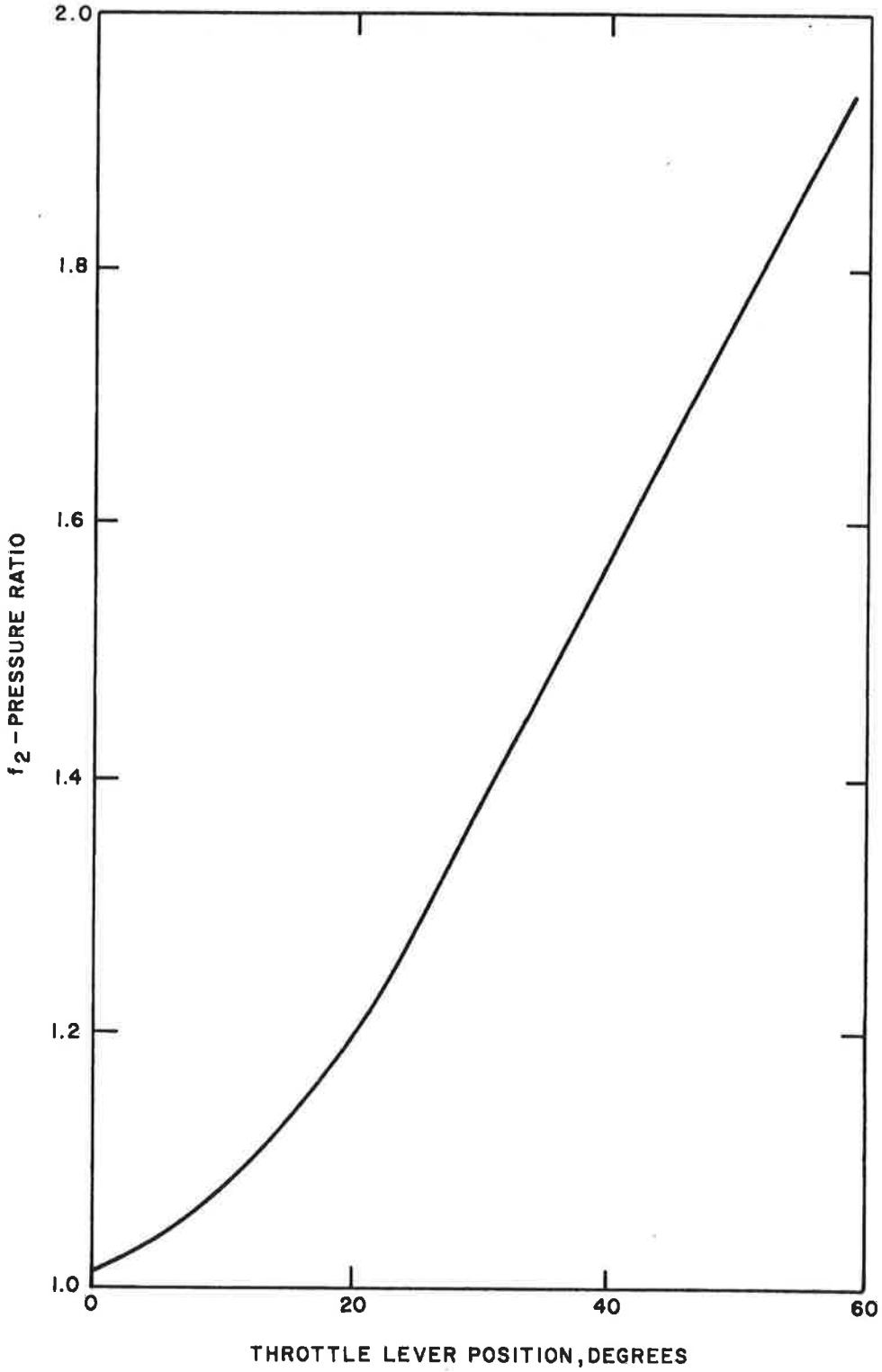

Figure 32. Pressure Ratio

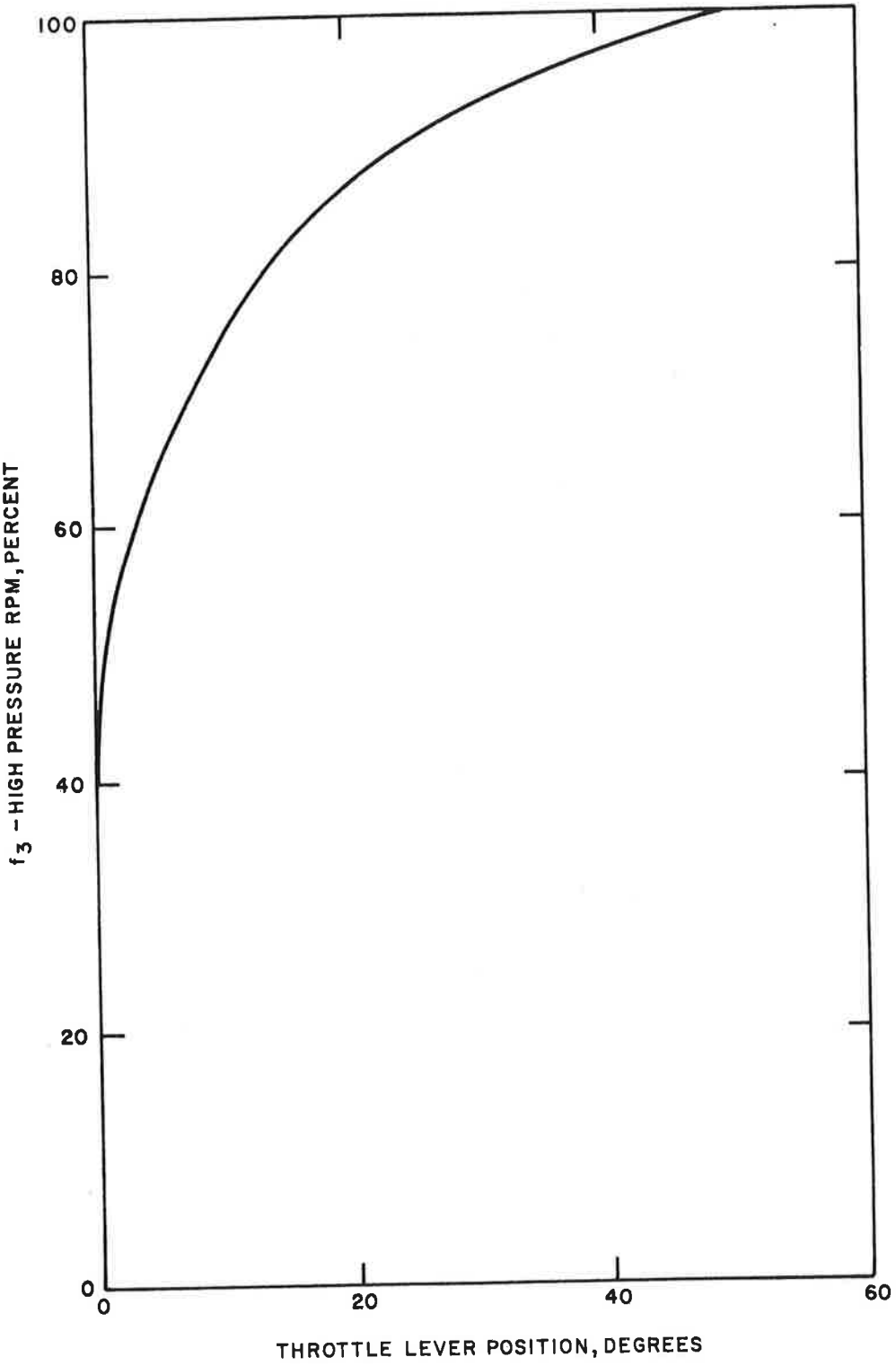

Figure 33. High Pressure RPM, Percent

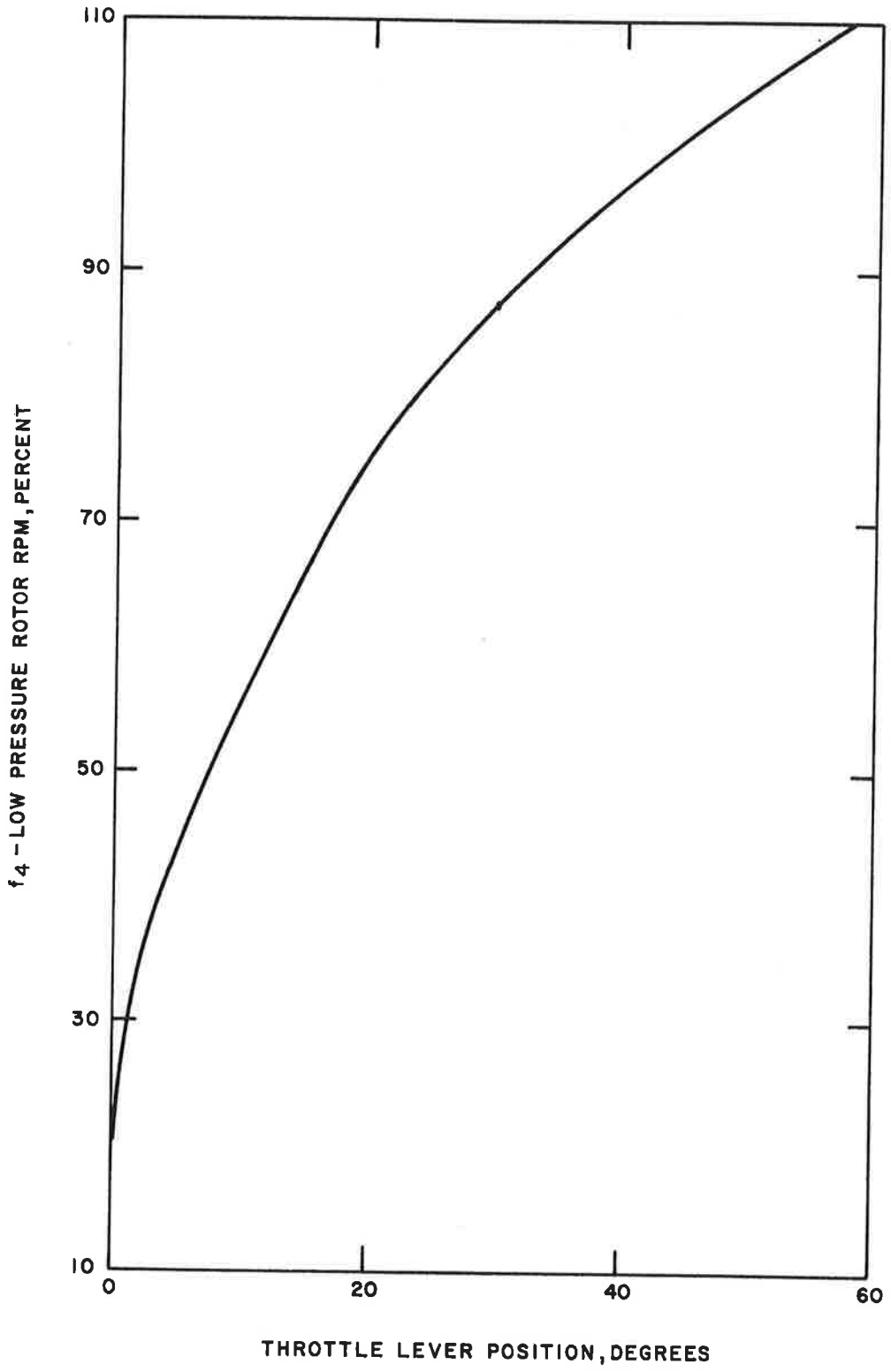

Figure 34. Low Pressure RPM, Percent

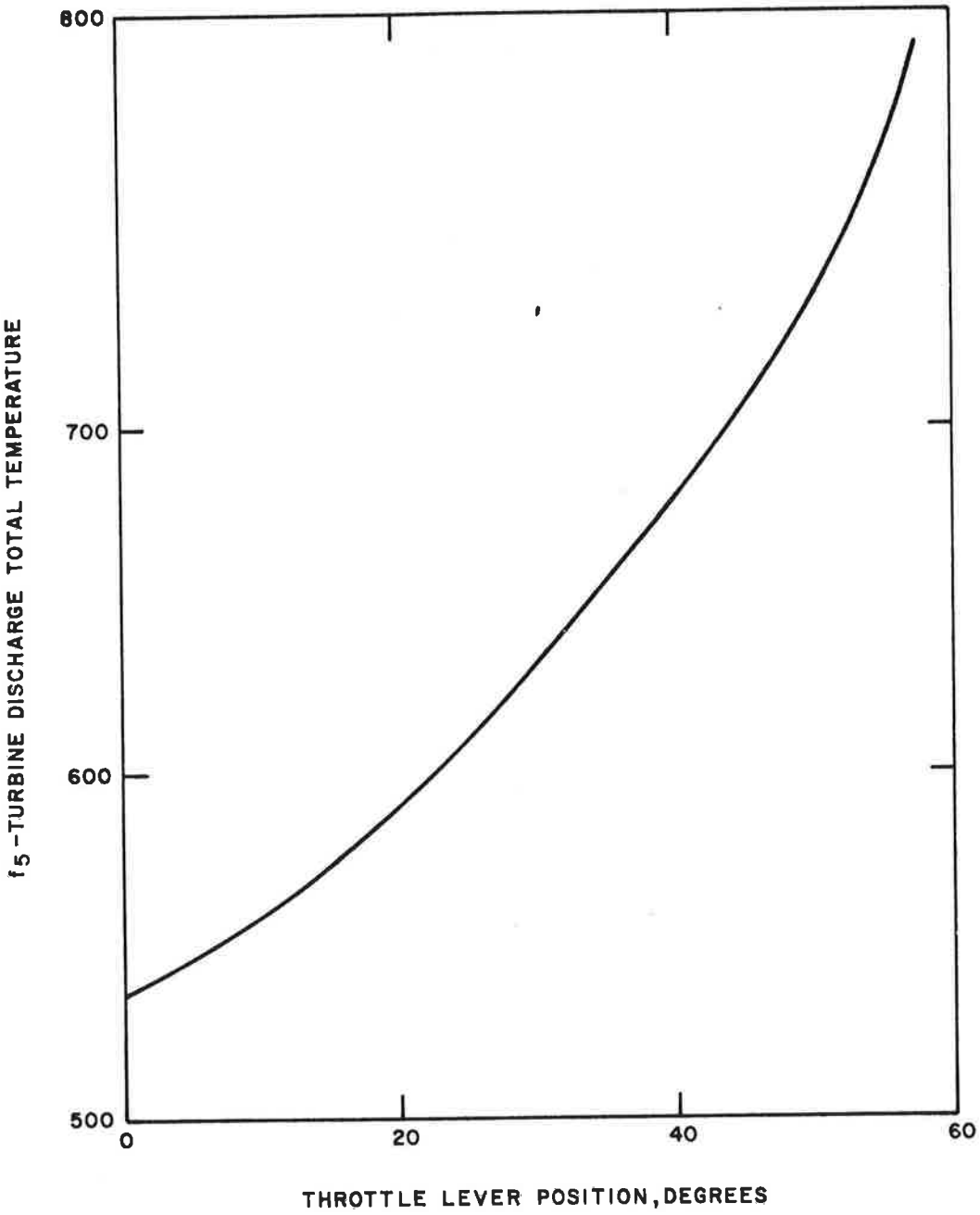

Figure 35. Exhaust Temperature

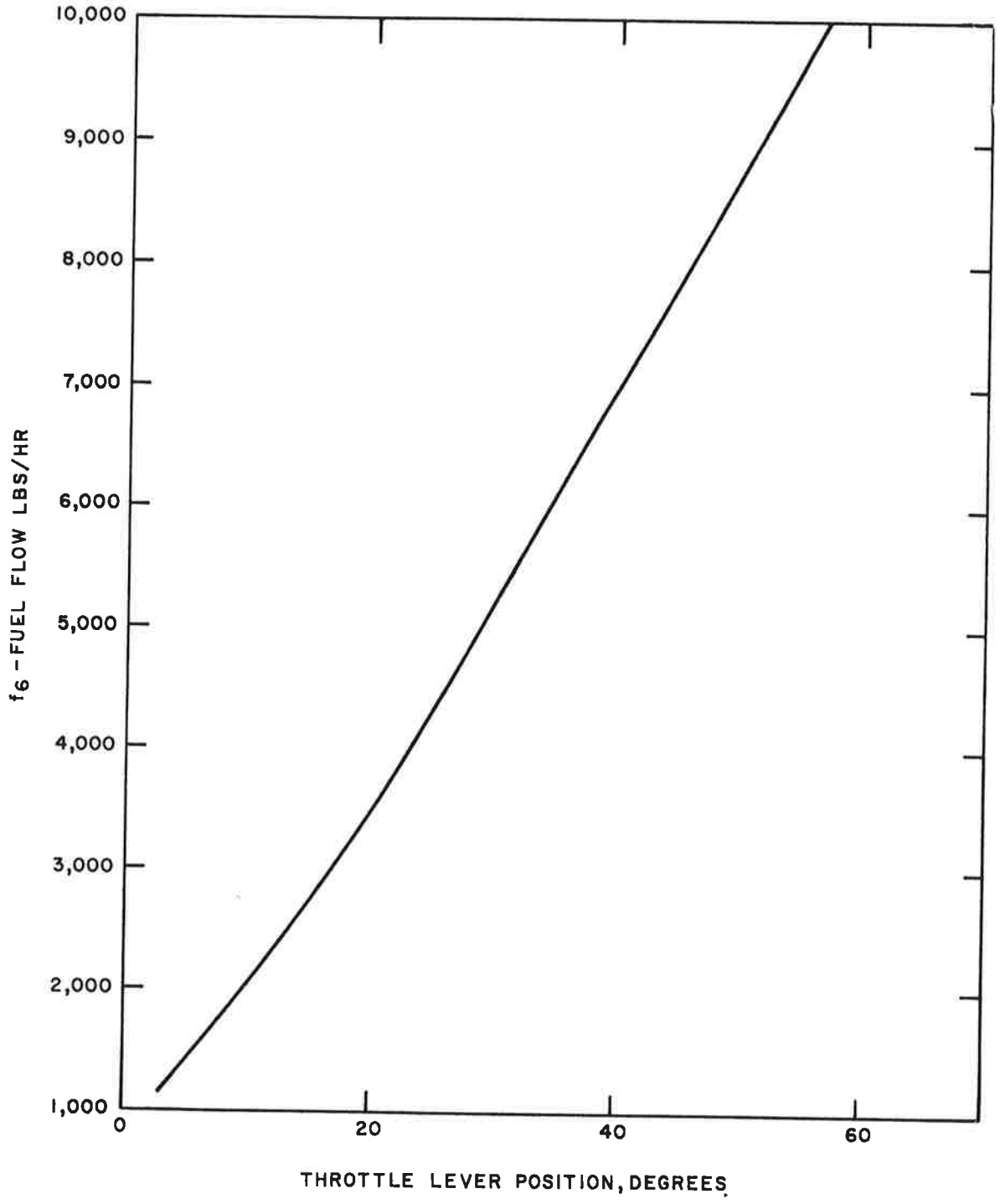

Figure 36. Fuel Flow (Pounds/Hour)

MANUAL FLIGHT CONTROL SYSTEM DESCRIPTION

LONGITUDINAL CONTROL SYSTEM

The longitudinal control system consists of an adjustable horizontal stabilizer for trim and an elevator for maneuvering flight. The horizontal stabilizer incidence can be varied from -13° to +1.5° with respect to the fuselage reference line. The stabilizer is pivoted at 25 per cent of the free mean aerodynamic chord in order to keep the actuation loads small. Normal operation of the stabilizer is accomplished by an electric motor actuated by control switches on the pilot's and copilot's control wheel. Manual operation for small trim changes or in the case of emergency is possible through the use of the manual trim wheel located on the control pedestal.

The elevator deflection limits are 23.5° up and 15° down with respect to the stabilizer. The elevator is partially balanced by an internal aerodynamic balance plate which is vented to the surface near the elevator hinge. Dampers prevent damage to the elevator due to gusts while the airplane is on the ground. The dampers nominally engage during the last 5° of elevator travel, thus they have essentially no effect on the control forces during flight.

The elevator is controlled by the pilot through a control tab which has an aerodynamic ratio of 1:1 at full deflection. The aerodynamic ratio is the ratio of the tab deflection to the resulting elevator deflection and is controlled by regulating the flow through the internal balance plate. Another factor in obtaining the desired control characteristics is the follow-up ratio, which is the ratio of the anti-balance tab deflection to the elevator deflection when the elevator is moved with the control system fixed. The elevator follow-up ratio is 1:1. The elevator is also equipped with a stabilizer actuated tab which is designed to make the elevator trail properly during flight. The schematic and block diagrams of the longitudinal control system are shown in Figure 37.

The elevator tab characteristics are presented in Figures 38 and 39 and for flaps up and flaps down. The elevator linkage ratios are given in Table 16. Figure 40 gives the relations between the elevator tab, elevator, and column position for the no air load case. Figure 41 shows the elevator control force due to the centering spring. Thus, with these curves it is possible to calculate the stick forces with the following equation:

$$F_{stick} = F_{spring} + (C_{H_t} \bar{q} S \bar{c}) (G) + F_{friction}$$

where F_{stick} = stick force (lb)

F_{spring} = spring force, (lb) from Figure 41

$C_{H(t)}$ = tab hinge moment coefficient, from Figures 38 and 39.

$\bar{q} = \frac{V_e^2}{295}$ (PSF)

$S\bar{c} = 11.43$ ft^2

$F_{friction} = \pm 2$ lb.

Pitching moments of the stabilizer about its hinge line are shown in Figure 42. These data may be used to calculate air loads on the stabilizer jack screw and its consequent effect on manual stabilizer trim wheel forces.

$$M_{hinge\ line} = C_{M_{tail}} \bar{q} \ (Sc_{tail})$$

The longitudinal control force with no airload is shown in Figure 43. This plot includes the elevator friction force.

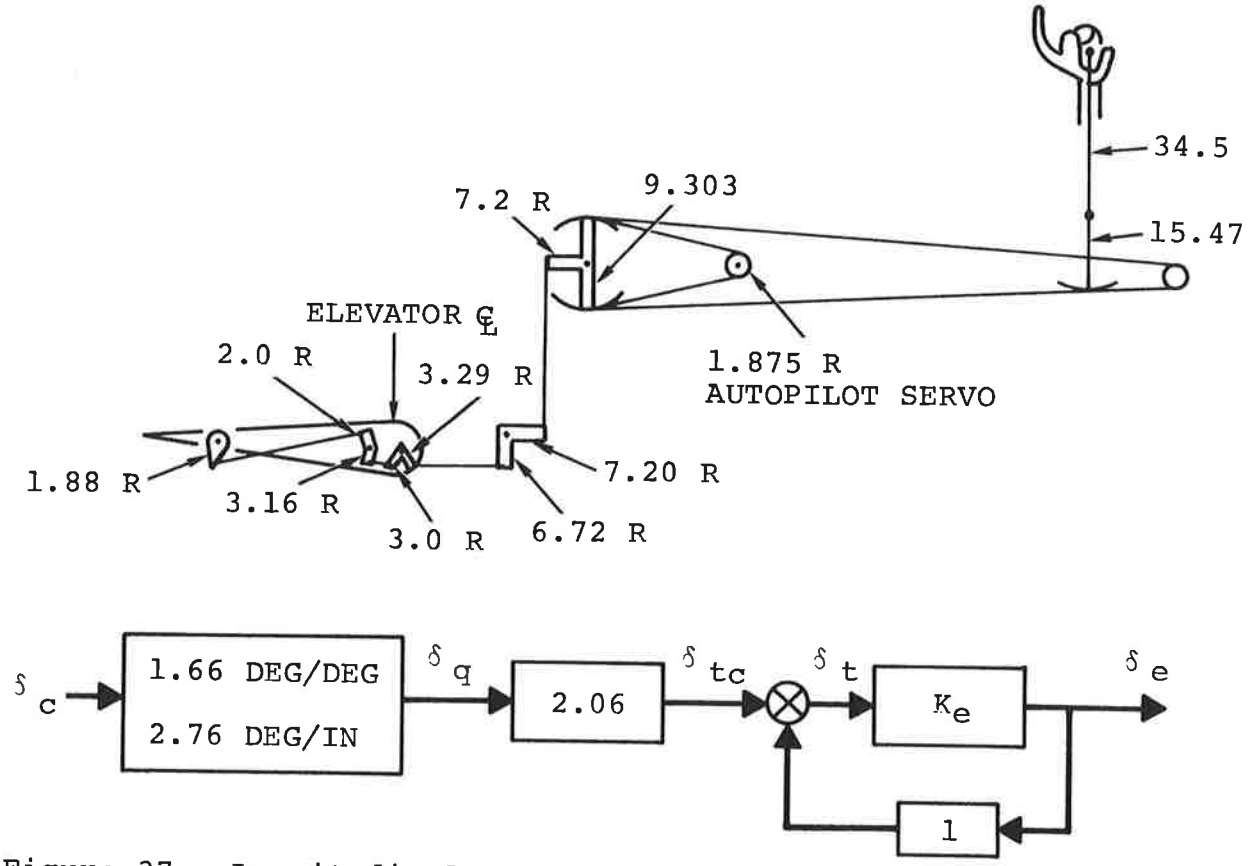

Figure 37. Longitudinal Control System Schematic and Block Diagram

TABLE 16. ELEVATOR - LINKAGE RATIOS

δ_c —— Column Motion

δ_q —— Quadrant Motion, Degrees

δ_{tc} —— Commanded Tab Motion, Degrees

δ_t —— Tab Motion, Degrees

δ_e —— Elevator Motion, Degrees

K_e —— Aerodynamic Gain = 1.67 For Approach Configuration and $\delta_e < 10$

$$\frac{\delta_q}{\delta_c} = \frac{15.47}{9.303} = 1.66 \frac{DEG}{DEG}$$

$$\frac{\delta_q}{\delta_c} = \frac{1.66\ (57.3)}{34.5} = 2.76 \frac{DEG}{INCH}$$

$$\frac{\delta_{tc}}{\delta_q} = \frac{7.2\ (6.72)\ (3.0)\ (2.0)}{7.2\ (3.29)\ (3.10)\ (1.88)} = 2.06 \frac{DEG}{DEG}$$

$$\frac{\delta_{tc}}{\delta_c} = \frac{\delta tc}{\delta_q} \frac{\delta_q}{\delta c} = 2.06\ (2.76) = 5.69 \frac{DEG}{INCH}$$

$$\frac{\delta_e}{\delta_{tc}} = \frac{K_e}{1 + K_e} = \frac{1.67}{2.67} = .625 \frac{DEG}{DEG} \quad (APPROACH)$$

[Reference 4 Boeing Document D6-9850 (Page 18)]

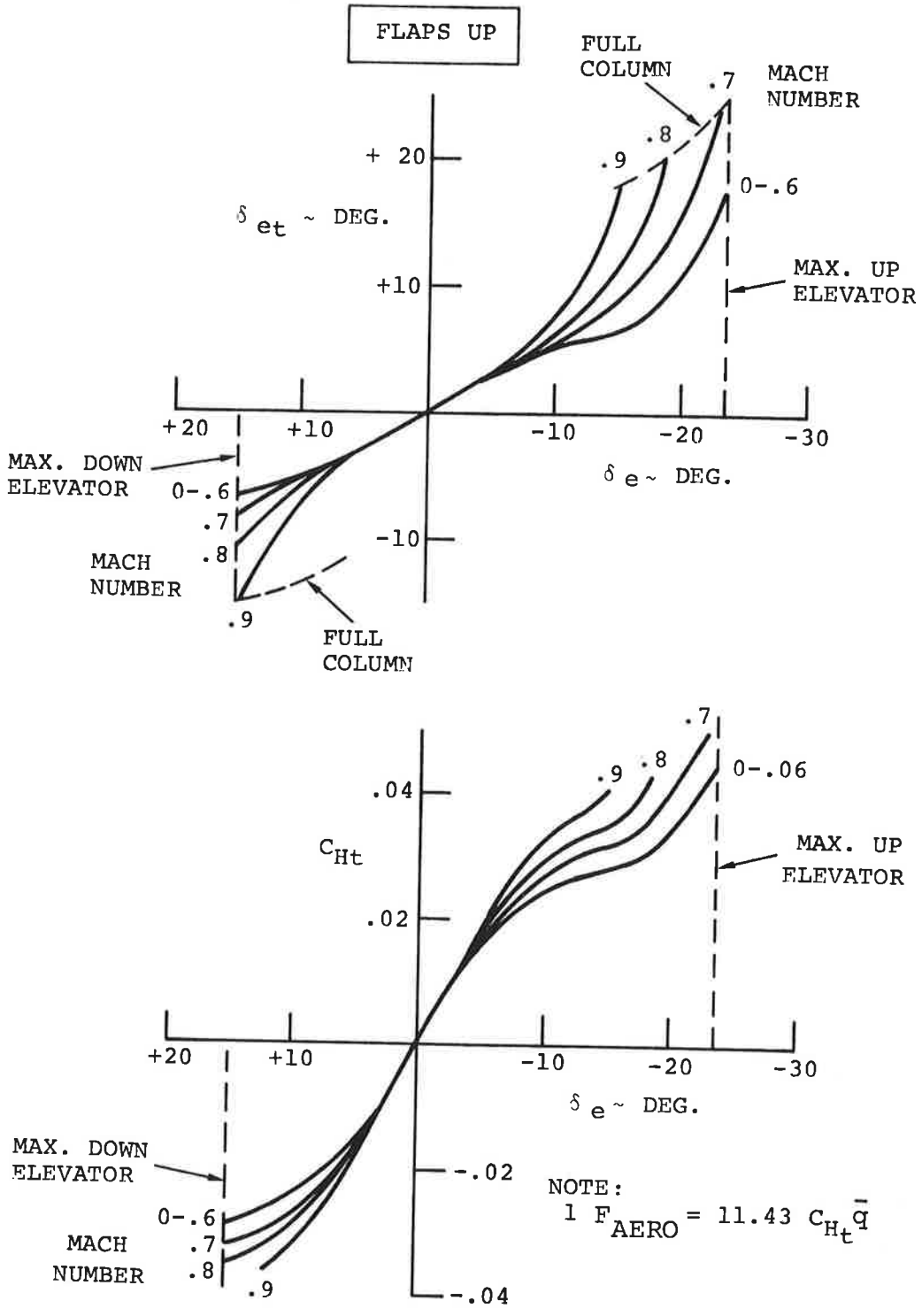

Figure 38. Elevator Tab Characteristics, Flaps Up.

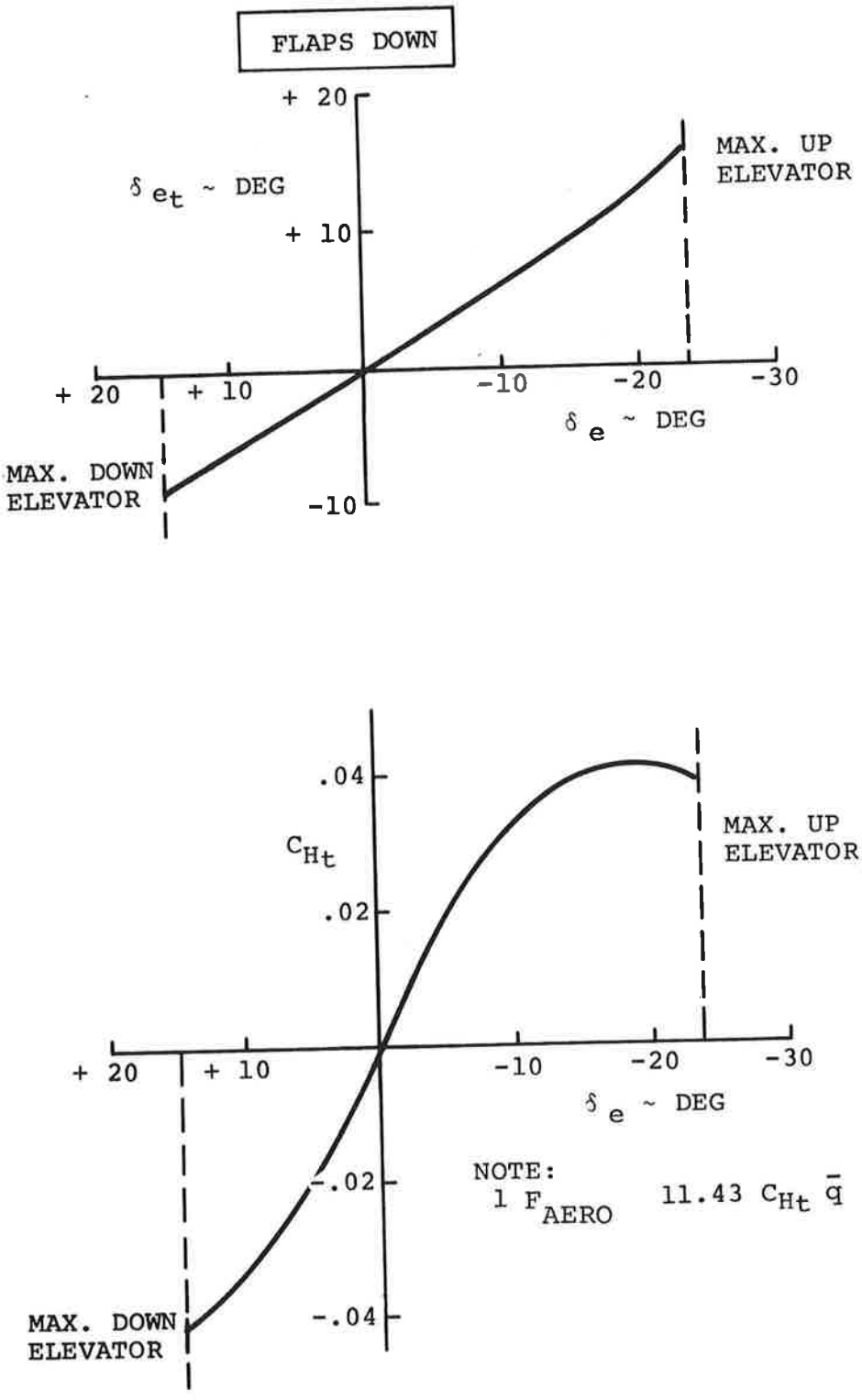

Figure 39. Elevator Tab Characteristics, Flaps Down.

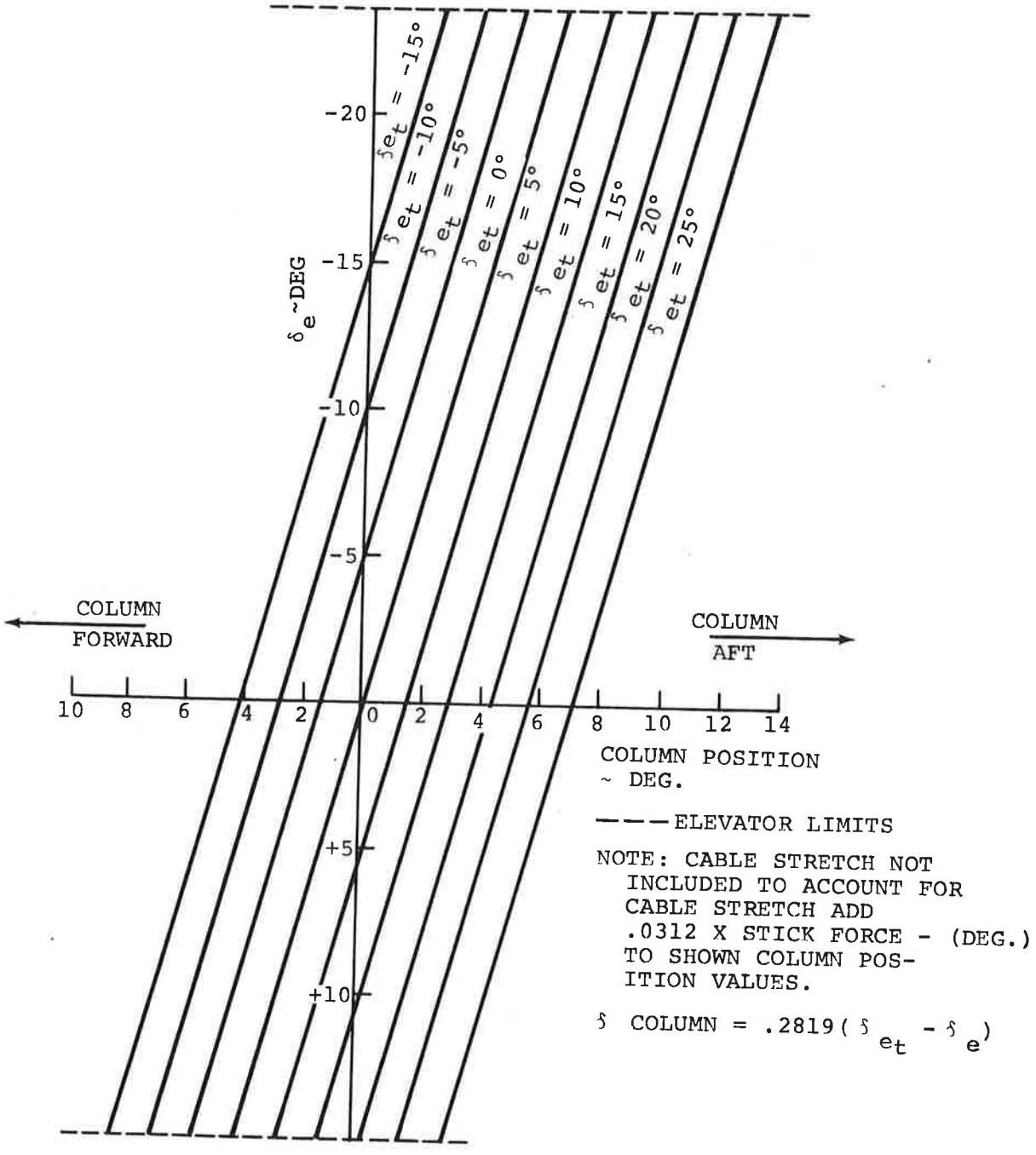

Figure 40. Longitudinal Control Motion (No Air Load).

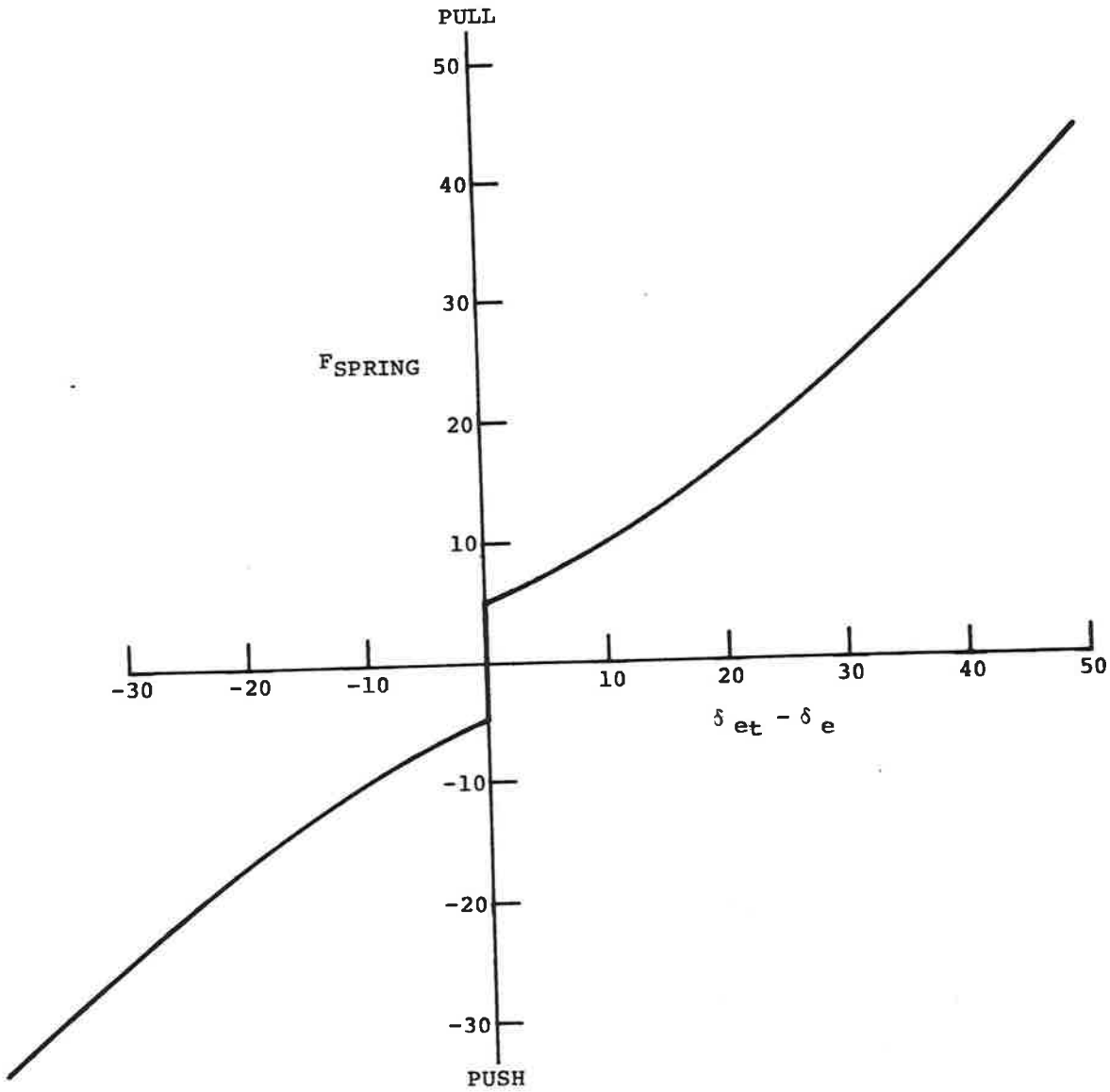

Figure 41. Elevator Control Tab Centering Spring Force.

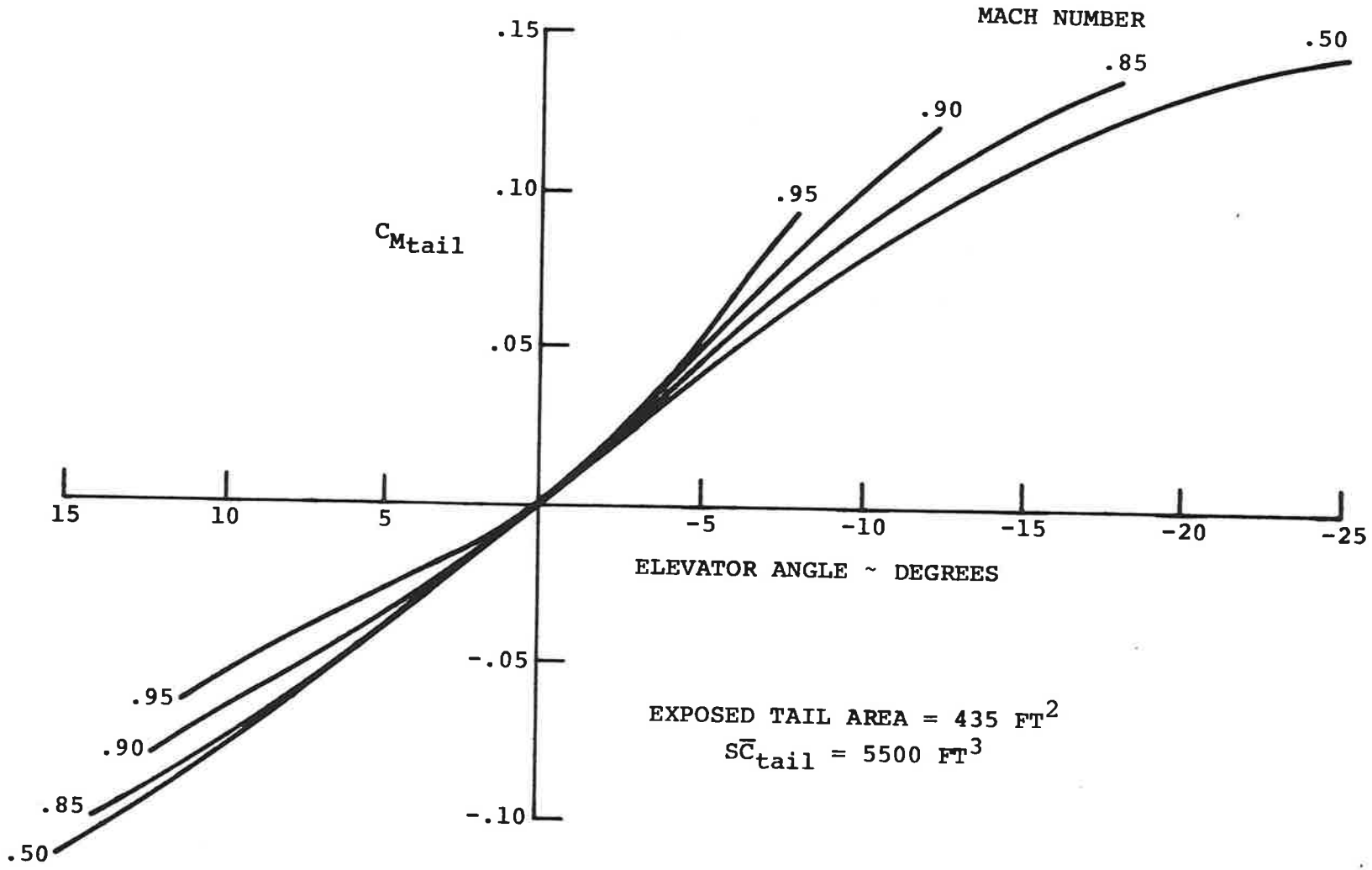

Figure 42. Horizontal Tail Moment (About Stabilizer Hinge Line).

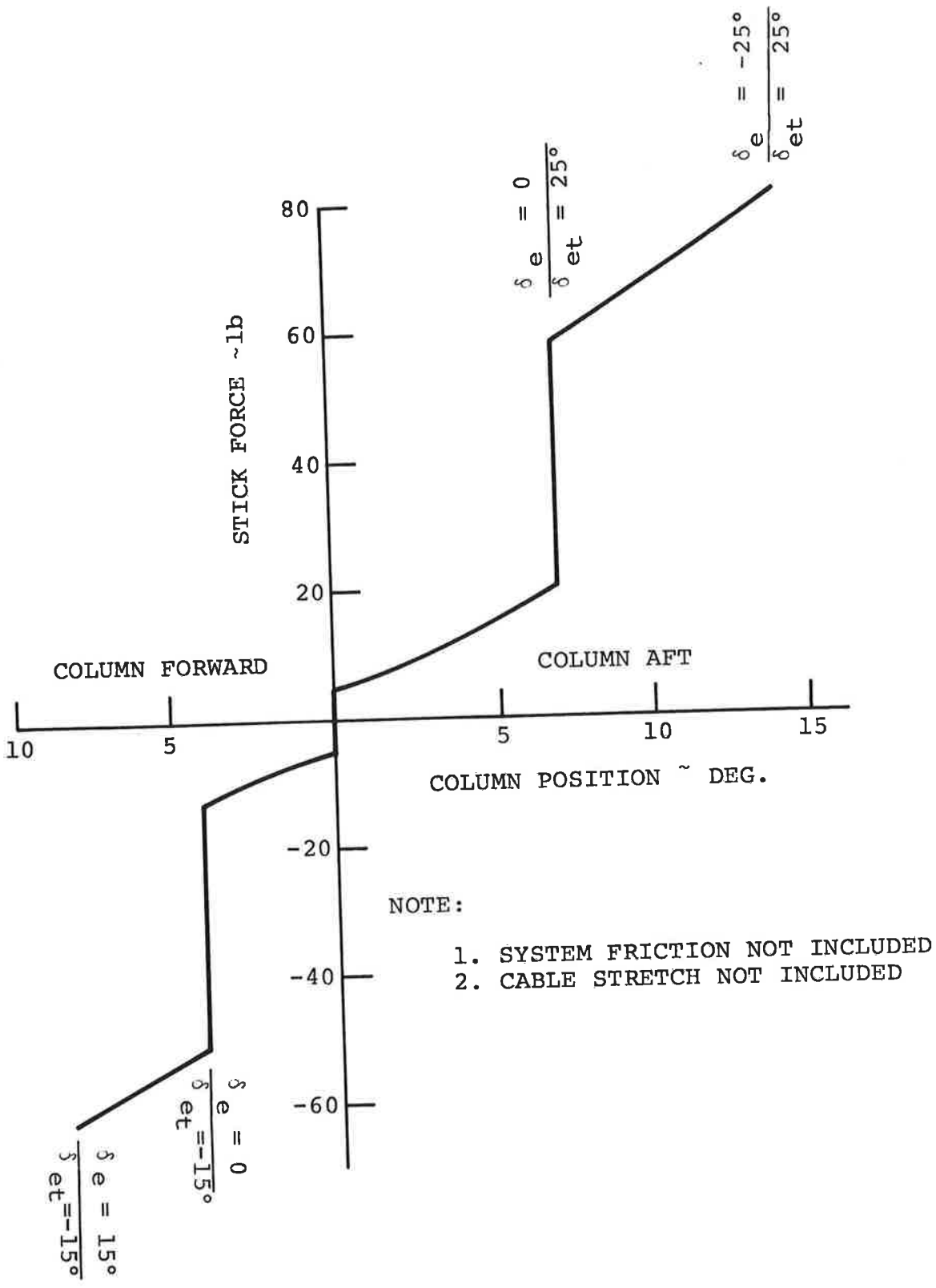

Figure 43. Longitudinal Control Force (no air load)

LATERAL CONTROL SYSTEM

The schematic and block diagrams of the lateral control system are shown in Figure 45. The lateral control system consists of an inboard aileron, located between the inboard and outboard flaps which corresponds to the region aft of the inboard nacelle strut, two spoilers consisting of two segments each located on the upper surface of the wing forward of the inboard and outboard flaps, and an outboard aileron extending outward from the outboard flap.

The inboard aileron is the primary lateral control surface since it is used throughout the complete flight regime. It is actuated by means of a spring tab which in turn is pilot operated through the control wheel. Aerodynamic balancing is obtained from a nose overhang and two internal plate balances. The spring tab has a 1:1 follow up ratio with respect to the aileron which supplies an antibalance (or stabilizing) action to the aileron when the control wheel is fixed.

A double acting preloaded spring is located between the tab control and the wing frame and serves to give both feel and centering action. In addition, aileron trim is obtained from the spring. The aileron trim wheel in the cockpit displaces the spring cartridge along its axis by means of a cable drive to a screw arrangement. The aileron linkage ratios are given in Table 17.

The relationship between inboard aileron deflection and the spring tab is shown in Figure 46 for flaps up and flaps down. Figure 48 gives the relationship between the inboard aileron, spring tab and control wheel position. The spoilers operate either as a lateral control device or as airbrakes. The spoilers are hydraulically actuated with the control valve being operatated from the inboard aileron quadrant. Each of the four spoilers has a followup arrangement on it so that the spoiler deflection is an implicit function of the control valve setting. The inboard and outboard spoilers are actuated by separate hydraulic systems. Individual spoiler operation may therefore be accomplished by deactivating the hydraulic system of the set desired inactive. Maximum spoiler deflection may be obtained up to an equivalent airspeed of 200 knots. At speeds above this, the spoiler deflection is limited to that which can balance the hinge moment produced by hydraulic pressure. Figure 47 presents the variation of maximum spoiler angle as a function of equivalent airspeed, and Figure 48 shows the relationship between spoiler angle and control wheel position.

The airbrakes are operated hydraulically through the follow-up circuit in the spoiler control valve. Figure 47 shows air-

brake schedule as a function of aircraft speed and Figure 49 shows the spoiler deflection schedule as a function of pilot's control. The outboard airbrakes are deflected 7° when the flaps move from 40° to 50° in order to improve the longitudinal stability characteristics. This deflection is accomplished by an actuating cam on the flaps which forces the spoiler up against hydraulic pressure.

Spoiler actuation can occur simultaneously with airbrake operation since the controls enter the hydraulic circuit by independent routes. Figure 49 shows the relationship between spoiler angle and control wheel position for several airbrake positions.

The outboard aileron is a secondary lateral control surface since it is operative for flaps down flight only. It is actuated by the inboard aileron through the aileron bus system. Figure 50 gives the ratio of inboard to outboard aileron deflection as a function of flap deflection. A geared flap interconnect permits the aileron to be deflected with the flaps down and to be locked in a neutral position with flaps up. The outboard aileron is very nearly aerodynamically balanced with a geared tab and pressure regulated plate balance. The geared balance tab has a 1:1 balance ratio.

WHEEL FORCE CHARACTERISTICS

$$F = F_{S_T} + F_{S_C} \pm F_{Frict.} + F_{Aero.} + F_{Inertia}$$

where

F = Total wheel force supplied by one hand in tangiental manner at the wheel rim (7 in. radius) measured in pounds.

F_{S_T} = Trim spring force. See Figure 44.

F_{S_C} = Centering spring force. See Figure 44.

$F_{Frict.}$ = Wheel force due to system friction

= 4.5 pounds $\pm$ signs corresponds to $\pm \frac{dSw}{dt}$ respectively

$F_{Aero.}$ = Wheel force due to control tab air loads

$F_{Inertia}$ = Wheel force due to control system inertia expressed in units of pounds.

$= I \frac{d^2Sw}{dt^2}$ where I has units of $\frac{\#\ \text{wheel force x sec.}^2}{\text{degree}}$

TABLE 17. AILERON - LINKAGE RATIOS

δ_w —— Control Wheel Motion, Degrees

δ_q —— Inboard Quadrant Motion, Degrees

δ_{tc} —— Commanded Tab Motion, Degrees

δ_t —— Tab Motion, Degrees

δ_a —— Inboard Aileron Motion, Degrees

K_a —— Aerodynamic Gain = 1.27 for Approach Configuration and $\delta_a < 15$

$$\frac{\delta_q}{\delta_w} = \frac{2.47}{11.12} = .222 \ \frac{DEG}{DEG}$$

$$\frac{\delta_{t_c}}{\delta_q} = \frac{2.80\ (1.75)}{1.70\ (1.75)} = 1.65 \ \frac{DEG}{DEG}$$

$$\frac{\delta_{tc}}{\delta_w} = \left(\frac{\delta_{t_c}}{\delta_q}\right)\left(\frac{\delta_q}{\delta_w}\right) = 1.65\ (.222) = .366 \ \frac{DEG}{DEG}$$

$$\frac{\delta_a}{\delta_{t_c}} = \frac{K_a}{1 + K_a} = \frac{1.27}{2.27} = .56 \ \frac{DEG}{DEG} \quad \text{(APPROACH)}$$

[Reference 4 Boeing Document D6-9850 (Page 14)]

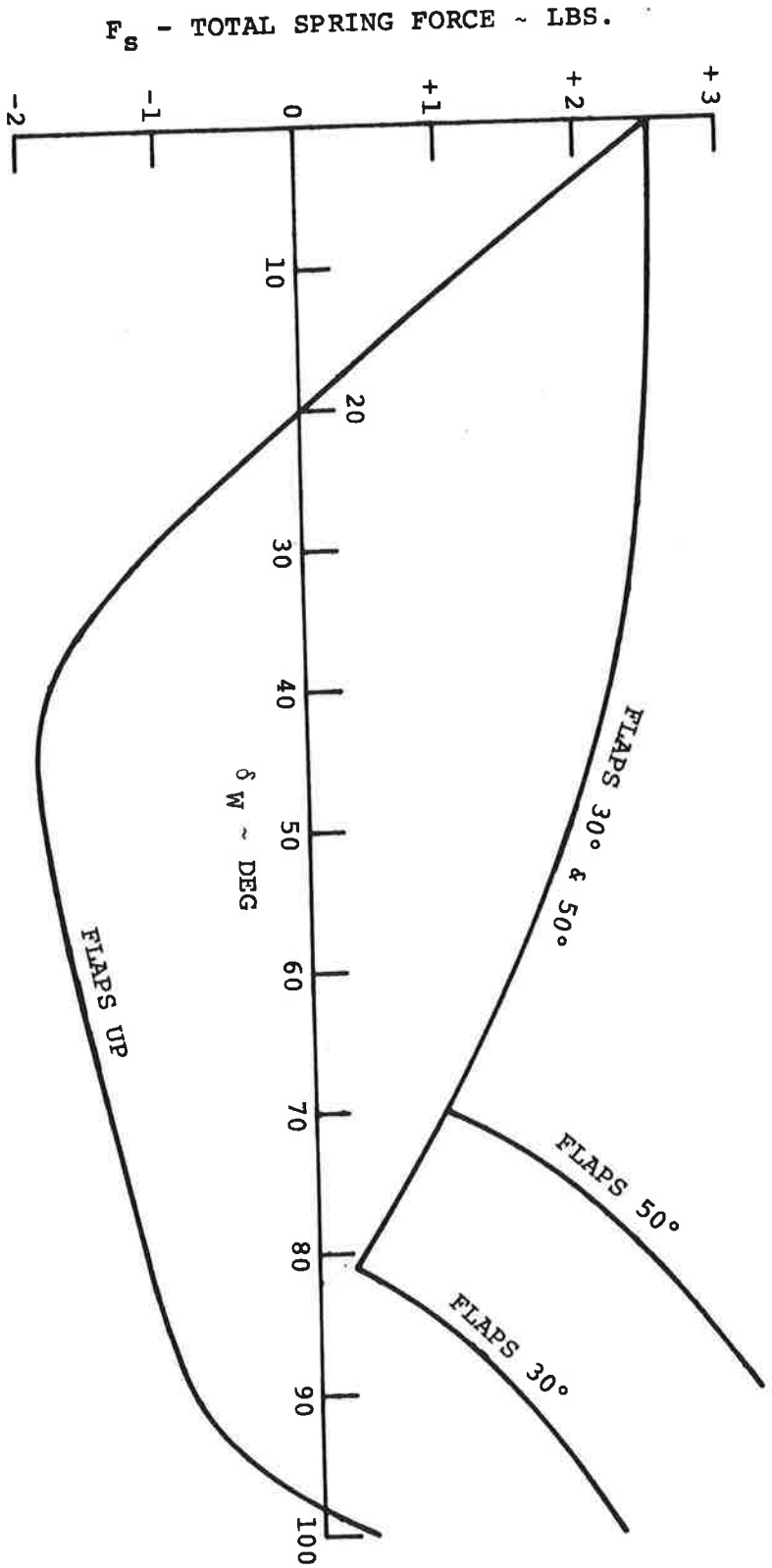

Figure 44. Combined Trim and Centering Spring Force.

Sw = Control wheel angle in degrees (+ corresponds to right wheel notion

I = .00224 (pound wheel force)/(deg/sec.^{2})

FLAPS UP (ASSUMED APPLICABLE FOR ALL MACH NUMBERS)

$$F_{Aero.} = .00151 \times \bar{q} \times \delta_w$$

where $-\delta_{w_1} \leq \delta_w \leq +\delta_{w_1}$

and $F_{Aero.} = \bar{q}\,[.00151 \times \delta_w + .0032 \times (\delta_w - \delta_{w_1})]$

when $\delta_{w_1} \leq \delta_w \leq \delta_{w_2}$

FLAPS 30°, 40°, 50° DEF.

$$F_{Aero.} = .0023 \times \bar{q} \times \delta_w$$

when $-\delta_{w_1} \leq \delta_w \leq +\delta_{w_1}$

and $F_{Aero} = \bar{q}\left[.0023 \times \delta_{w_1} + .00708\,(\delta_w - \delta_{w_1})\right]$

when $\delta_{w_1} \leq \delta_w \leq \delta_{w_2}$

$$\delta_{w_1} = \begin{cases} 73.5^\circ \text{ for flaps } 50^\circ \\ 80.0^\circ \text{ for flaps } 40^\circ \\ 82.0^\circ \text{ for flaps } 30^\circ \\ 81.5^\circ \text{ for flaps up} \end{cases}$$

$$\delta w_2 = \begin{cases} 93.0^\circ \text{ for flaps } 50^\circ \\ 96.0^\circ \text{ for flaps } 40^\circ \\ 97.5^\circ \text{ for flaps } 30^\circ \\ 100.0^\circ \text{ for flaps up} \end{cases}$$

δ_{w_1} = corresponds to wheel angle when aileron reaches stops. For flaps down limit aileron angle is defined by outboard aileron reaching 20°.

δ_{w_2} corresponds to wheel angle when aileron control tab reaches 20°.

$\bar{q}$ is dynamic pressure measured in PSF units

when $\delta_w = \delta_{w_2}$ additional wheel force is caused by stretching the control cables

$$\text{then} \quad F_{RATE} = .025 \times \delta_{w2} + 7.92 \left(\delta_w - \delta_{w2} \right)$$

$$\text{and} \quad F_{Aero} = \bar{q} \left[.00151 \times \delta_{w1} + .00302 \left(\delta_{w2} - \delta_{w1} \right) \right] \quad \text{for flaps up}$$

$$= \bar{q} \left[.0023 \times \delta_{w1} + .00700 \left(\delta_{w2} - \delta_{w1} \right) \right] \quad \text{for flaps down}$$

Account should be taken of cable stretch in determining the final corrected wheel angle

Define

δ_w' = Corrected wheel angle, considering cable stretch.

δ_w = Uncorrected wheel angle.

then

$$\delta_w' = \delta_w + .187 \sum \text{FORCES}$$

Figure 51 shows the lateral control force for the no airload case.

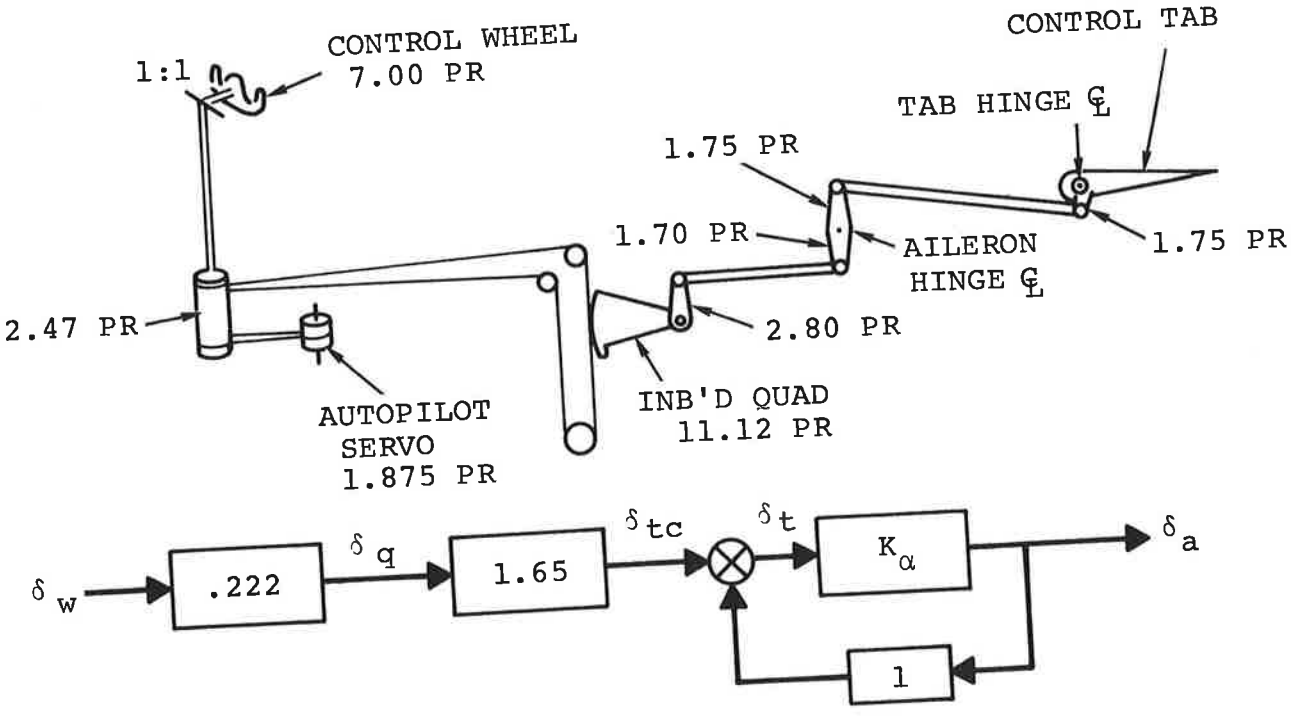

Figure 45. Lateral Control System Schematic and Block Diagram

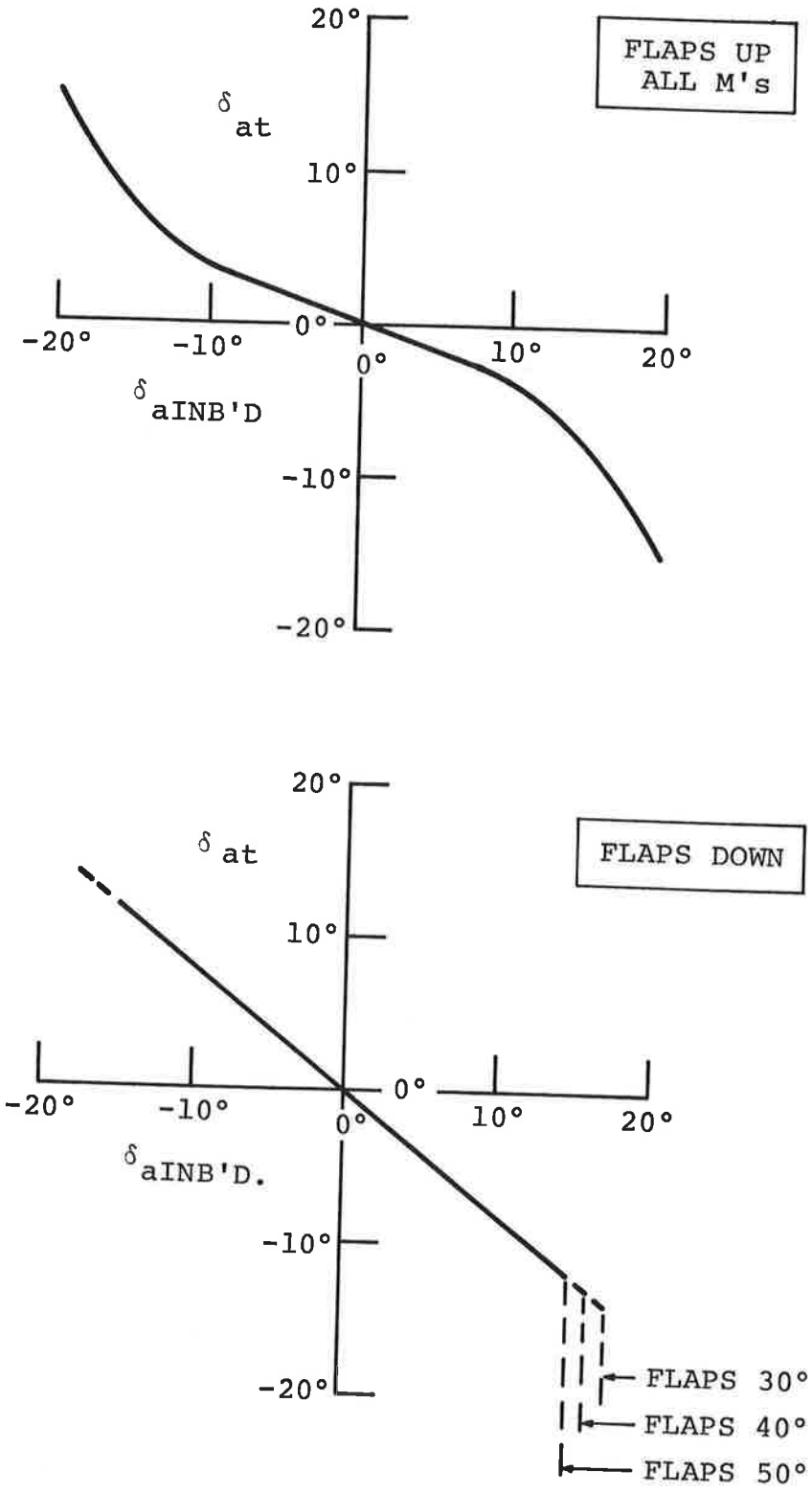

Figure 46. Aileron Tab Characteristics (inb'd).

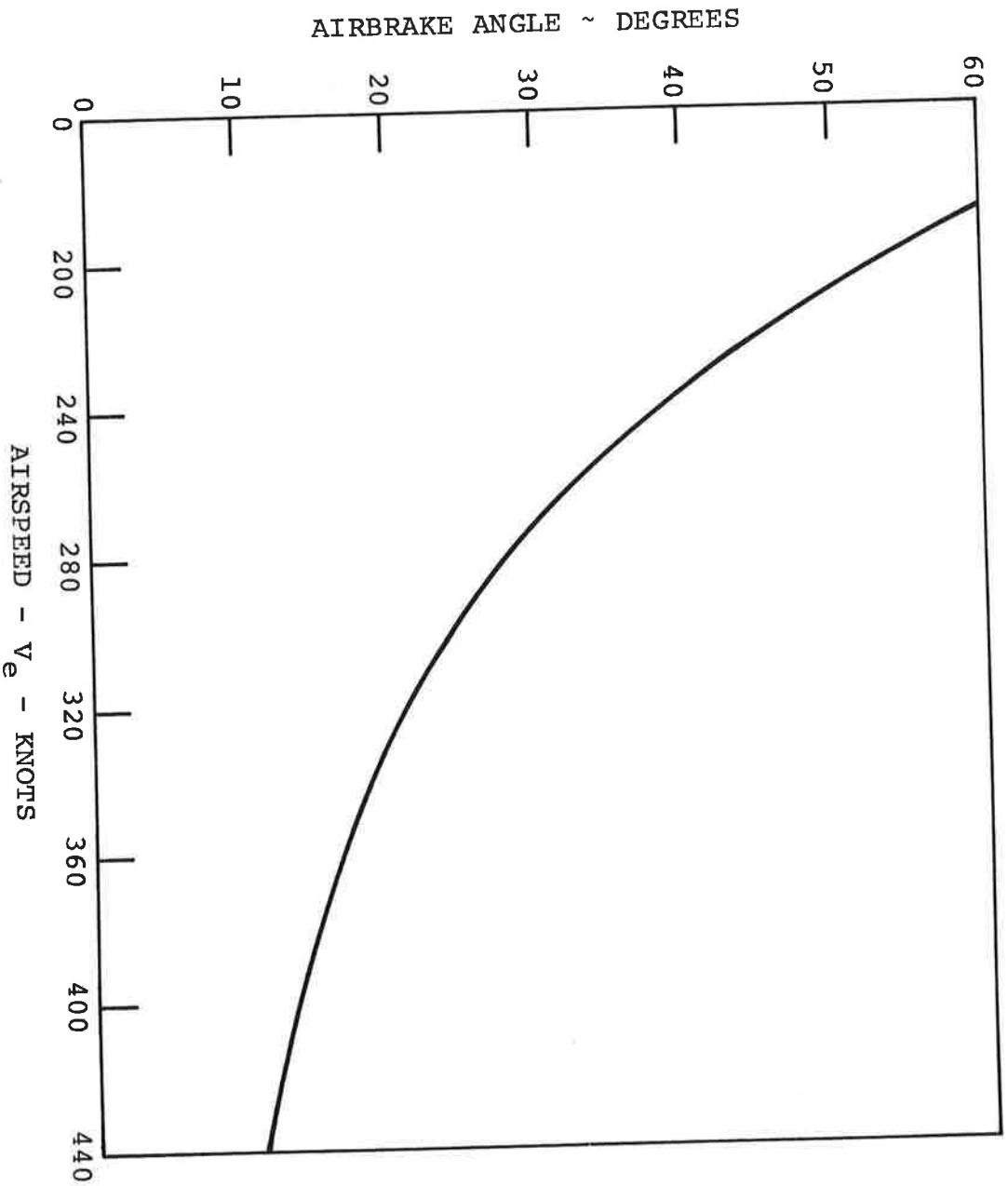

Figure 47. Airbrake Schedule.

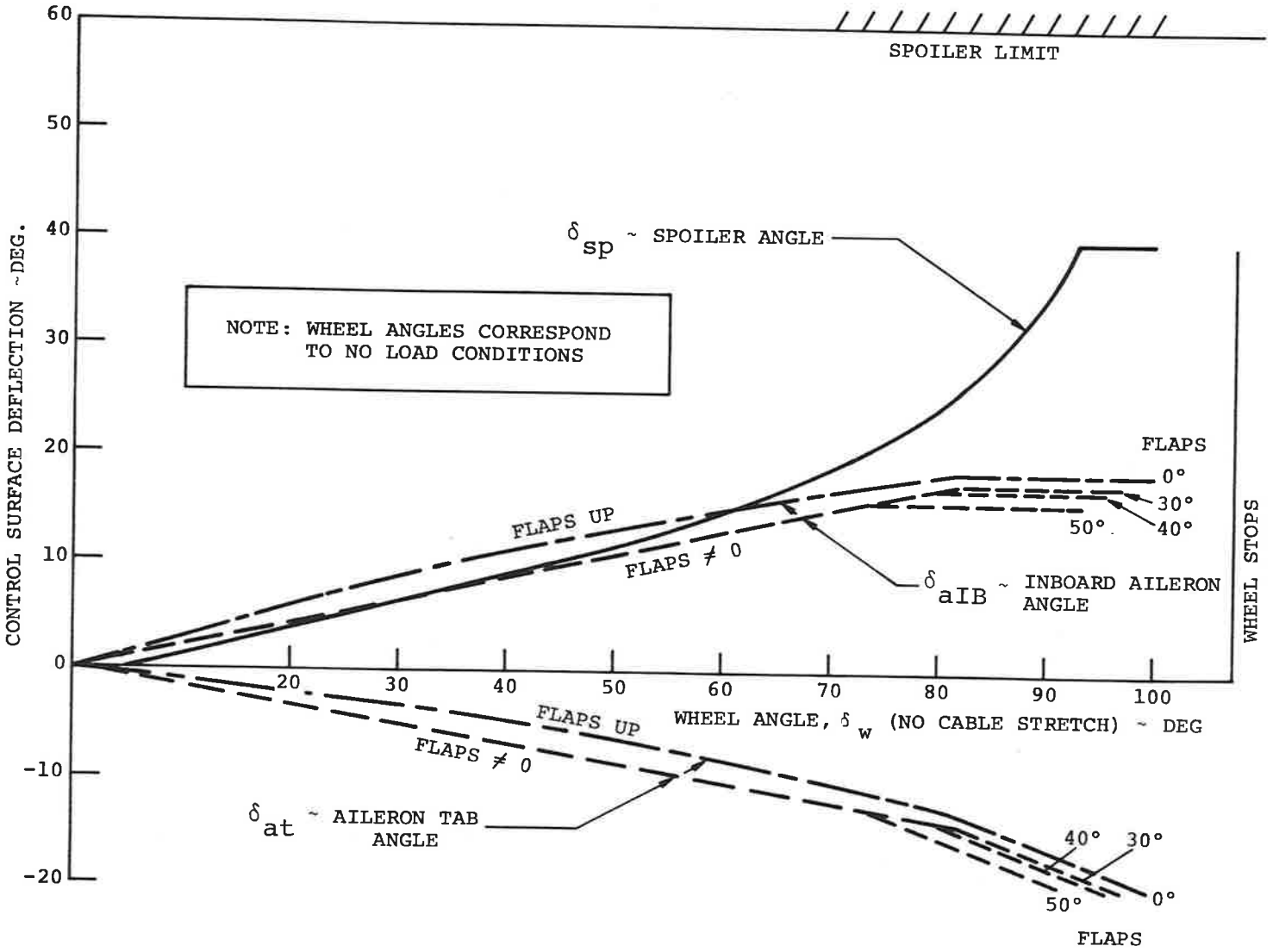

Figure 48. Lateral Control Motion.

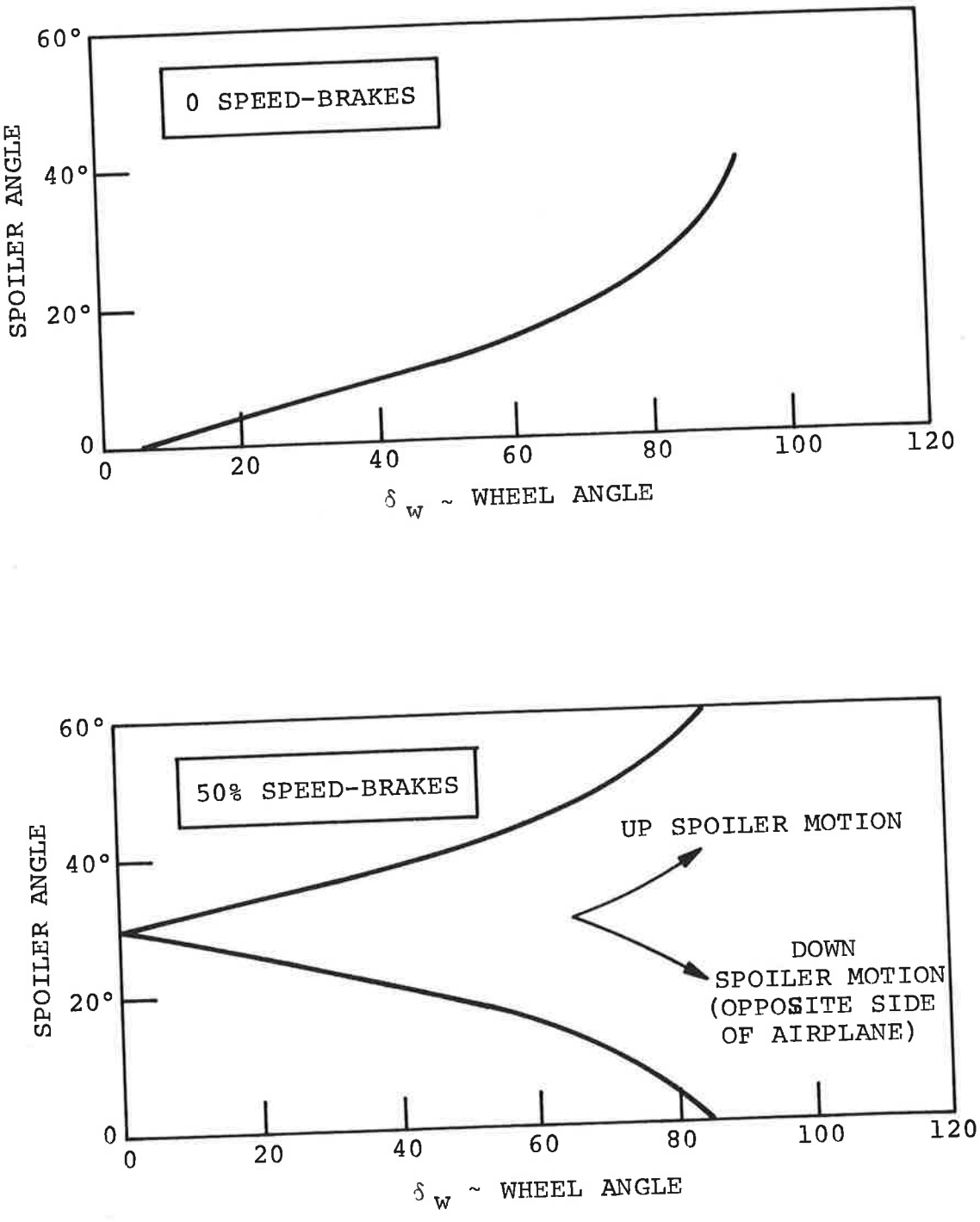

Figure 49. Spoiler Program With Speed Brakes.

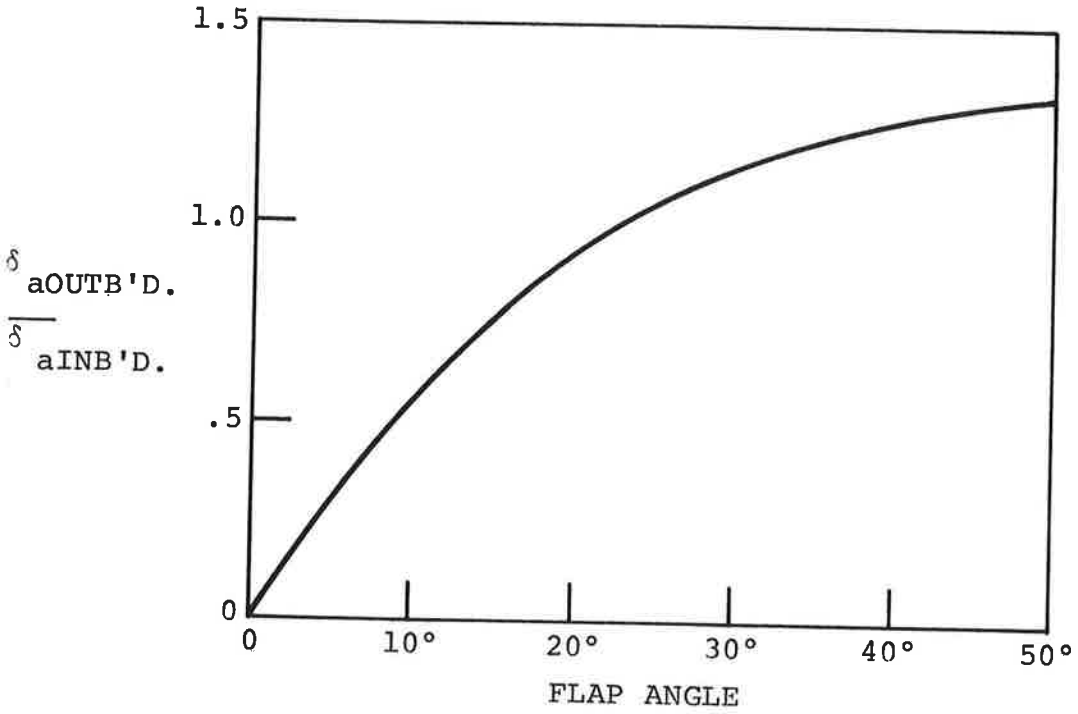

NOTE:
CHANGE IN GEAR RATIO CAUSED BY
INTER CONNECT WITH OUTBOARD FLAP

Figure 50. Outboard Aileron Motion.

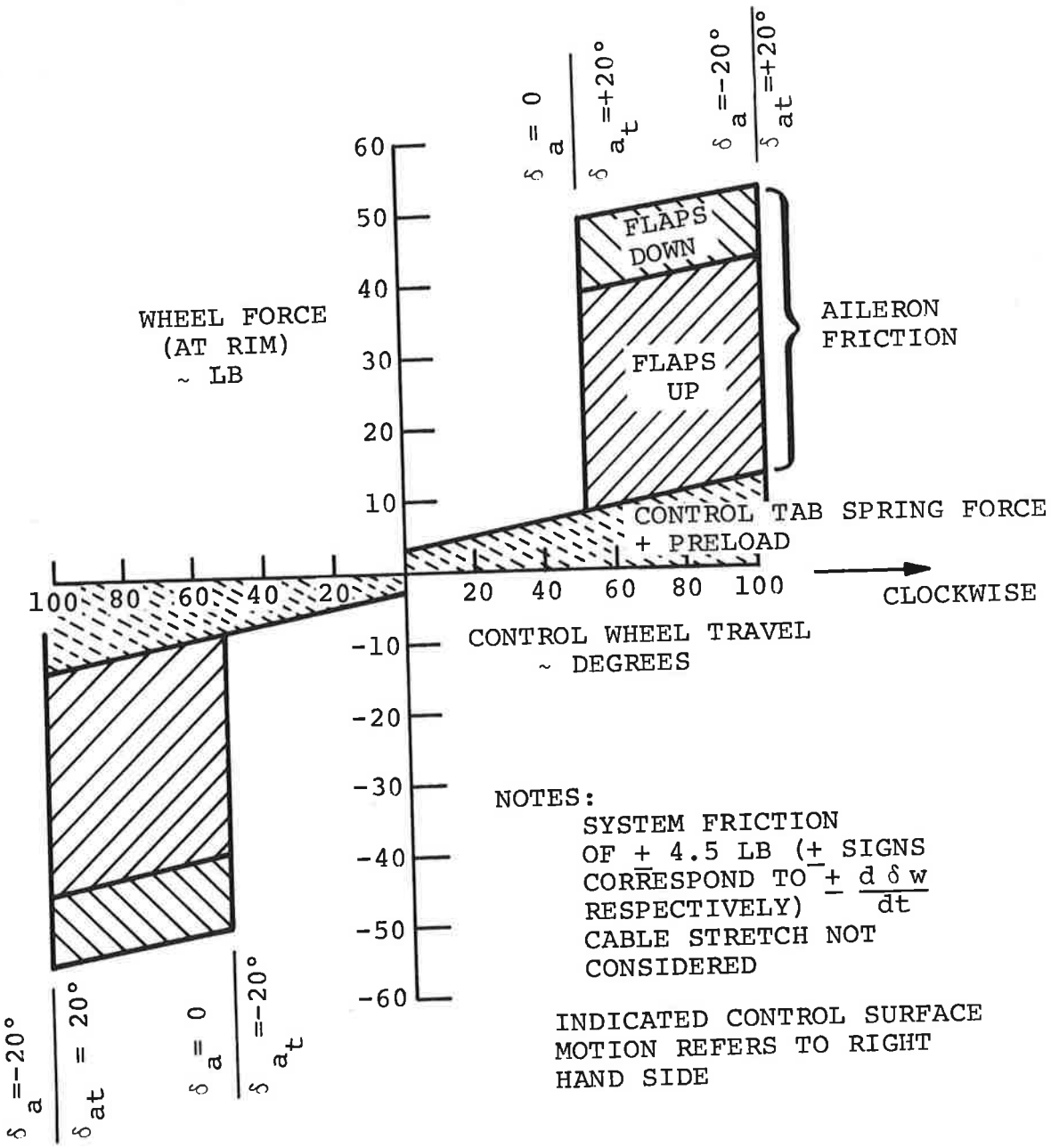

Figure 51. Lateral Control Force (no air load).

DIRECTIONAL CONTROL SYSTEM

FULL TIME / PROGRAMMED RUDDER BOOST

The directional control system of the 720-B consists of the vertical stabilizer, a ventral fin and the rudder. Three methods are used simultaneously to balance the rudder hinge moments: rudder tab, balance panels and a hydraulic boost.

The rudder operating range is divided into full time boost and programmed boost regimes. The full time boost range extends from 17° to 25° of rudder deflection. In this range the hydraulic boost and balance panels are entirely responsible for balancing rudder hinge moments and provide the necessary moments for rudder deflection. The tab direction is reversed from balancing action at -6.8° to a maximum anti-balancing action at $+20^{\circ}$. The pedal feel is obtained from three sources:

a. "Q" bellows (Figure 52)
b. "Q" spring, mechanical (Figure 52)
c. Centering spring (Figure 52)

The "Q" bellows cause the pedal forces to be a function of the airplane dynamic pressure ($\bar{q}$).

In the programmed boost region ($0-17^{\circ}$ δ_r) the rudder hinge moments are balanced by three methods:

a. Hydraulic boost (partial)
b. Rudder tab
c. Balance panels

The pedal forces in this region are a function of:

a. Tab hinge moments (Figure 53)
b. Centering spring (Figure 52)

Table 18 and Figure 54 give the directional control system gains and schematic and block diagrams respectively.

The hydraulic boost provides partial or programmed assistance in this region, thus reducing tab load and assuring a tab to rudder ratio of $-.4$ ($\delta_t/\delta_r = -.4$).

Balance panels nos. one, two and three provide assistance through all rudder deflection ranges. Panels 4 and 5 have been deactivated for all airplanes using a rudder boost system.

In order to stay within structural limits of the airplane, boost is limited in programmed and full boost range. See Figure 58 for a boost limit line. Above the boost line any further rudder deflection will be due to tab deflection only.

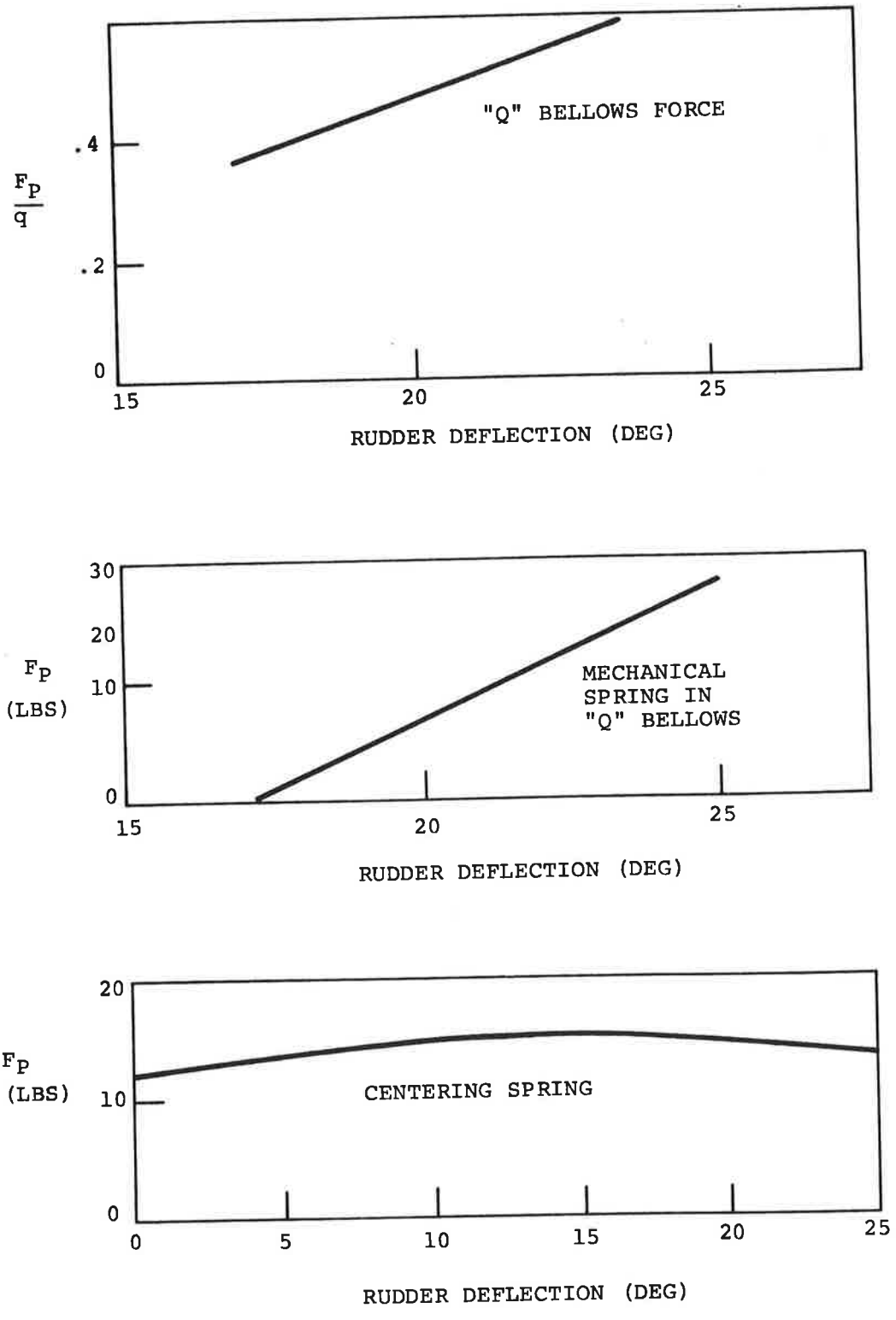

Figure 52. Pedal Forces in Full Boost Range.

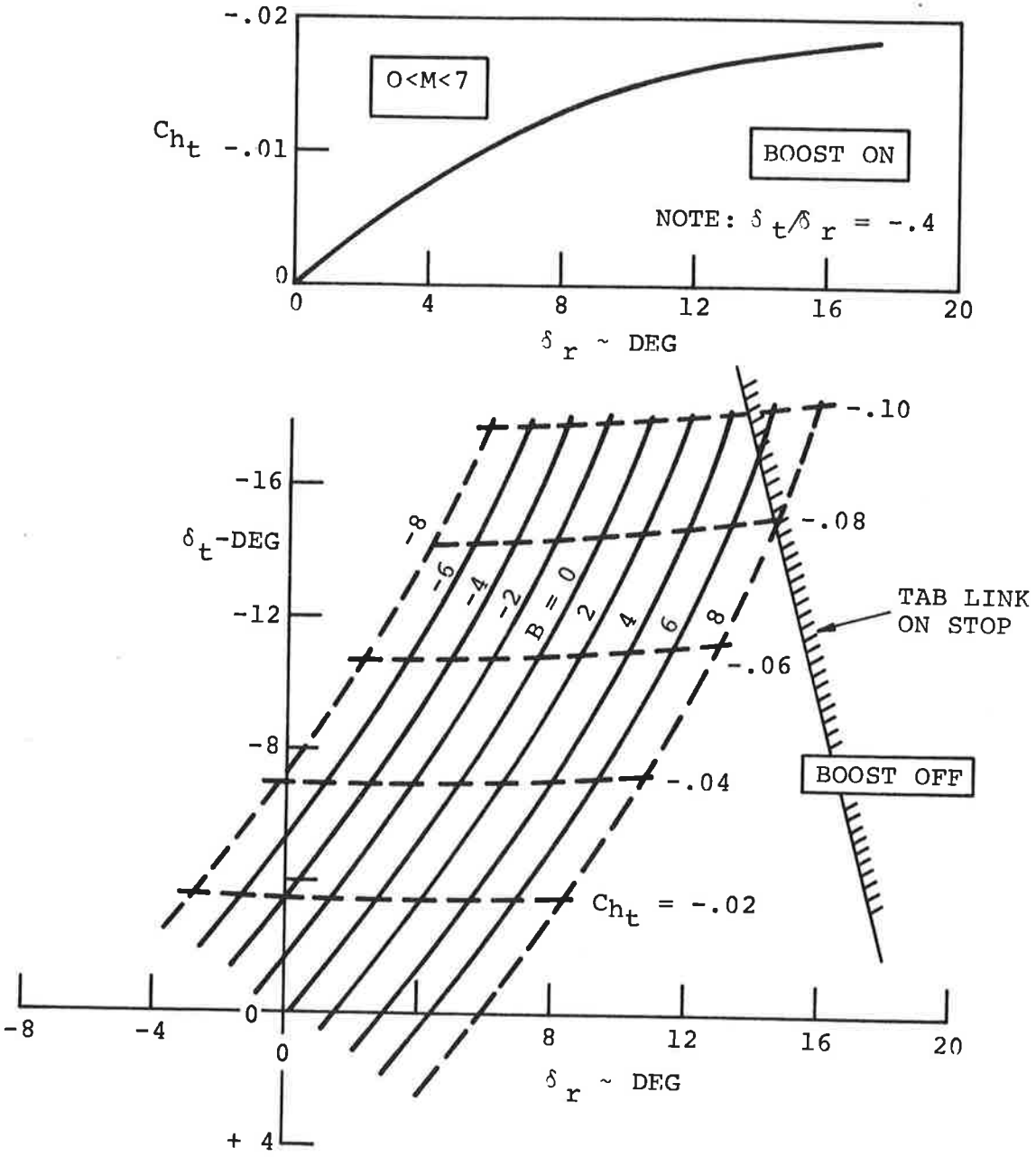

NOTES:

1. $\frac{F_A}{q} = -20.1\ C_{h_t}$
2. PROGRAMMED FULL TIME BOOST
3. BASED ON N74612 & N5088K FLIGHT TEST DATA
4. BALANCE CONFIGURATION "6"

Figure 53. Tab, Rudder, Sideslip and C_{h_t} Relation.

TABLE 18. RUDDER-PROGRAMMED BOOST

δ_p —— Pedal Motion, Inches

δ_q —— Quadrant Motion, Degrees

δ_r —— Rudder Motion, Degrees

x_i —— Tab Input Rod Motion, Inches

x_v —— Valve Input Rod Motion, Inches

$$\frac{\delta_q}{\delta_p} = \frac{57.3 \quad (4.34) \quad (15.47)}{19.25 \quad (2.82) \quad (7.14\ )} = 9.925 \ \frac{\text{DEG}}{\text{INCH}}$$

$$\frac{\delta_r}{\delta_q} = \frac{3.92 \quad (4.76)}{4.50 \quad (4.96)} = .835 \ \frac{\text{DEG}}{\text{DEG}}$$

$$\frac{\delta_r}{\delta_p} = \left(\frac{\delta_r}{\delta_q}\right)\left(\frac{\delta_q}{\delta_p}\right) = .835 \ (9.925) = 8.30 \ \frac{\text{DEG}}{\text{INCH}}$$

$$\frac{x_i}{\delta_p} = \frac{4.76 \ (4.39) \ (9.925)}{57.3 \ (4.96)} = .730 \ \frac{\text{IN.}}{\text{IN.}}$$

$$\frac{x_y}{x_i} = \frac{3.92}{4.39} = .893$$

$$\frac{\delta_r}{x_y} = \frac{57.3}{4.5} = 12.72 \ \frac{\text{DEG}}{\text{INCH}}$$

Reference: Boeing Document D6-9850

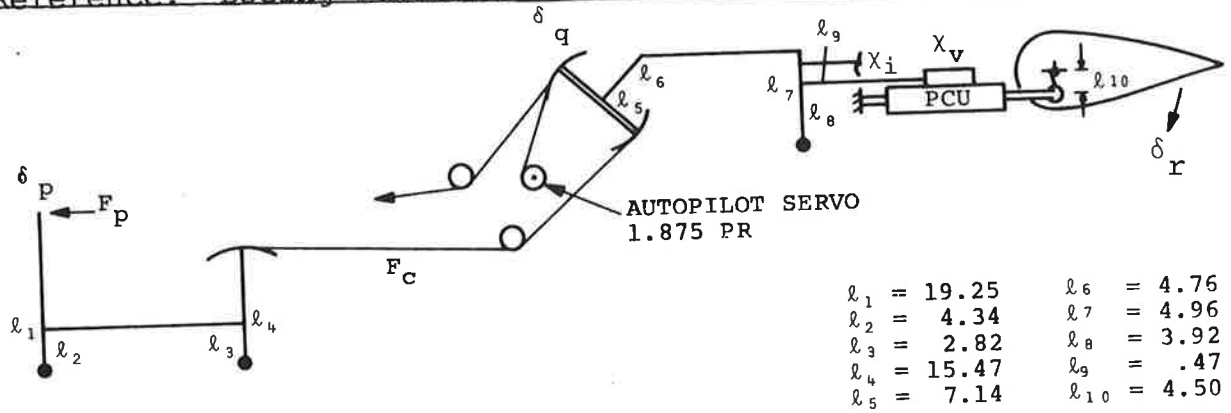

$\ell_1 = 19.25$ $\ell_6 = 4.76$
$\ell_2 = 4.34$ $\ell_7 = 4.96$
$\ell_3 = 2.82$ $\ell_8 = 3.92$
$\ell_4 = 15.47$ $\ell_9 = .47$
$\ell_5 = 7.14$ $\ell_{10} = 4.50$

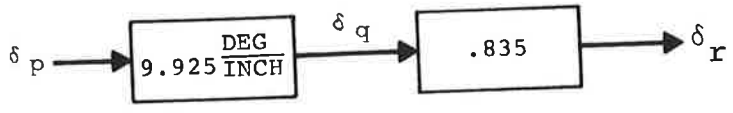

Figure 54. Directional Control System Schematic

Consequently, the tab to rudder ratio of -.4 does not hold in this region.

BOOST OFF

For boost off condition the rudder hinge moments are balanced by:

a. Rudder tab
b. Balance panels

The pedal forces are a function of:

a. Tab hinge moments (Figure 53)
b. Centering spring (Figure 52)
c. Trim spring (Figure 57)

DIRECTIONAL CONTROL FORCES

Pedal forces can be calculated in the following manner:

1. For programmed boost range ($0^{\circ} \leq \delta_r \leq 17^{\circ}$)

   $F_p = + F_A + F_{SC} + F_{Inertia} \pm F_{Frict.}$

   F_A = Air load given as function of C_{h_t} in Figure 53

   F_{SC} = Centering spring force

   $F_{Inertia} = .0916 \ddot{\delta}_{r_t} - .0635 \delta_r$

   $F_{Frict.} = \pm 8$ Lbs.

2. For full time boost range ($17^{\circ} \leq \delta_r \leq 25^{\circ}$)

   $F_p = F_{QB} = F_{QS} + F_{SC} + F_{Frict.}$

   F_{QB}= "Q" bellows force

   F_{QS}= "Q" bellows mechanical spring force

   F_{SC}= Centering spring force

   $F_{Frict.} = \pm 8$ Lbs.

3. For boost off condition ($0^{\circ} \leq \delta_r \leq 25^{\circ}$)

   $F_p = + F_A + F_{SC} + F_{S_T} \pm F_{Frict.} + F_{Inertia}$

   F_A = Aerodynamic force given as function of C_{h_t} in Figure 53

F_{S_C} = Centering spring force

F_{S_T} = Trim spring force

$F_{Inertia} = .0916 \ddot{\delta}_{r_t} - .0635 \delta_r$

Additional information relating to the directional control system forces and deflections is given in Figures 55, 56, 58 and 59.

AS THE PEDAL IS DEPRESSED, BOOST IS PROGRAMMED INTO THE SYSTEM ACCORDING TO THE POWER ASSIST LINE, RESULTING IN A δ_t / δ_r = -.4 RATIO FOR RUDDER DEFLECTIONS BELOW 17°. THIS IS TRUE OF ANY FLIGHT CONDITION WHICH IS NOT BOOST LIMITED FOR RUDDER DEFLECTIONS OF 17° TO 25° THE SYSTEM RELIES COMPLETELY ON HYDRAULIC BOOST

FORWARD PEDAL STOPS AT 12.36° (4.2")

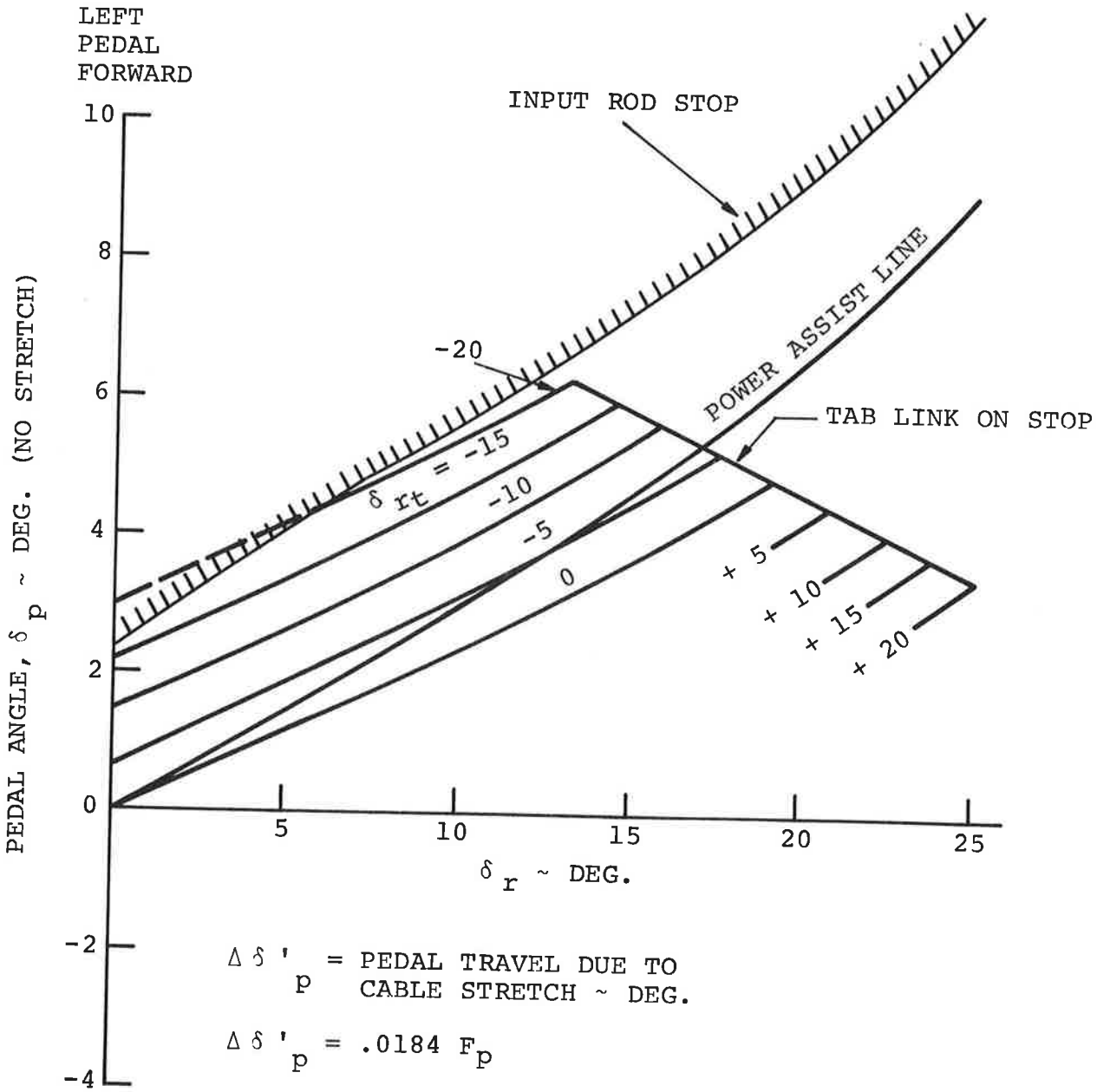

$\Delta\delta'_p$ = PEDAL TRAVEL DUE TO CABLE STRETCH ~ DEG.

$\Delta\delta'_p = .0184\ F_p$

Figure 55. Rudder Pedal Travel (no stretch).

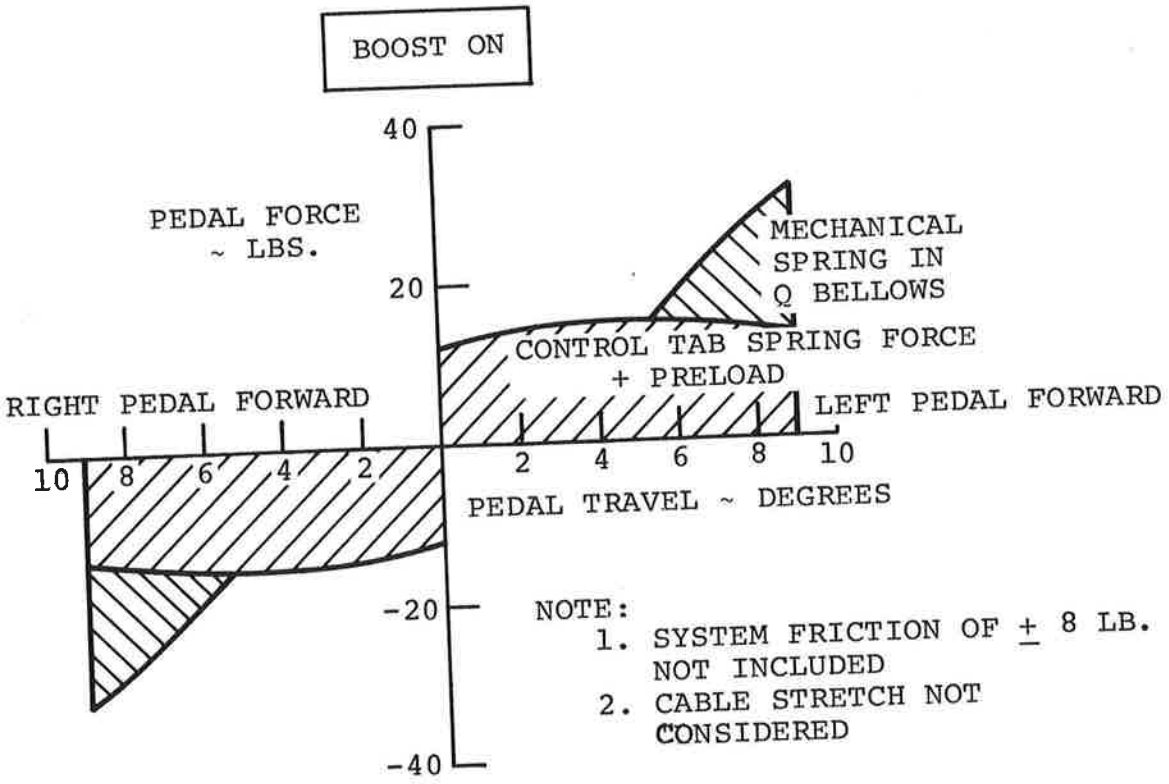

Figure 56. Directional Control Force (no air loads).

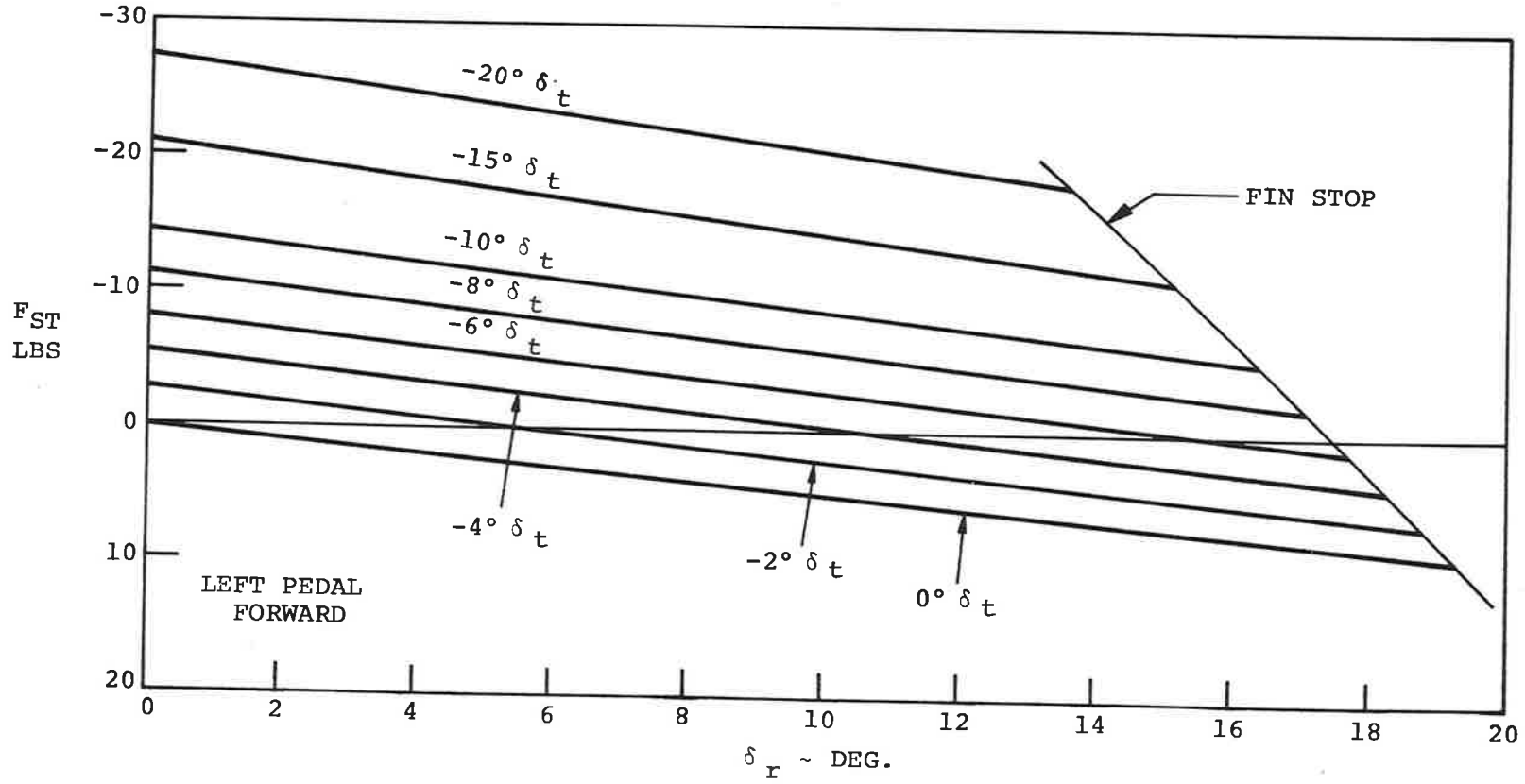

Figure 57. Rudder Trim Spring Characteristics.

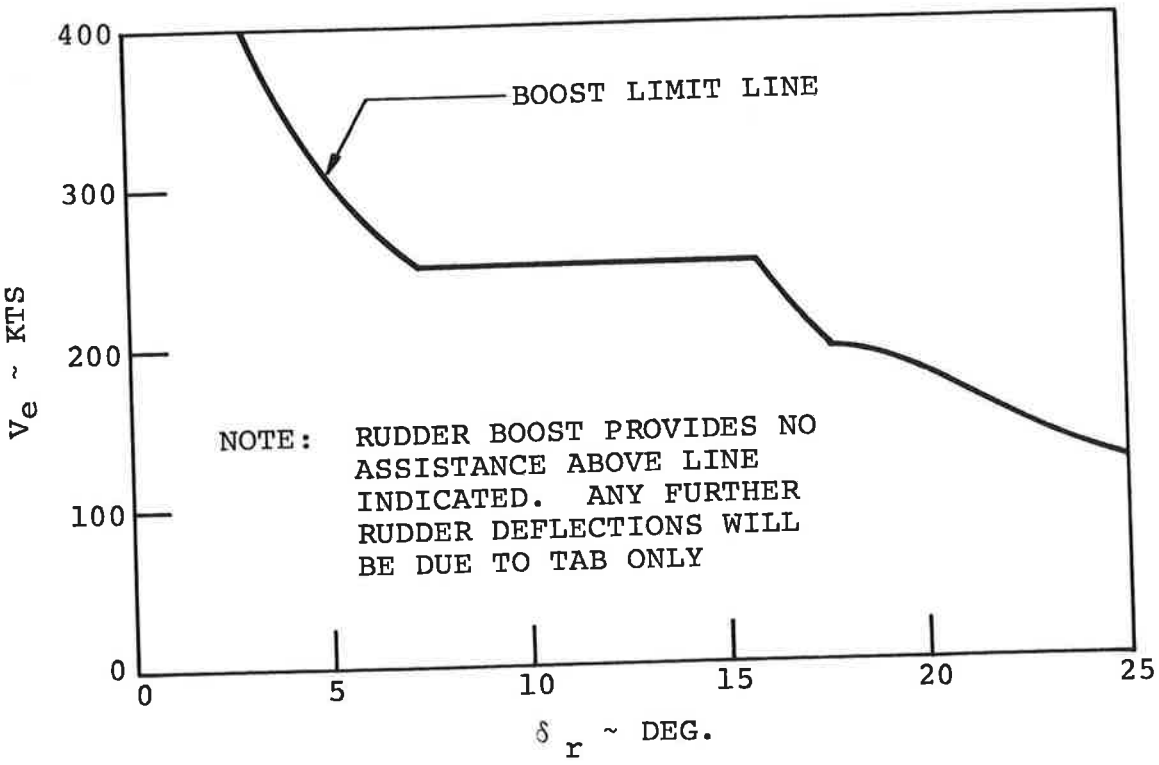

Figure 58. Boost Limit Full Boost System.

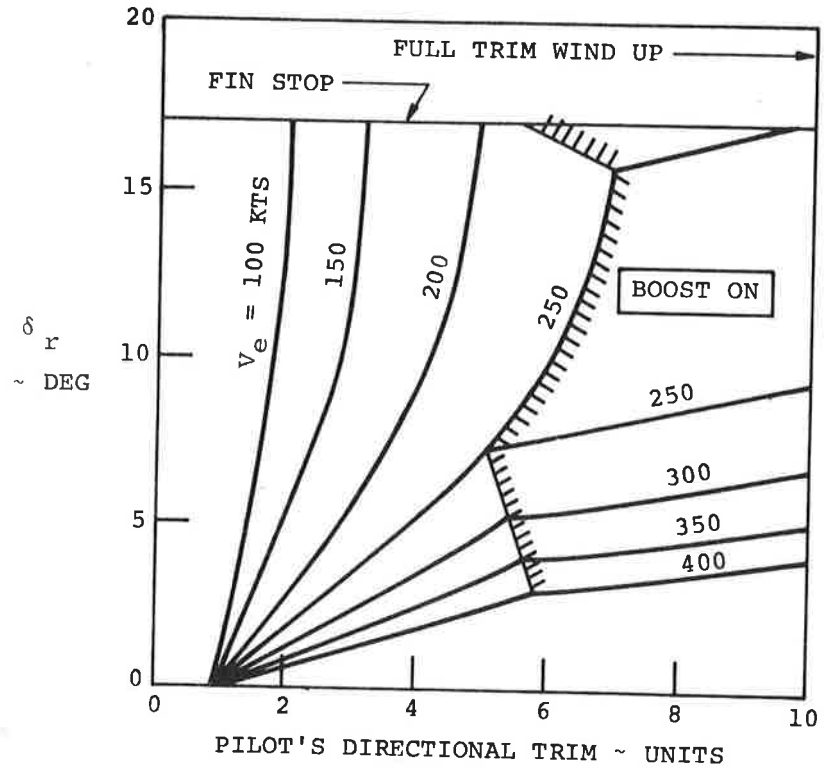

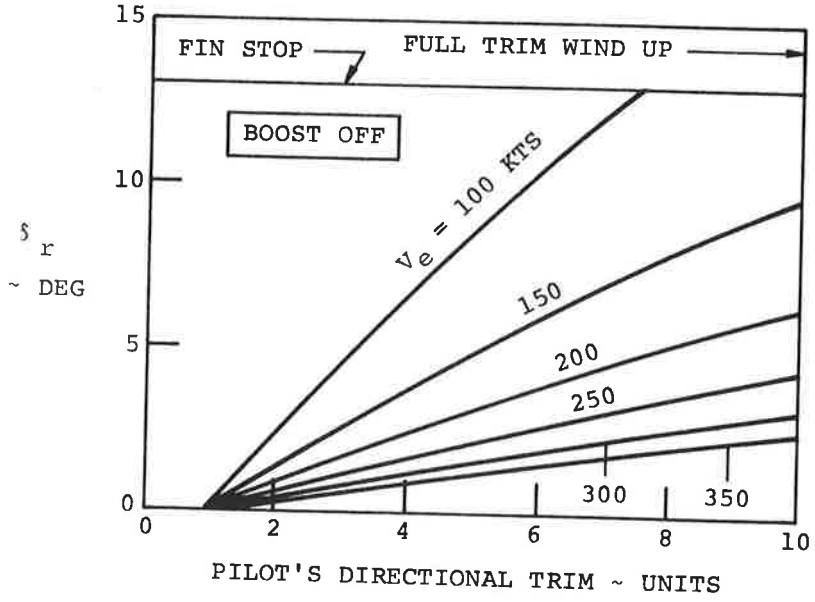

NOTE: 1. δ_t / δ_r = -.4 IN BALANCE TAB RANGE
2. APPLICABLE TO ALL AIRPLANES WITH FULL TIME BOOST

Figure 59. Directional Trim Capability Full Boost System.

AUTOMATIC FLIGHT CONTROL SYSTEM DESCRIPTION

GENERAL

This section presents a description of a typical autopilot as it has been simulated for the Boeing 720-B aircraft model. This autopilot provides three axes of control - pitch, roll, and yaw - which can be engaged individually or simultaneously. Brief descriptions of the individual controls operation are given in the following paragraphs followed by a description of the autopilot operation. Block diagrams of the three axes of control are shown in Figures 65, 66, 67.

CONTROLS OPERATION

PITCH CONTROL

Pitching moment is provided by tab control of the elevator surfaces. Follow-up links provide surface feedback to the control tabs. A schematic of the elevator control system is illustrated in Figure 60 Mechanical ratios are formulated in Table 19. Elevator-Tab characteristics are illustrated in Figure 61.

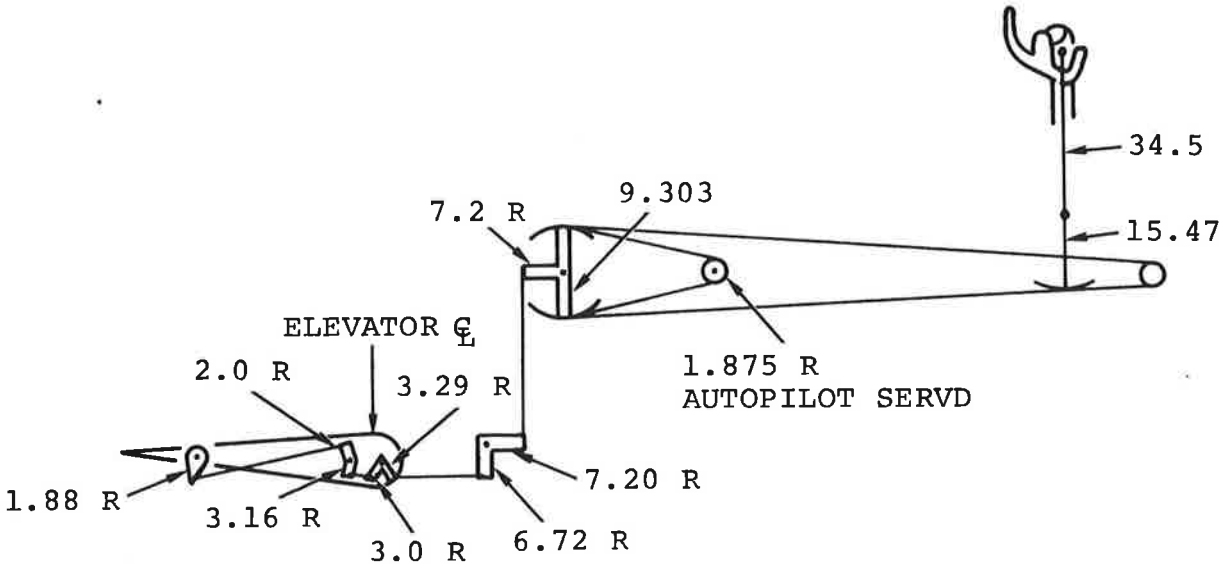

Figure 60. Elevator Control System Schematic

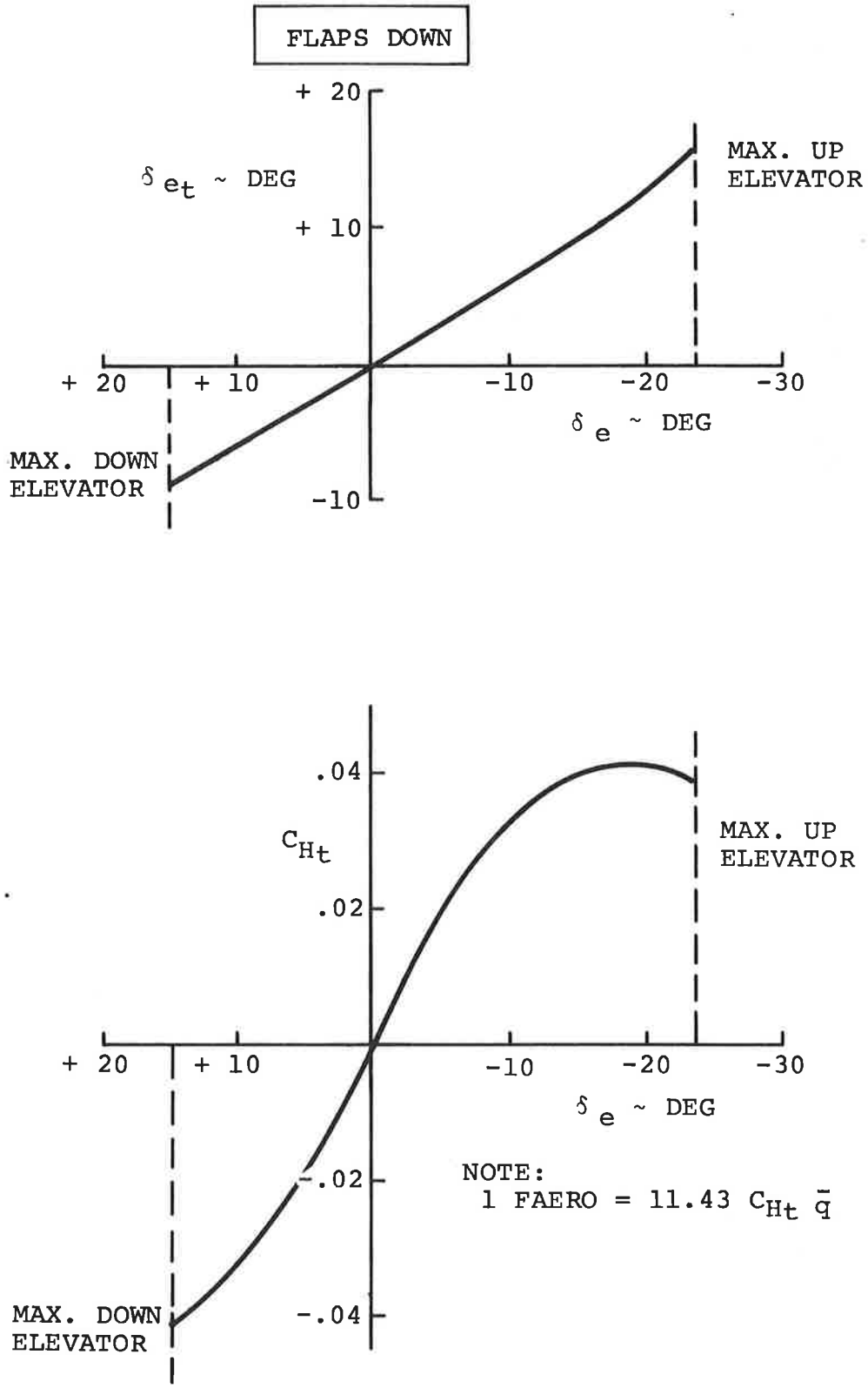

Figure 61. Elevator - Tab Characteristics - Flaps Down.

TABLE 19. ELEVATOR - LINKAGE RATIOS

δ_c —— Column Motion

δ_q —— Quadrant Motion, Degrees

δ_{tc} —— Commanded Tab Motion, Degrees

δ_t —— Tab Motion, Degrees

δ_e —— Elevator Motion, Degrees

δ_{es} —— Autopilot Servo Motion, Degrees

K_e —— Aerodynamic Gain = 1.67 for Approach Configuration and $\delta_e < 10°$

$$\frac{\delta_q}{\delta_c} = \frac{15.47}{9.303} = 1.66 \ \frac{DEG}{DEG}$$

$$\frac{\delta_q}{\delta_c} = \frac{1.66\ (57.3)}{34.5} = 2.76 \ \frac{DEG}{INCH}$$

$$\frac{\delta_{tc}}{\delta_q} = \frac{7.2\ (6.72)\ (3.0)\ \ (2.0\ )}{7.2\ (3.29)\ (3.16)\ (1.88)} = 2.06 \ \frac{DEG}{DEG}$$

$$\frac{\delta_{tc}}{\delta_c} = \left(\frac{\delta_{tc}}{\delta_q}\right)\ \left(\frac{\delta_q}{\delta_c}\right) = 2.06\ (2.76) = 5.69 \ \frac{DEG}{INCH}$$

$$\frac{\delta_q}{\delta_{es}} = \frac{1.875}{9.303} = .202 \ \frac{DEG}{DEG}$$

$$\frac{\delta_{tc}}{\delta_{es}} = \left(\frac{\delta_{tc}}{\delta_q}\right)\ \left(\frac{\delta_q}{\delta_{es}}\right) = 2.06\ (.202) = .416 \ \frac{DEG}{DEG}$$

$$\frac{\delta_e}{\delta_{tc}} = \frac{K_e}{1 + K_e} = \frac{1.67}{2.67} = .625 \ \frac{DEG}{DEG} \ (APPROACH)$$

$$\left.\frac{\delta_e}{\delta_{es}}\right|_{APPR} = \left(\frac{\delta_e}{\delta_{tc}}\right)\ \left(\frac{\delta_{tc}}{\delta_{es}}\right) = .625\ (.416) = .26 \ \frac{DEG}{DEG}$$

[Reference 4 Boeing Document D6-9850 (Page 18)]

ROLL CONTROL

Rolling moment is provided by inboard ailerons, outboard ailerons, and spoilers. The inboard ailerons are control tab operated and the outboard ailerons are actuated by the inboard ailerons whenever the flaps are extended. Follow-up links provide surface feedback to the control tabs. A schematic of the inboard aileron control system is illustrated in Figure 62. Mechanical ratios are formulated in Table 20.

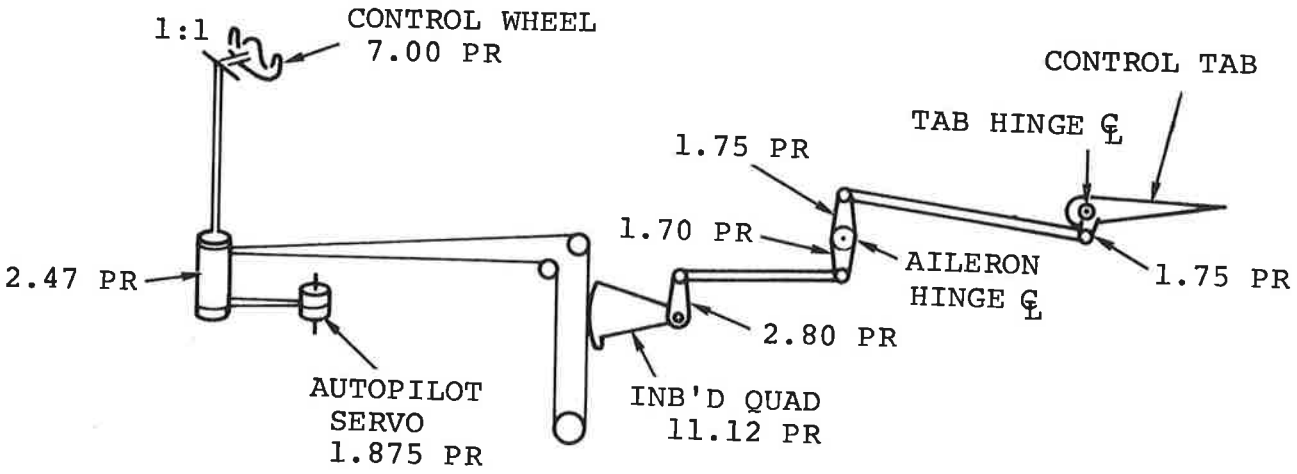

Figure 62. Aileron Control System Schematic

YAW CONTROL

Full Time Series Yaw Damper

Yawing moment is provided by program boost through a series type hydraulic power package shown in Figure 63. During boost on operation, a follow-up line provides surface feedback to reposition the control valve. The control tab operates in anti-balance during boost "on" condition and as a balance tab during manual reversion. Mechanical ratios are formulated in Table 21.

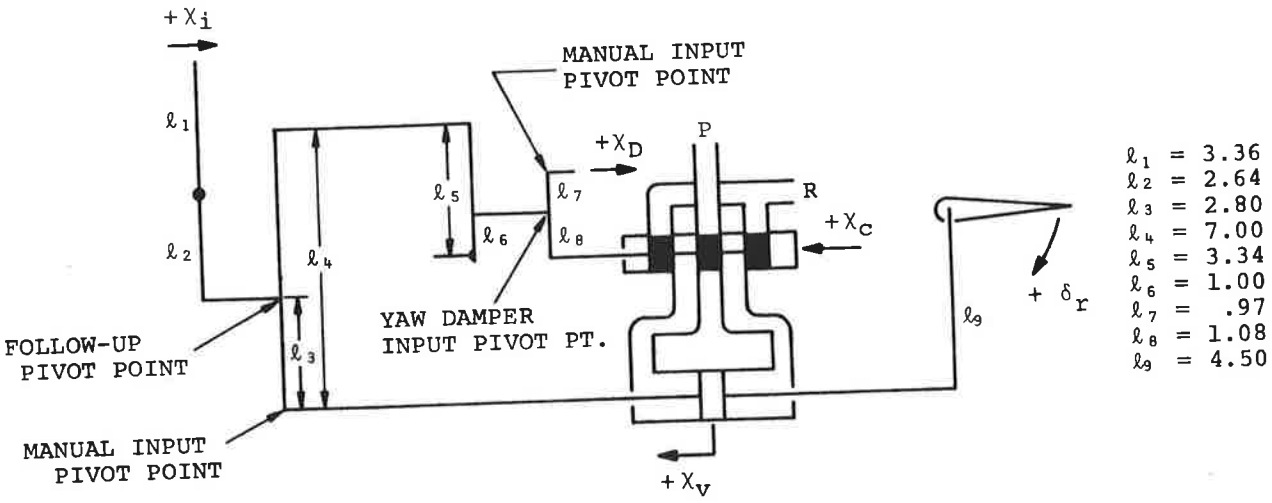

Figure 63. Rudder Control System Schematic, (Full Time Series Yaw Damper)

Programmed Boost

Yawing moment is provided by programmed boost through a hydraulic power control unit (PCU). During boost-on operation, the body of the PCU moves in response to control valve motion and in so doing, it shuts off the flow from the control valve. The control tab operates as a balance tab during boost-on and boost-off conditions. A schematic of the programmed boost rudder system is illustrated in Figure 64. Mechanical ratios are formulated in Table 22.

TABLE 20. AILERON - LINKAGE RATIOS

δ_w —— Control Wheel Motion, Degrees

δ_q —— Inboard Quadrant Motion, Degrees

δ_{tc} —— Commanded Tab Motion, Degrees

δ_t —— Tab Motion, Degrees

δ_a —— Inboard Aileron Motion, Degrees

δ_{as} —— Autopilot Servo Motion, Degrees

K_a —— Aerodynamic Gain = 1.27 for Approach Configuration and $\delta_a < 15°$

$$\frac{\delta q}{\delta w} = \frac{2.47}{11.12} = .222 \ \frac{DEG}{DEG}$$

$$\frac{\delta tc}{\delta q} = \frac{2.80\ (1.75)}{1.70\ (1.75)} = 1.65 \ \frac{DEG}{DEG}$$

$$\frac{\delta tc}{\delta w} = \left(\frac{\delta tc}{\delta q}\right)\left(\frac{\delta q}{\delta w}\right) = 1.65\ (.222) = .366 \ \frac{DEG}{DEG}$$

$$\frac{\delta q}{\delta as} = \frac{1.875}{11.12} = .1685 \ \frac{DEG}{DEG}$$

$$\frac{\delta tc}{\delta as} = \left(\frac{\delta tc}{\delta q}\right)\left(\frac{\delta q}{\delta as}\right) = 1.65\ (.1685) = .278 \ \frac{DEG}{DEG}$$

$$\frac{\delta a}{\delta tc} = \frac{K_a}{1 + K_a} = \frac{1.27}{2.27} = .56 \ \frac{DEG}{DEG} \quad \text{(APPROACH)}$$

$$\left.\frac{\delta a}{\delta as}\right|_{APPR} = \left(\frac{\delta a}{\delta tc}\right)\left(\frac{\delta tc}{\delta as}\right) = .56\ (.278) = .156 \ \frac{DEG}{DEG}$$

[Reference 4 Boeing Document D6-9850 (Page 14)]

TABLE 21. RUDDER - FULL TIME YAW DAMPER

δ_p —— Rudder Pedal Motion, Inches

δ_r —— Rudder Motion, Degrees

x_i —— Manual Input Motion, Inches

x_D —— Yaw Damper Piston Motion, Inches

x_c —— Control Valve Motion, Inches

x_v —— Main Piston Motion, Inches

$$\frac{x_i}{\delta_p} = \frac{4.34\ (15.47)\ (4.46)\ (57.3)}{2.82\ (\ 7.14)\ (57.3)\ (19.25)} = .775\ \frac{\text{INCHES}}{\text{INCH}}$$

$$\frac{x_c}{x_i} = \frac{2.64\ (7.00)\ (1.00)\ (2.05)}{3.36\ (2.80)\ (3.34)\ (\ .97)} = 1.241\ \frac{\text{INCHES}}{\text{INCH}}$$

$$\frac{x_c}{x_v} = \frac{4.20\ (1.00)\ (2.05)}{2.80\ (3.34)\ (\ .97)} = .95\ \frac{\text{INCHES}}{\text{INCH}}$$

$$\frac{\delta_r}{x_v} = \frac{57.3}{4.5} = 12.72\ \frac{\text{DEG}}{\text{INCH}}$$

$$\frac{\delta_r}{\delta_p} = \left(\frac{\delta_r}{x_v}\right)\left(\frac{x_v}{x_c}\right)\left(\frac{x_c}{x_i}\right)\left(\frac{x_i}{\delta_p}\right) = \frac{(12.72)\ (1.241)\ (.775)}{.95}$$

$$= 12.91\ \frac{\text{DEG}}{\text{INCH}}$$

$$\frac{x_c}{x_d} = \frac{1.05}{.97} = 1.112\ \frac{\text{INCHES}}{\text{INCH}}$$

$$\frac{\delta_r}{x_D} = \left(\frac{\delta_r}{x_v}\right)\ \frac{x_v}{x_c}\ \frac{x_c}{x_D} = \frac{12.72}{.95}\ (1.112) = 14.92\ \frac{\text{DEG}}{\text{INCH}}$$

[Reference 4 Boeing Document D6-9850 (Page 10)]

TABLE 22. RUDDER - PROGRAMMED BOOST

δ_p —— Pedal Motion, Inches

δ_q —— Quadrant Motion, Degrees

δ_{rs} —— Autopilot Servo Motion, Degrees

δ_r —— Rudder Motion, Degrees

x_i —— Tab Input Rod Motion, Inches

x_v —— Valve Input Rod Motion, Inches

$$\frac{\delta_q}{\delta_p} = \frac{57.3\ (4.34)\ (15.47)}{19.25\ (2.82)\ (7.14)} = 9.925\ \frac{\text{DEG}}{\text{INCH}}$$

$$\frac{\delta_r}{\delta_q} = \frac{3.92\ (4.76)}{4.50\ (4.96)} = .835\ \frac{\text{DEG}}{\text{DEG}}$$

$$\frac{\delta_r}{\delta_p} = \left(\frac{\delta_r}{\delta_q}\right)\left(\frac{\delta_q}{\delta_p}\right) = .835\ (9.925) = 8.30\ \frac{\text{DEG}}{\text{INCH}}$$

$$\frac{\delta_q}{\delta_{rs}} = \frac{1.875}{7.14} = .263\ \frac{\text{DEG}}{\text{DEG}}$$

$$\frac{\delta_r}{\delta_{rs}} = \left(\frac{\delta_r}{\delta_q}\right)\left(\frac{\delta_q}{\delta_{rs}}\right) = .835\ (.263) = .220\ \frac{\text{DEG}}{\text{DEG}}$$

$$\frac{\delta_p}{\delta_{rs}} = \left(\frac{\delta_p}{\delta_q}\right)\left(\frac{\delta_q}{\delta_{rs}}\right) = \frac{.263}{9.925} = .0265\ \frac{\text{IN.}}{\text{DEG}}$$

$$\frac{x_i}{\delta_p} = \frac{4.76\ (4.39)\ (9.925)}{57.3\ (4.96)} = .730\ \frac{\text{IN.}}{\text{IN.}}$$

$$\frac{x_v}{x_i} = \frac{3.92}{4.39} = .893$$

$$\frac{\delta_r}{x_v} = \frac{57.3}{4.5} = 12.72\ \frac{\text{DEG}}{\text{INCH}}$$

[Reference 4 Boeing Document D6-9850]

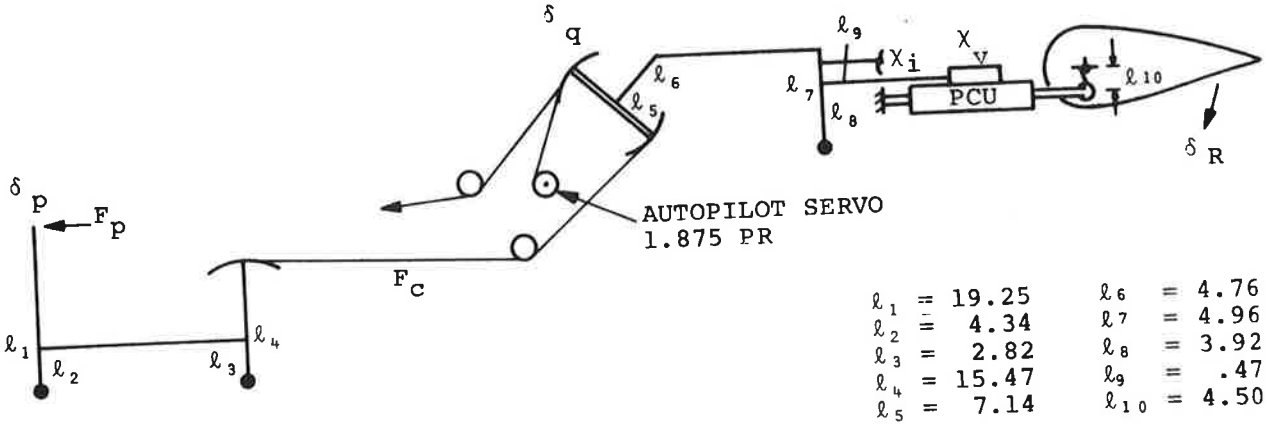

Figure 64. Rudder Control System Schematic (Programmed Boost)

AUTOPILOT OPERATION

Upon engagement, any particular mode of operation can be selected from among the following six basic modes and certain combinations thereof:

None Selected
MANUAL - (Maintain Course: at Engagement)
LOCALIZER - (Track the Localizer beam)
GS AUTO - (Track the glideslope beam with automatic engagement when the beam is intercepted. Autopilot must be in LOCALIZER in order to engage GS Auto)
GS MAN - (Track the Glideslope)
ALT. HOLD - (Maintain Altitude; at Engagement)

These modes and the permitted combinations are defined in Table 23.

* The material presented in this section was drawn from Reference 2. The reference data was not entirely complete and therefore the discussion of the autopilot operation may not be very accurate.

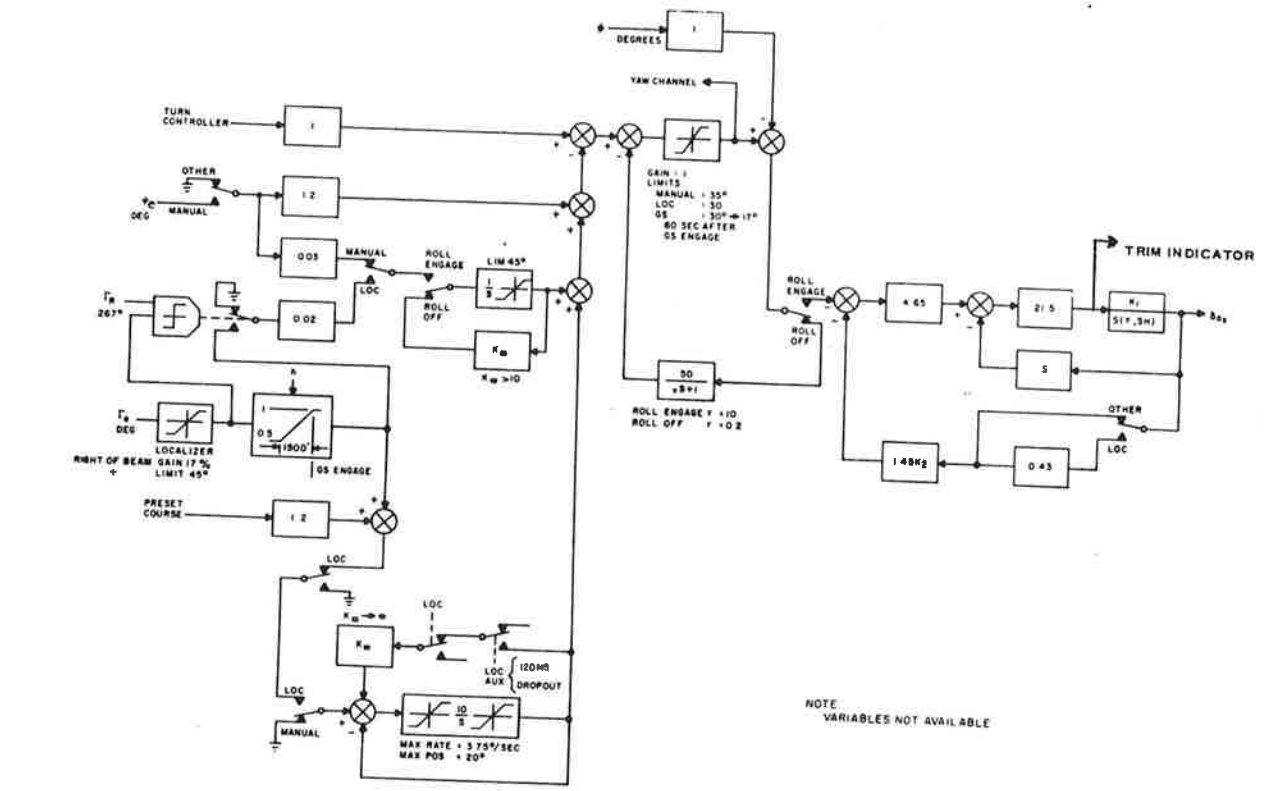

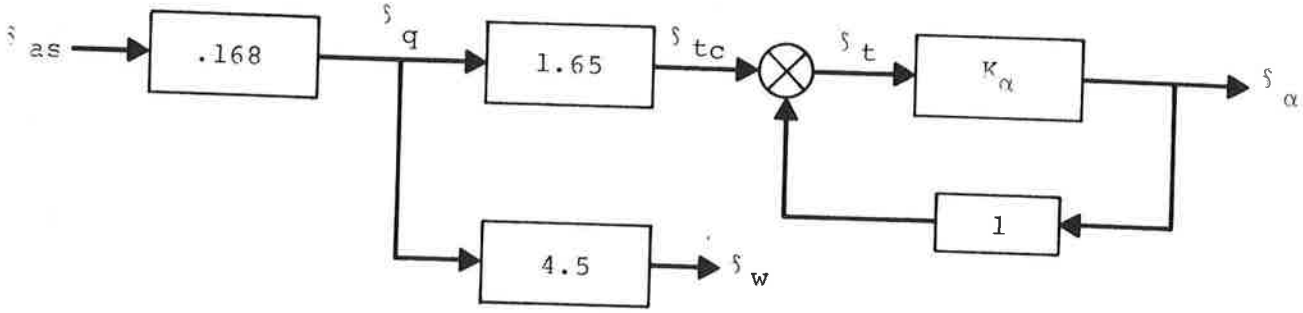

Figure 65. Block Diagram, Roll Channel.

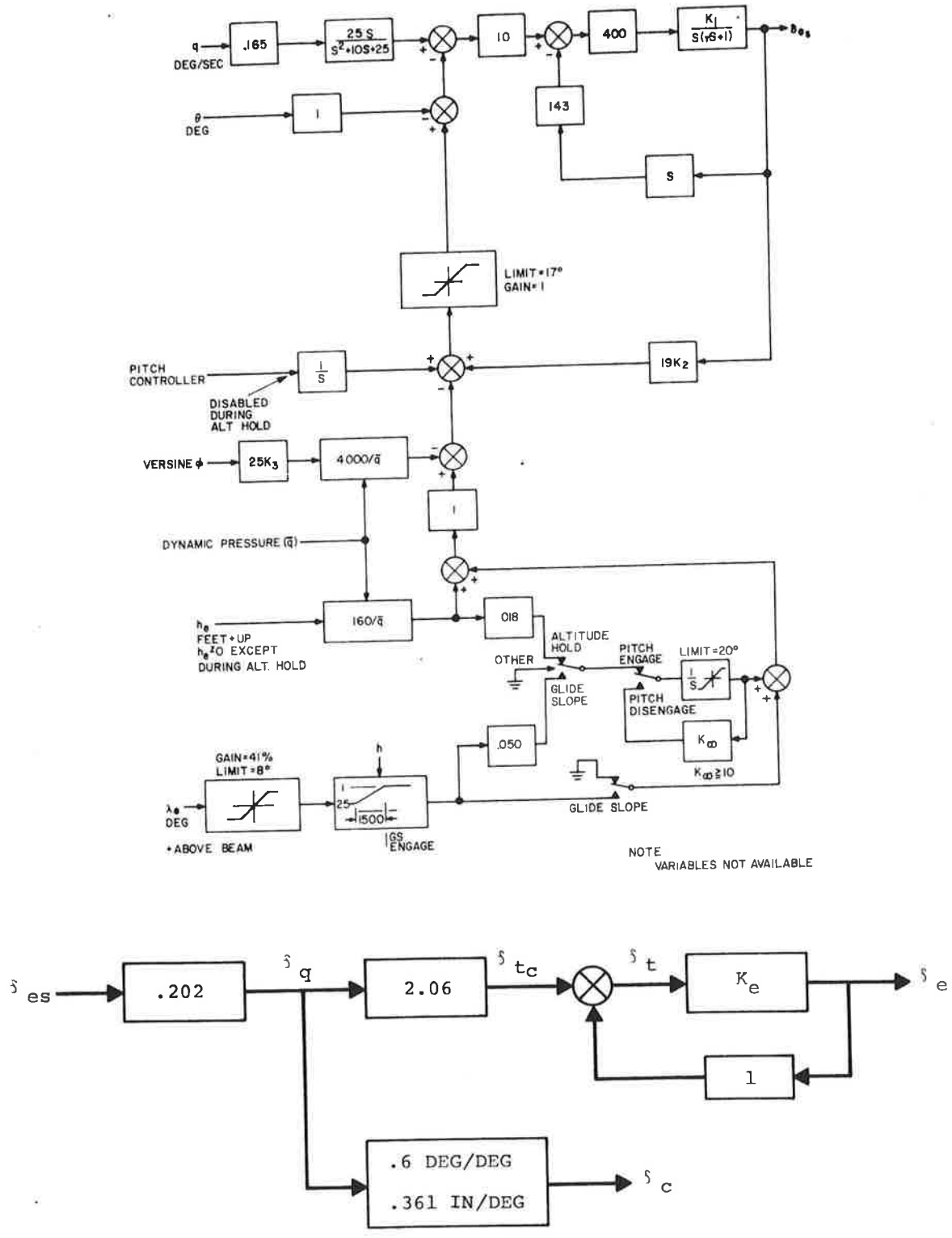

Figure 66. Block Diagram, Pitch Channel

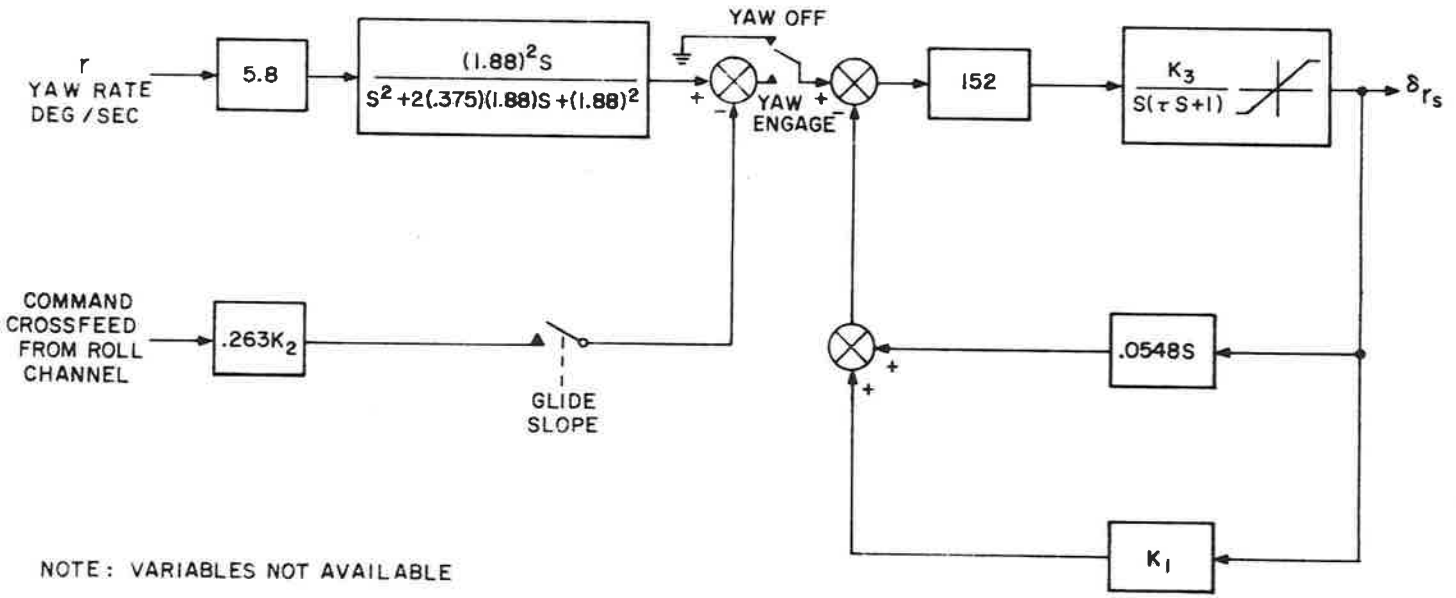

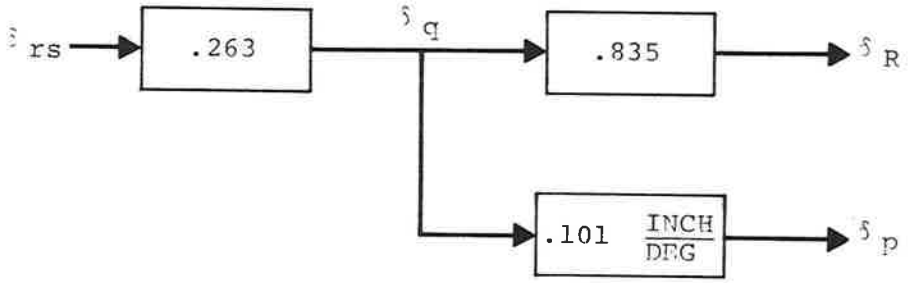

YAW DAMPER

Figure 67. Block Diagram, Yaw Channel

TABLE 23. SIX MODES AND DEFINITIONS

Mode	Definition
None Selected	Attitude Hold (pitch and roll) control via attitude command switches which cause attitude command to change at a fixed rate.
MANUAL	Heading Hold (at engagement value) pitch attitude hold with control via pitch attitude command switch.
MANUAL, ALT. HOLD	Heading and Altitude Hold (at engagement values)
LOCALIZER	Automatic tracking of the localizer beam. Pitch attitude hold with control via pitch attitude command switch.
LOCALIZER, ALT. HOLD	Automatic tracking of the localizer beam. Altitude hold at the engagement value
LOCALIZER, ALT. HOLD, GS AUTO	Automatic tracking of the localizer beam. Altitude hold at the engagement value until acquisition of the glide slope beam at which time glide slope tracking commences
LOCALIZER, GS MAN	Automatic tracking of the localizer beam. Glide slope tracking commences immediately upon selection of GS MAN.
GS MAN	Roll attitude hold with control via roll attitude command switch. Glideslope tracking commences immediately upon selection of GS MAN.

NONE SELECTED MODE (PITCH AND ROLL ATTITUDE)

When no modes are selected (Table 23) the system is in a pitch and roll attitude hold configuration. Attitude control is achieved via pitch and roll attitude command switches. Depressing these switches in the appropriate direction causes the aircraft to change attitude at a fixed rate. When the desired attitude has been achieved, the switches are released. The autopilot will then cause the aircraft to maintain this attitude until it is disengaged or a mode is selected which commands a new attitude.

In the roll channel, the bank angle is limited to $\pm$ 35 degrees by a bank angle command limiter. A block diagram of the roll channel configuration during attitude hold is included in Figure 65. In this configuration, the switches are set such that the turn controller is providing the only bank angle command to the roll system.

In the pitch channel, the pitch angle is limited ot $\pm$ 17 degrees. A washed-out pitch rate signal is used to augment the aircraft short period damping. A block diagram of the pitch channel configuration during attitude hold is included in Figure 66.

In the yaw channel, dutch roll damping is augmented by using a washed-out yaw rate signal to command a rudder deflection. A block diagram of the yaw channel is included in Figure 67.

MANUAL

Selection of the MANUAL mode affects the operation of the roll channel. The pitch and yaw channels are unaffected. In this mode the autopilot maintains the heading of the aircraft at the engagement value by commanding a bank angle as a function of the heading error. The bank angle is limited to $\pm$ 35 degrees by a bank angle command limiter. To force the aircraft to track the desired heading on a long term basis, a low-gain integrator is used to supplement the heading error signal. A block diagram of this mode is included in Figure 65.

Interlocking logic precludes the selection of the LOCALIZER, GS AUTO, or GS MAN modes when the MANUAL mode is selected.

LOCALIZER

Selection of the LOCALIZER mode affects the operation of the roll channel. A block diagram of the LOCALIZER mode is included in Figure 65. Once selected the LOCALIZER mode can only be activated if the absolute value of the localizer

error signal is less than a preset constant whose value was not specified in Reference 2. Should the error signal subsequently exceed this value, the LOCALIZER mode will automatically deactivate. Since there seems to be nothing in the system (either heading or psuedo velocity) that would prevent the undesirable S-turn maneuver during localizer capture, it is assumed that capture must be performed by the pilot either with the roll command switch or with the autopilot disengaged. After the beam has been captured, the pilot can then select the LOCALIZER mode to permit automatic beam tracking.

In this mode the sum of the straight gain localizer error, a preset course signal, and the integrated localizer error generate the bank angle command to cause the aircraft to track the localizer beam.

The integration of the localizer error signal is only permitted as long as the absolute value of the error is less than Γ_R (0.267 degrees). (The purpose of the preset course signal and its value are unclear to this author). During this mode the bank angle command is limited to $\pm$ 30 degrees by a bank angle command limiter until 60 seconds after glide slope track mode is engaged at which time the limit level is reduced to $\pm$ 17 degrees.

There seems to be no provision in autopilot design for any type of path damping (lagged roll angle, heading error, or differentiated localizer error) which is necessary for system stability. It is assumed that some form of heading error is probably used to provide path damping although this was not apparent from the material in Reference 2.

A desensitization gain is included in the localizer error signal path. This gain decreases with decreasing altitude to counteract the effect of the increasing sensitivity of the localizer error signal as the aircraft approaches the localizer antenna.

ALTITUDE HOLD

A block diagram of the altitude holde mode is included in Figure 66. In this mode the autopilot maintains the altitude of the aircraft (at the engagement value) by commanding a pitch attitude as a function of altitude error. The aircraft short period damping is augmented by a washed-out pitch rate signal. The aircraft is forced to track the engagement altitude in steady state by a low-gain integrator which operates on the altitude error. This same integrator is used during glide slope track as well as during altitude hold.

If the GS AUTO mode has also been selected, the autopilot will automatically switch to the GS track mode when the centerline of the glide slope beam is crossed. If the GS MAN mode is selected by the pilot while the system is in ALTITUDE HOLD, the autopilot will disengage altitude hold and engage the GS track mode.

GLIDE SLOPE TRACK MODE

The glide slope track mode can be engaged either automatically by selecting GS AUTO or manually by selecting GS MAN. If GS AUTO has been selected by the pilot, he must have also selected LOCALIZER for automatic activation of GS track. Generally ALTITUDE HOLD is also selected with GS AUTO. In this case, when the aircraft crosses the centerline of the glide slope beam, the GS track mode will automatically be activated and the altitude hold mode will be disengaged. If the pilot chooses to engage GS track manually, he may select GS MAN. In this case the GS track mode will be activated immediately and if it has been engaged the altitude hold mode will disengage.

In the GS track mode the elevator servo command is the sum of washed-out pitch rate, pitch angle, and straight gain and integrated glide slope error signals. The washed-out pitch rate is used to augment the aircraft's short period damping. A block diagram of the GS track mode is included in Figure 66.

During GS track, the roll angle command signal is fed to the yaw channel to improve the localizer beam tracking performance.

FLARE MODE

Flare is introduced automatically at the appropriate time. Flare is accomplished upon crossing the inner marker by disengaging the glideslope and engaging a program altitude descent. The programmed change of altitude is an exponential decay from the existing altitude at the time of flare engagement to a desired altitude (touchdown).

The altitude error signal commands a pitch up maneuver as a function time in accordance to:

$$h_e = (h_o - h_F)\, e^{-t/\tau} - (h - h_F)$$

where

h_e = altitude error
h_o = initial altitude at start of flare
h_F = preset final altitude (unspecified)
h = actual altitude
t = time from start of flow
τ = preset time constant (unspecified)

APPROACH AND LANDING MODE DESCRIPTION

The purpose herein is to provide readily useable data on the operations required to prepare a 720B aircraft for the approach and landing mode.

Normal operation for the approach and landing mode is based on providing good economy of fuel consumption as well as, during the descent phase, not exceeding a specified maximum cabin rate-of-descent of 300 feet/minute.

As an example, a 720B airplane cruising at 20,000 ft. altitude, in preparation for the approach and landing mode, should be at approximately 340KIAS cruise speed. The initiation of the approach and landing mode should take place at approximately 50 n. miles from touchdown. At this point, the descent and engine throttling back should begin.

When the aircraft reaches the 3000 ft. altitude, the speed should be approximately 180 KIAS. At this stage the flaps should be deflected to 30° and the speed increased to approximately 200 KIAS. Approximately 5-8 minutes later the landing gear should be extended.

When the aircraft reaches the outer marker (altitude approximately 1500 feet) the flaps are deflected to 50° and the approach speed changed to 190 KIAS.

Figure 68 illustrates a typical approach and landing pattern.

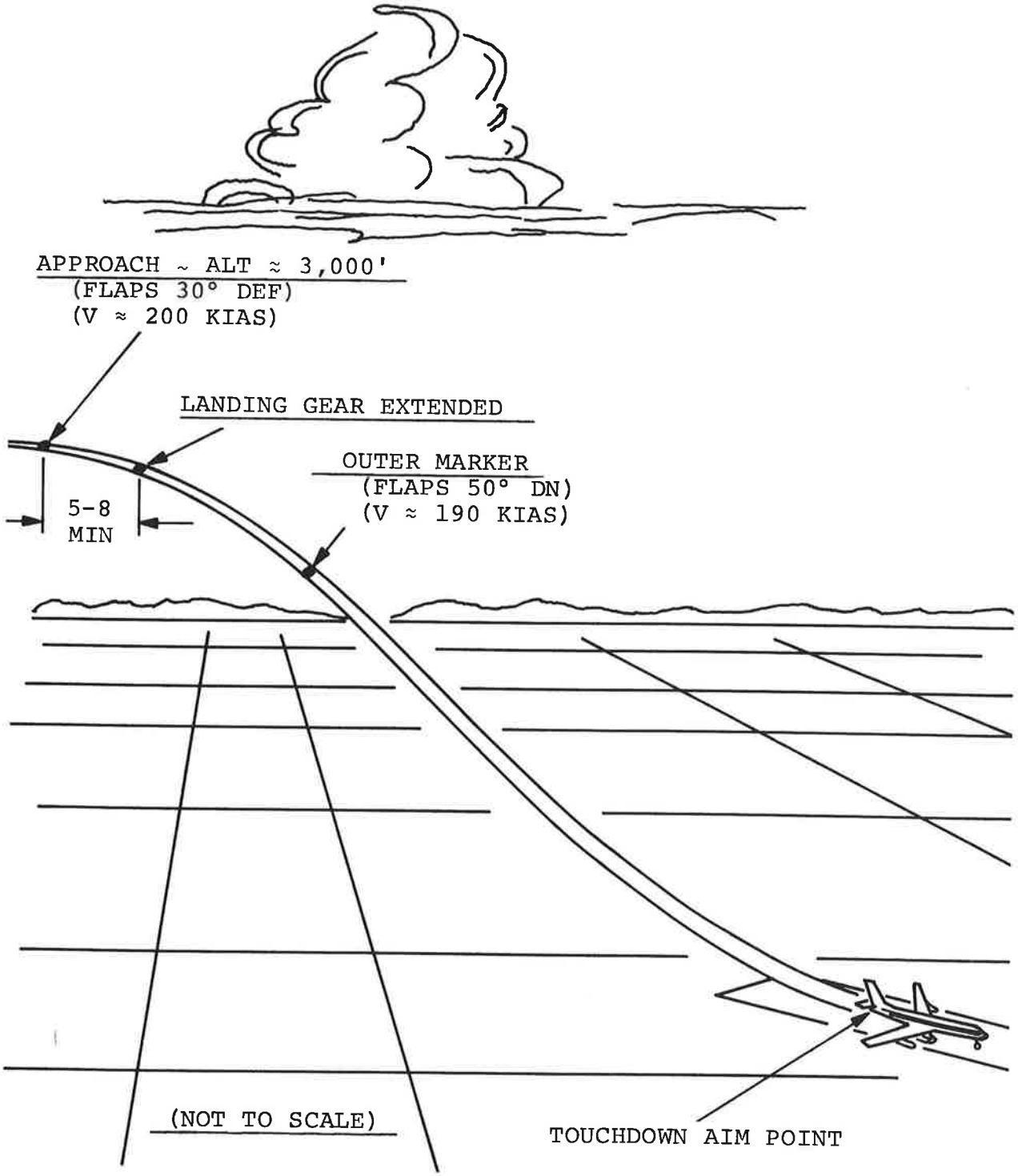

Figure 68. Typical Approach and Landing Pattern.

PROPOSED SIMULATOR BLOCK DIAGRAM

It was originally intended that TSC recommend procedures for implementing the continuous flight regime model for the Boeing 720B aircraft on the NAFEC hybrid computation facility. Since the hardware availability and constraints at NAFEC are not known at this time, the simulator block diagram shown in Figure 69 is proposed as a guideline.

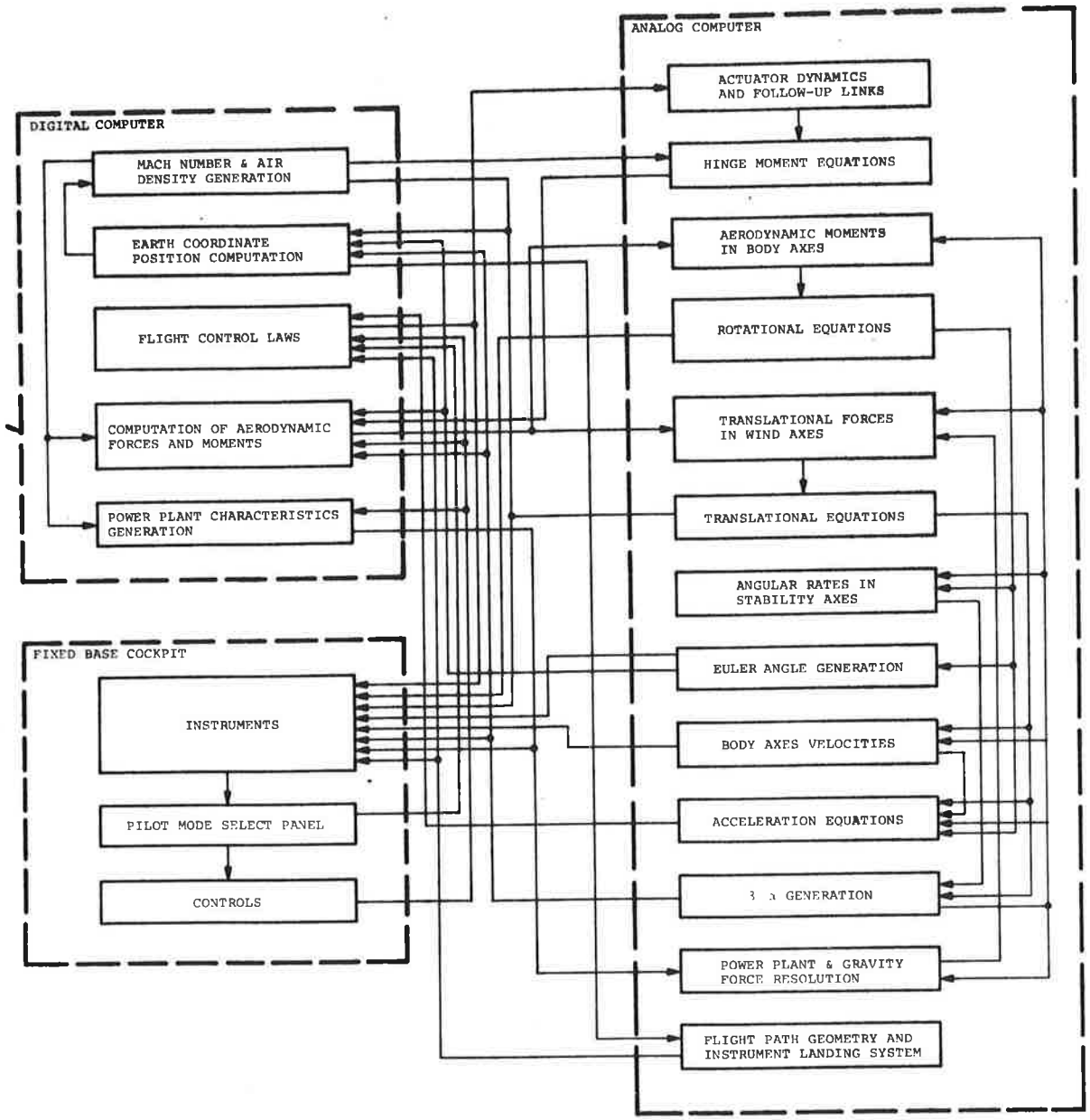

Figure 69. Proposed Hybrid Computer Simulation.

REFERENCES

1. Zuckerberg, H. and Robb, A.F., *Airframe Rigid-Body Equations of Motion and Aircraft Data in the Approach and Landing Mode for the CV-880 and Boeing 720B Airplanes*, STC-DOT-TSC-43-71-816, June 1971.
2. Hughes Document 2732. 50/147 dated April 1965, *Transport Approach and Landing Simulator: Aircraft and Autopilot Simulation.*
3. Boeing Document D6-1154-7, *Aerodynamic Data for the 720B Flight Simulator, (A supplement to D6-1154).*
4. Boeing Document D6-9850, *Airplane Data for Automatic Pilot Design, Boeing Model 720B.*
5. Etkin, B. *Dynamics of Flight*, John Wiley & Son.
6. U. S. Standard Atmosphere Supplements, 1966 Environmental Science Services Administration, NASA, USAF.